1-1-2002

Condensation Heat Transfer in Horizontal Micro-Fin Tubes

Cheahun Kung

CONDENSATION HEAT TRANSFER IN HORIZONTAL MICRO-FIN TUBES

By

Chea-Chun Kung

A Thesis
Submitted to the Faculty of
Mississippi State University
in Partial Fulfillment of the Requirements
for the Degree of Master of Science
in Mechanical Engineering
in the Department of Mechanical Engineering

Mississippi State, Mississippi

December 2002

CONDENSATION HEAT TRANSFER IN HORIZONTAL

MICRO-FIN TUBES

By

Chea-Chun Kung

Approved:

Louay M. Chamra Associate Professor of Mechanical Engineering (Major Professor)	B. Keith Hodge Professor of Mechanical Engineering (Committee Member)
George A. Adebiyi Professor of Mechanical Engineering (Committee Member)	Carl A. James Assistant Research Professor of Mechanical Engineering (Committee Member)
Rogelio Luck Associate Professor and Graduate Coordinator of Department of Mechanical Engineering	A. Wayne Bennett Dean of the College of Engineering

Name: Chea-Chun Kung

Date of Degree: December 13, 2002

Institution: Mississippi State University

Major Field: Mechanical Engineering

Major Professor: Dr. Louay M. Chamra

Title of Study: CONDENSATION HEAT TRANSFER
IN HORIZONTAL MICRO-FIN TUBES

Pages in Study: 110

Candidate for Degree of Master in Science

Three existing condensation heat transfer models are validated using 544 experimental data points for pure refrigerants and refrigerant mixtures. The Cavallini et al. (1999) model predicts well with the pure-refrigerant data sets. However, the Cavallini et al. (1999) model fails to predict the refrigerant-mixture data sets. The Yu and Koyama (1998) model, which is applicable for the pure refrigerants only, fails to predict most of the R22 data sets. The Kedzierski and Goncalves (1999) model, which is applicable for both pure refrigerants and refrigerant mixtures, yields relatively high mean absolute deviations for most of the pure-refrigerant data sets. The Kedzierski and Goncalves (1999) model does not account for the mass transfer thermal resistance in refrigerant mixtures. A new pure-refrigerant model and a new refrigerant-mixture semi-empirical model have been developed. Both the new models successfully predict the experimental data for pure refrigerant and for refrigerant mixtures.

DEDICATION

I would like to dedicate this research to my parents, Gim-Him Kung and Ah-Kee Teh, my sister, Chea-Win, my brother, Chea-Hoong, and my girl friend, Celine Lim, for their encouragements and endless support.

ACKNOWLEDGEMENTS

I would like to express my sincere gratitude to many people who have provided guidance and assistance to materialize this thesis. Dr. Louay M. Chamra, my major professor, who has offered his absolute support and invaluable time to assist me throughout my entire masters program and my thesis preparation process. I also would like to express my sincere appreciation to my thesis committee members, Dr. B. Keith Hodge, Dr. George A. Adebiyi, and Dr. Carl A. James, for their precious advices and valuable assistances.

TABLE OF CONTENTS

LIST OF TABLES

TABLE Page

TABLE Page

LIST OF FIGURES

FIGURE Page

NOMENCLATURE

a	Radius of curvature of the liquid-vapor interface between the micro fins (m)
A	Total heat transfer surface area (m^2)
A_c	Cross-sectional flow area inside tube (m^2)
A_f	Unflooded area at the fin flank and fin tip (m^2) (equation 2.30)
A_i	Unflooded area at the inter-fin space (m^2) (equation 2.31)
b	Width of micro-fin valley bottom (m)
Bo	Bond number adopted from Webb (1988) (equation 2.6)
c	Heat transfer enhancement factor (equation 2.29)
c_p	Specific heat (J/kg-K)
d_i	Inner-tube diameter (m)
d_h	Hydraulic diameter (m)
d_o	Outer-tube diameter (m)
$(dp/dz)_f$	Frictional pressure gradient (Pa/m)
e	Micro-fin fin height (m)
E	Fridel parameter (equation 4.24)
f_{LO}	Friction factor based on total flow assumed as liquid
f_{GO}	Friction factor based on total flow assumed as gas
F	Fridel parameter (equation 4.25)
Fr	Froude number (equation 2.5)

g	Gravitational acceleration (m/s^2)
G	Total mass flux (kg/m^2-s)
Ga	Galileo number (equation 2.13)
h	Heat transfer coefficient (W/m^2-K)
h_B	Film condensation contribution (equation 2.26)
h_F	Forced convective condensation contribution (equation 2.27)
i_{fg}	Latent heat of condensation (J/kg)
i_{fg_m}	Specific enthalpy of isobaric condensation of the mixture (J/kg)
Ja	Jakob number (equation 2.21)
k	Thermal conductivity (W/m-K)
L	Heated test section length (m)
m	Mass flow rate (kg/s)
MAD	Mean absolute deviation
N	Total number of data points
Nu	Nusselt number
Nu_F	Forced convective condensation component (equation 2.8)
Nu_B	Natural convective condensation component (equation 2.12)
n_g	Number of micro-fins
P	Pressure (Pa)
p_R	Reduced pressure (equation 2.20)
p	Micro-fin pitch (m)
Ph	Phase-change number (equation 2.14)
Pr	Prandtl number (dimensionless)

q	Surface heat flux (W/m^2)
R	Radius of the cylindrical surface equivalent to the actual liquid-vapor interface (m)
R_0	Distance between the center of the tube and fin tip (m)
R_r	Distance between the center of the tube and the bottom of the groove (m)
Re	Reynolds number (dimensionless)
Rx	Geometry parameter proposed by Hori and Shinohara (1991) (equation 2.4)
Rx_f	Empirically-fitted relative roughness (equation 4.34)
s	Spacing between the fin root (m)
S	Perimeter of one fin and channel taken perpendicular to the axis of the fin (m)
S_v	Dimensionless specific volume (equation 2.22)
t	Width of micro-fin top (m)
th	Tube-wall thickness (without micro-fin) (m)
T	Temperature (K)
T^+	Dimensionless temperature
ΔT	Wall superheat (K)
ΔTG	Temperature glide for refrigerant mixture effect (K)
u	Velocity (m/s)
u^*	Friction velocity (m/s)
u^+	Dimensionless velocity
x	Vapor quality
X_{tt}	Martinelli Parameter (equation 2.11)

Δx	Change in vapor quality
y	Distance measured from boundary (m)
y^+	Dimensionless distance from the wall
We	Weber number (equation 4.27)

Greek Symbols

β	Micro-fin apex angle (^{o}, degree)
γ	Micro-fin helix angle (^{o}, degree)
μ	Dynamic viscosity (kg/ms)
ν	Kinematic viscosity (m^2/s)
τ	Shear stress (Pa)
ε	Void fraction (equation 2.15)
ε_H	Eddy diffusivity of heat (m^2/s)
ε_M	Eddy diffusivity of momentum (m^2/s)
α_T	Thermal diffusivity
δ	Liquid film thickness (m)
δ^+	Dimensionless liquid film thickness
η_A	Heat transfer area enlargement ratio
Δ	Difference
Φ	Two-phase multiplier
Φ_{LO}	Two-phase multiplier from the new model (equation 4.23)
ρ	Density (kg/m^3)

σ	Surface tension (N/m)
θ	Fin-tip angle (rad)
ϕ	Angle from the top of the tube (rad)
ϕ_o	Stratified liquid angle (rad)
ϕ_f	Liquid hold-up angles (rad)

Subscripts

cr	Critical condition
eq	Equivalent
experimental	Experimental results
f	Frictional
GO	Total fluid assumed as vapor
i	Inlet
l	Liquid-phase only
LO	Total fluid assumed as liquid
m	Two-phase mixture
out	Outlet
predicted	Prediction results
sat	Saturation
t	Turbulent
T	Total
v	Vapor-phase only
w	Wall

CHAPTER I

INTRODUCTION

Micro-fin tubes have been widely used in commercial air-conditioning industry since the early eighties. The typical micro-fin tubes available for industrial applications are made of copper. Micro-fin tubes have proved to be more efficient in refrigeration systems than conventional smooth tubes. The use of the micro-fin tubes beneficially enhances the heat transfer without causing similar increases in pressure drop and refrigerant charge, in both single-phase and two-phase applications. According to Cavallini et al. (1999), micro-fin tubes generally exhibit heat transfer enhancements, with respect to equivalent smooth tubes under the same operating conditions, from 80 to 140%, with pressure-loss increases from 20 to 80%.

The major geometrical parameters of the micro-fin tubes are the outer diameter, d_o, the root diameter, d_i, the fin tip diameter, d_t, the fin height, e, and the half-tip or half-apex angle, β. The other characteristic dimensions are the spiral (helix) angle, γ, of individual fins with respect to the tube axis, the number of fins, n_g, around the circumference in a tube, and the ratio of the surface area of the micro-fin tubes to that of a smooth tube if the micro-fins were removed. Fins may be rectangular or trapezoidal, or triangular in shape. Micro-fin tubes normally have a set of 50 to 70 spiral fins with the spiral angle from 6 to 35^{o}, fin-height range from 0.075 to 0.4 mm, and the apex angles, β,

tend to range between 25^{o} and 90^{o}. Figure 1.1 presents the characteristic geometrical parameters of inside micro-fin tubes.

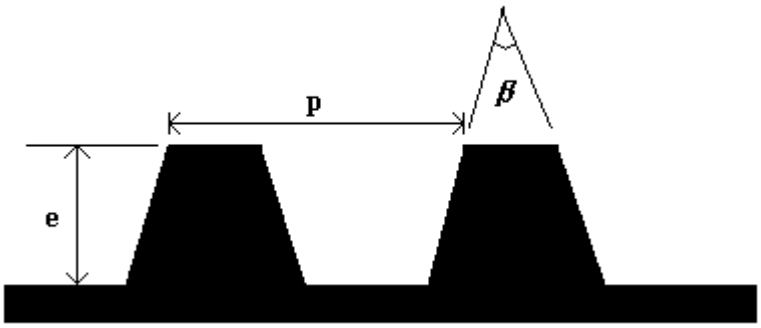

Figure 1.1 The characteristic geometrical parameters of inside micro-fin tubes

In the past decades, many researchers have studied and determined the performance of both smooth tubes and micro-fin tubes by using the chlorine-based pure refrigerants as the working fluids. A number of correlations have been successfully developed to predict the heat transfer coefficients of pure refrigerants flowing inside smooth tubes and micro-fin tubes. However, the implementation of Montreal Protocol in 1987 mandated the replacement of chlorine-containing pure refrigerants by the new alternative refrigerants, which have zero ozone depletion potential and reduced global-warming potential. These new refrigerants are pure HFC (Hydrofluorocarbon) refrigerants and mixtures of HFC refrigerants. However, the characteristics of these new alternatives are not clearly understood and only limited research have been conducted on them. Thus, the traditional well-established correlations for computing condensation heat transfer coefficients inside micro-fin tubes may be quite inadequate with the use of these new alternative refrigerants.

The main objective of this research is to carefully review the previous research concerning in-tube condensation for micro-fin tubes using pure refrigerants and refrigerant mixtures. Three existing condensation heat transfer models are further analyzed and evaluated to examine their validity with the available experimental data. A new condensation heat transfer model for both pure refrigerants and refrigerant mixtures is formulated. This new condensation heat transfer model is capable of predicting the condensation heat transfer coefficient for various types of HFC refrigerants flowing inside different geometry of micro-fin tubes.

CHAPTER II

LITERATURE SURVEY

Many mathematical models are available to predict the condensation heat transfer coefficients of alternative refrigerants or alternative refrigerant mixtures flowing inside micro-fin tubes. These models are categorized into empirical or semi-empirical models. Several models have been chosen for further study. Their abilities to predict the heat transfer coefficients are examined using the existing data. The following literature survey is divided into two parts: the correlations for pure refrigerants flowing inside micro-fin tubes and the correlations for refrigerant mixtures flowing inside micro-fin tubes.

Correlations for Pure Refrigerants Flowing inside Micro-Fin Tubes

Four correlations for pure refrigerants are studied and assessed. These four correlations are: Cavallini et al. (1999), Yu and Koyama (1998), Kedzierski and Goncalves (1999), and Shikazono et al. (1998).

Cavallini et al. (1999) developed a correlation to predict the heat transfer coefficients of pure refrigerants during condensation inside enhanced tubes. This model was modified from the Cavallini and Zecchin equation (Cavallini and Zecchin, 1971, 1974) for conventional smooth tubes. The Cavallini et al. (1999) model had been compared with the available pure refrigerant data for enhanced tubes. The model

achieved a mean absolution deviation of around 15% with more than 72% of the calculated values within ± 20% of the experimental data. Mean absolute deviation (*MAD*) is the average of the normalized difference between the predicted heat transfer coefficient and the experimental heat transfer coefficient. The Cavallini et al. (1999) correlation was validated on existing experimental data points for pure refrigerants R12, R22, R32, and R134a.

Cavallini and Zecchin (1971, 1974) developed the typical structure of a single-phase heat transfer correlation. However, its use was also suggested to predict the mean heat transfer coefficient over the whole tube length by referring to the arithmetic average of the inlet and outlet values of Reynolds number. The Cavallini et al. (1999) model has the form of a forced convection equation

$$Nu = \frac{h \cdot d_i}{k_l} = 0.05 \cdot \mathrm{Re}_{eq}^{\ 0.8} \cdot \mathrm{Pr}_l^{\frac{1}{3}} \cdot Rx^s (Bo \cdot Fr_l)^t \tag{2.1}$$

where

$$\mathrm{Re}_{eq} = \frac{4 \cdot m \cdot \left[(1-x) + x \cdot (\frac{\rho_l}{\rho_v})^{\frac{1}{2}} \right]}{\pi \cdot d_i \cdot \mu_l} \tag{2.2}$$

$$\mathrm{Pr}_l = \frac{\mu_l \cdot c_{pl}}{k_l} \tag{2.3}$$

$$Rx = \frac{1}{\cos(\gamma)} \cdot \left[\frac{2 \cdot e \cdot n_g \cdot \left(1 - \sin\left(\frac{\beta}{2} \right) \right)}{\pi \cdot d_i \cdot \cos(\frac{\beta}{2})} + 1 \right] \tag{2.4}$$

$$Fr_l = \frac{G^2}{\rho_l^{\ 2} \cdot g \cdot d_i} \tag{2.5}$$

$$Bo = \frac{g \cdot \rho_l \cdot e \cdot \pi \cdot d_i}{8 \cdot \sigma \cdot n_g} \tag{2.6}$$

In the Cavallini et al. (1999) correlation, two non-dimensional groups were introduced into the original equation to account for the heat transfer enhancement due to the micro-fins: the parameter, *Rx*, and the product of the Bond number, *Bo*, and the Froude number, Fr_l. The geometry enhancement parameter, *Rx*, is equal to the ratio between the exchange area enhancement factor for micro-fin tubes suggested by Hori and Shinohara (1991) and the cosine function of the spiral angle, γ; represents the effect of the heat transfer area increase. The Bond number, adopted from Webb (1988), is used to account for surface tension effects. The inside diameter at the fin tip of the tube is to be used as the geometrical parameter in the Reynolds number, Re_{eq}, and the Nusselt number, *Nu*. The exponents, *s*, and, *t*, are empirical constants derived by a best-fitting procedure from the available experimental data. There are some limits on the Cavallini et al. (1999) model. The operating range limits of the model is reported in Table 2.1:

Table 2.1 Operating Ranges of the Cavallini et al. (1999) Model

$\mathrm{Re}_{eq} > 15000$	$3 < \mathrm{Pr}_l < 6.5$	$0.3 < Bo \cdot Fr_l < 508$	$7^\circ < \gamma < 30^\circ$

Yu and Koyama (1998) developed a correlation to predict the condensation heat transfer coefficient of pure refrigerants inside micro-fin tubes. The correlation was formulated based on the Haraguchi et al. (1994) for conventional smooth tubes. They believed that the enhancement effect on the heat transfer coefficient inside micro-fin tubes was caused mainly by the heat transfer area enlargement ratio, η_A. The Yu and

Koyama (1998) correlation compared well (within 30%) with their own data for R134a, R123, and R22 and data from other sources. The experimental data of Koyama et al., Miyara et al., and Hayashi show a good agreement with the correlation. In the Yu and Koyama (1998) model, a new parameter, η_A, was introduced into the Haraguchi et al. (1994) model to account for the heat transfer enhancement effect due to the presence of micro-fins. The heat transfer area enlargement ratio, η_A, is an important parameter for pure refrigerant condensation in horizontal micro-fin tubes. The Yu and Koyama (1998) correlation is as follows:

$$Nu = \frac{h \cdot d_i}{k_l} = \left(Nu_F{}^2 + Nu_B{}^2\right)^{1/2} \tag{2.7}$$

where Nu_F is the forced convective condensation component and, Nu_B, is the natural convective condensation component.

Based on turbulent liquid-film theory, the forced convective condensation component is expressed as

$$Nu_F = 0.152 \cdot \left[0.3 + 0.1 \mathrm{Pr}_l{}^{1.1}\right](\Phi_v / X_{tt})\mathrm{Re}_l{}^{0.68} \tag{2.8}$$

where

$$\mathrm{Re}_l = \frac{G \cdot (1-x) \cdot d_i}{\mu_l} \tag{2.9}$$

$$\Phi_v = 1.1 + 1.3 \cdot \left[\frac{G \cdot X_{tt}}{\left[g \cdot d_i \cdot \rho_v \cdot (\rho_l - \rho_v)\right]^{0.5}}\right]^{0.35} \tag{2.10}$$

$$X_{tt} = \left(\frac{1-x}{x}\right)^{0.9}\left(\frac{\rho_v}{\rho_l}\right)^{0.5}\left(\frac{\mu_l}{\mu_v}\right)^{0.1} \tag{2.11}$$

The natural convective condensation component is written as

$$Nu_B = \frac{0.725}{\eta_A^{1/4}} \cdot H(\varepsilon) \cdot \left(\frac{Ga \cdot \mathrm{Pr}_l}{Ph_l} \right)^{0.25} \tag{2.12}$$

where

$$Ga = \frac{g \cdot \rho_l^{\,2} \cdot d_i^{\,3}}{k_l^{\,2}} \tag{2.13}$$

$$Ph_l = \frac{c_{pl}\left(T_{sat} - T_{wi}\right)}{i_{fg}} \tag{2.14}$$

$$\varepsilon^{-1} = 1 + \left[\frac{(1-x) \cdot \rho_v}{x \cdot \rho_l} \right] \cdot \left[0.4 + 0.6 \cdot \frac{\left[x \cdot \left(\frac{\rho_l}{\rho_v} \right) + 0.4 \cdot (1-x) \right]^{0.5}}{\left[x + 0.4 \cdot (1-x) \right]^{0.5}} \right] \tag{2.15}$$

$$H(\varepsilon) = \varepsilon + A\sqrt{\varepsilon}\left(1 - \sqrt{\varepsilon}\right) \tag{2.16}$$

$$A = 10(1-\varepsilon)^{0.1} - 8.0 \tag{2.17}$$

where *A* is a function of the void fraction, which is estimated by Smith's correlation (1970). $H(\varepsilon)$ is a modification for the difference of the condensed liquid film between the inner surface of the tube and the plate wall on which the Nusselt theory is suitable. The $H(\varepsilon)$ function only depends on the void fraction.

Kedzierski and Goncalves (1999) correlated their measured convective-condensation Nusselt numbers for all refrigerants to a single expression consisting of products of dimensionless numbers. They set up an experimental apparatus to measure the convective-condensation heat transfer inside micro-fin tubes. Four refrigerants were used in their experiment: R134a, R410a (R32/R125, 50/50% mass fraction), R125, and R32. The Kedzierski and Goncalves (1999) model is applicable to both pure refrigerants

and refrigerant mixtures flowing inside micro-fin tubes. The correlation predicted existing data from the literature acceptably well. However, the correlation poorly predicted the heat transfer performance of micro-fin tubes with cross-grooves.

The convective-condensation Nusselt numbers were correlated by applying the law of corresponding states philosophy presented by Cooper (1984). According to Cooper (1984), the fluid properties that govern nucleate pool boiling can be represented by a product of the reduced pressure (P_r/P_c), the acentric factor ($-\log_{10}(P_r/P_c)$), and other dimensionless variables to various powers. Thus, Kedzierski and Goncalves (1999) applied the reduced-pressure terms of Cooper (1984) and several other locally-evaluated terms to correlate the measured local Nusselt numbers for all the condensing flow conditions and refrigerants. Their expression has following form:

$$Nu = \frac{h \cdot d_h}{k_l} = 2.256 \cdot \mathrm{Re}^{\beta_1} \cdot Ja^{\beta_2} \cdot \mathrm{Pr}_l^{\beta_3} \cdot p_R^{\beta_4} \cdot \left(-\log_{10}\left(p_R\right)\right)^{\beta_5} \cdot S_v^{\beta_6} \qquad (2.18)$$

where $\beta_1 = 0.3032,\ \beta_2 = 0.232 \cdot x,\ \beta_3 = 0.393,\ \beta_4 = -0.578 \cdot x^2$

$\beta_5 = -0.474 \cdot x^2,\ \beta_6 = 2.531 \cdot x$

$$\mathrm{Re} = \frac{G \cdot d_h}{\mu_l} \qquad (2.19)$$

$$p_R = \frac{P}{P_{cr}} \qquad (2.20)$$

$$Ja = \frac{i_{fg}}{c_{pl} \cdot \Delta T} \qquad (2.21)$$

$$S_v = \frac{\left(\frac{\rho_l}{\rho_v}\right) - 1}{\left[x \cdot \left(\frac{\rho_l}{\rho_v} + 1 - x\right)\right]} \tag{2.22}$$

The Reynolds number, *Re*, the Jakob number, *Ja*, the Prandtl number, *Pr*, the reduced pressure drop, p_R, the dimensionless specific volume, S_v, and the quality, x, are all evaluated locally at the saturated condition. The hydraulic diameter of the micro-fin tube is used in their correlations and is written as

$$d_h = \frac{4 \cdot A_c \cdot \cos(\gamma)}{n_g \cdot S} \tag{2.23}$$

The measured condensation Nusselt numbers for the micro-fin tubes have been compared with the predictions from Equation (2.18). Equation (2.18) correlates 95% of the pure-component and near-azeotropic convective-condensation Nusselt numbers to within approximately ±21%.

Shikazono et al. (1998) proposed a general analytical model to predict the heat transfer coefficient of pure refrigerants inside horizontal micro-fin tubes. The model basically followed the smooth tube correlation proposed by Haraguchi et al. (1994). The correlation proposed by Haraguchi et al. (1994) is written as:

$$h = \left(h_B{}^2 + h_F{}^2\right)^{\frac{1}{2}} \tag{2.24}$$

The total condensation coefficient is composed of the contributions of film condensation, h_B, and forced convective condensation, h_F. Shikazono et al. (1998) utilized Equation 2.24 as the basis for the micro-fin tube model since they had incorporated the effects of micro-fins into the expression. For the micro-fin tube, the

film-condensation term was estimated from the product of the total unflooded area and the local enhancement factor, while the forced convective condensation was set equal to that of a smooth tube. The predicted results showed good agreement with experimental results, and that the effects of the parameters that characterize a micro-fin tube were well predicted for the first-order approximation.

Three assumptions were adopted for the Shikazono et al. (1998) modeling condensation in micro-fin tubes:

1. The film-condensation contribution is the essential mechanism in heat transfer enhancement of micro-fin tubes.
2. The unflooded area can be approximately determined from the balance of gravity and the surface tension force.
3. Film condensation effectively occurs in the region where the inner surface remains unflooded. Capillary forces pull the liquid from the bottom of the pipe to the grooved channel, and the vapor effectively condenses on the tip which remains unflooded.

Shikazono et al. (1998) believed that film condensation was a major contribution in micro-fin tubes. With the assumptions above, the film-condensation contribution was multiplied by an enhancement factor and the total condensation heat transfer coefficient is written as

$$h = \left[\left(c \cdot h_B \right)^2 + {h_F}^2 \right]^{\frac{1}{2}} \tag{2.25}$$

where c is the heat transfer enhancement factor.

The film condensation coefficient, h_B, and the forced convective condensation coefficient, h_F, in the Shikazono et al. (1998) model are written as

$$h_B = \frac{1}{\pi} \cdot \frac{k_l}{d_i} \cdot \int_0^{\phi_0} \frac{\sin(\phi)^{\frac{1}{3}}}{\left(2 \cdot \int_0^{\phi} \sin(\beta)^{\frac{1}{3}} \cdot d\beta\right)^{\frac{1}{4}}} d\theta \cdot \left(\frac{Ga \cdot \mathrm{Pr}}{Ph_l}\right)^{\frac{1}{4}} \tag{2.26}$$

$$h_F = 0.0152 \cdot \frac{k_l}{d_i} \cdot \left(1 + 0.6 \cdot \mathrm{Pr}^{0.8}\right) \cdot \frac{\Phi_v}{X_{tt}} \cdot \mathrm{Re}_l^{\,0.77} \tag{2.27}$$

where $$\Phi_v = 1 + 0.5 \cdot \left[\frac{G}{\sqrt{g \cdot d_i \cdot \rho_v \cdot (\rho_l - \rho_v)}}\right]^{0.75} \cdot X_{tt}^{\,0.35} \tag{2.28}$$

The Martinelli parameter, X_{tt}, is calculated by Equation (2.11), the phase change number, Ph_l, is found using Equation (2.14), and the Galilleo number, Ga, is computed by Equation (2.13).

In the Shikazono et al. (1998) model, the heat transfer enhancement factor, c, is written as a ratio of the unflooded area of the micro-fin tube and that of the smooth tube:

$$c = \frac{c_1 \cdot A_f + c_2 \cdot A_i}{2 \cdot \phi_0 \cdot R_r \cdot (b + t)} \tag{2.29}$$

where

$$A_f = (2\cdot\phi_0\cdot R_0\cdot t) + 2\cdot\int_0^{\phi_{f1}} \frac{\left[R_r - a + a\cdot\sin\left(\frac{\beta}{2}\right)\right]^2 - {R_0}^2}{\cos\left(\frac{\beta}{2}\right)} d\phi$$
$$+ 2\cdot\int_{\phi_{f1}}^{\phi_{f2}} \frac{\left[R_r - \frac{a\cdot\cos\left(\frac{\beta}{2}\right) - \frac{s}{2}}{\tan\left(\frac{\beta}{2}\right)}\right]^2 - {R_0}^2}{\cos\left(\frac{\beta}{2}\right)} d\phi \qquad (2.30)$$

$$A_i = 2\cdot\int_0^{\phi_{f1}} R_0\cdot\left[s - a\cdot\cos\left(\frac{\beta}{2}\right) + \left[\left(a - a\cdot\sin\left(\frac{\beta}{2}\right)\right)\cdot\tan\left(\frac{\beta}{2}\right)\right]\right] d\phi \qquad (2.31)$$

where c_1 and c_2 are the weighing factors for the two unflooded areas, A_f, and A_i. Since c must asymptote to unity when fin pitch tends to infinity, the constant c_2 is determined as c_2=1. The coefficient c_1 is assumed to be a function of the curvature at the fin tip since the heat transfer enhancement factor should depend on the surface tension force that acts on the condensate at the fin tip. The coefficient c_1 is given as

$$c_1 = 1 + 6\cdot\frac{\beta - \pi}{\left(\frac{2\cdot\pi}{9} - \pi\right)} \qquad (2.32)$$

The predicted results from Shikazono et al. (1998) model show good agreement with experimental results for three different refrigerants (R22, R13a, and R32). The dependence of the condensation coefficient on quality is predicted fairly well. The Shikazono et al (1998) model showed that the forced-convection condensation contribution has only a minor effect on the total condensation coefficient for micro-fin

tubes. The prediction from the film-condensation contribution only gave fairly good results for the flow rate range tested.

Correlations for Refrigerant Mixtures Flowing inside Micro-Fin Tubes

The Cavallini et al. (1999) model was originally developed for pure refrigerants inside micro-fin tubes. The model was expanded for zeotropic refrigerant mixtures by using the Silver (1947) and Bell and Ghaly (1973) procedure to account for the mass transfer thermal resistance between the liquid and vapor phases. There is a non-equilibrium condition between a vapor and a liquid phase caused by the slip velocity between the phases. The procedure is written as below:

$$h_m = \left[\frac{1}{h} + \frac{\frac{\delta Q_{SV}}{\delta Q_T}}{h_v} \right]^{-1} \tag{2.33}$$

$$\frac{\delta Q_{SV}}{\delta Q_T} \approx x \cdot c_{pv} \cdot \left(\frac{\Delta TG}{i_{fg\_m}} \right) \tag{2.34}$$

where h is the heat transfer coefficient from the Cavallini et al. (1999) correlation (Eqs.(2.1-2.6)) for pure refrigerants with the properties of the refrigerant mixture (liquid and vapor at their equilibrium composition), h_v is the heat transfer coefficient of the vapor phase flowing alone in the duct, ($\delta Q_{SV}/\delta Q_T$) is the ratio between the sensible heat duty removed by cooling the vapor and the total heat flow rate exchanged, and i_{fg_m} is the enthalpy of isobaric condensation of the mixture. The heat transfer coefficient for the vapor phase only is determined from the Dittus-Boelter equation. For a maximum temperature glide, ΔTG, around 7-8^{o}C, this ratio is often assumed to be constant. The

temperature glide is defined as the temperature difference between the bubble-point temperature and the dew-point temperature of the refrigerant mixtures. The model shows an absolute mean deviation of around 15% compares with most of the available experimental data.

The Kedzierski and Goncalves (1999) model is an empirical mathematical model. They had collected the convective-condensation heat transfer data for R410a inside micro-fin tubes as well. The measured convective-condensation Nusselt numbers for all of the tested refrigerants were correlated to a single expression consisting of products of dimensionless parameters. The correlation shown in Equation 2.18 is applicable to both pure refrigerants and refrigerant mixtures. The correlation predicts existing condensation Nusselt number datas for micro-fin tubes from the literature acceptably well.

CHAPTER III

CONDENSATION HEAT TRANSFER MODELS

Three correlations for condensation inside micro-fin tubes are further evaluated. The three correlations are the Cavallini et al. (1999) model, the Yu and Koyama (1998) model, and the Kedzierski and Goncalves (1999) model. The Shikazono et al. (1998) model is not considered for further evaluation because of the details to compute the recommended enhancement factor for micro-fin tubes in most of the available experimental data sets are insufficient. The Cavallini et al. (1999), the Yu and Koyama (1998), and the Kedzierski and Goncalves (1999) models are validated by using the available experimental data.

Experimental Database

To validate the existing condensation heat transfer models, the available experimental data for pure refrigerants and refrigerant mixtures flowing inside micro-fin tubes were collected from the published papers. A database was created for both pure refrigerants and refrigerant mixtures experimental data. Tables 3.1 and 3.2 present the collected pure refrigerants experimental data for flow inside micro-fin tubes. Tables 3.3 and 3.4 contain the experimental data for refrigerant mixtures. Tables 3.1 and Table 3.3 list the flow conditions (saturation pressure, P_{sat}, saturation temperature, T_{sat}, heat flux, q, mass flux, G, and mean vapor quality, x). Table 3.2 and Table 3.4 delineate the tube

geometries (outer tube diameter, d_o, minimum wall thickness, *th*, fin height, *e*, number of fins, n_g, helix angle, γ, apex angle, β, and the heated test section length, *L*).

Table 3.1 Flow Conditions for Pure Refrigerants Flowing inside Micro-Fin Tubes

Reference	Runs	Fluid	P_{sat} (kPa)	T_{sat} (°C)	q (kW/m^2)	G (kg/m^2-s)	x (mean)
Bogart and Thors (1999)	17	R22		40.6		200 – 800	0.80 – 0.10
Chamra et al. (1996)	24	R22		24		40 – 200	0.80 – 0.20
Ebisu et al. (1994)	7	R22		50		85 – 530	0.80 – 0.10
Eckels et al. (1991)	20 20	R134a R12		30 – 50		130 – 420	0.88 – 0.05
Eckels et al. (1998a)	12	R134a	1010	40		80 – 400	0.88 – 0.05
Eckels et al. (1998b)	16	R134a	1010	40		120 – 400	0.88 – 0.05
Eckels et al. (1999)	15 19	R22 R134a		40		100 – 630	0.95 – 0.05
Goto et al. (1995)	52	R22		40		48 – 598	0.90 – 0.10
Hitachi Cable (1987)	12	R22	1540	40		100 – 300	0.50
Muzzio et al. (1995)	24	R22		35		80 – 410	0.50
Muzzio et al. (1998)	37	R22	1350	35		80 – 410	0.80 – 0.10
Schlager L.M. (1988)	27	R22	1543 – 1561	40.2-40.7		120 – 405	0.898 – 0.092
Schlager et al. (1989)	15	R22		39 – 42		180 – 550	0.90 – 0.10
Shinohara and Tobe (1985)	9	R22	1400			100 – 300	0.60
Tang et al. (2000)	35	R22 R134a		40 40		250 – 850 250 – 750	0.50 0.50
Uchida et al. (1996)	6	R22		35	2.3 – 37.2	100 – 500	0.90 – 0.10
Yasuda et al. (1990)	17	R22		40		100 – 350	0.60

Table 3.2 Tube Geometries for Pure Refrigerants Flowing inside Micro-Fin Tubes

Reference	Tube Material	d_o (mm)	th (mm)	e (mm)	n_g	γ (°)	β (°)	L (m)
Bogart and Thors (1999)	Copper	9.53	0.33	0.203	60	18	50	3.66
Chamra et al. (1996)	Copper	15.88	0.5	0.35	74-80	15 – 27	30	2.44
Ebisu et al. (1994)	Copper	7.0	0.3	0.18	50	18	40	3.0
Eckels et al. (1991)	Copper	9.52	0.40	0.20	60	15	50	3.67
Eckels et al. (1998a)	Copper	9.52 12.70	0.30 0.40	0.2 0.2	60 60	18 17	50 50	3.66 3.66
Eckels et al (1998b)	Copper	9.52	0.30	0.20	60	17	50	3.66
Eckels et al. (1999)	Copper	9.53 15.88 7.94	0.305 0.635 0.3	0.203 0.305 0.203	60 60 50	18 27 18	51 45 57	3.78 3.81 3.78
Goto et al. (1995)	Copper	9.52 6.35	0.27 0.27	0.17 0.14	60 55	25 16	50	1.0
Hitachi Cable (1987)	Copper	9.50-9.52	0.28 0.29	0.2 – 0.21	60	17 18	40 – 53	0.50
Muzzio et al. (1995)	Copper	9.52	0.3 0.34	0.15– 0.23	54-65	18 25	40 – 90	2.6
Muzzio et al. (1998)	Copper	9.52	0.30	0.195	54	18	40	2.24
Schlager L.M. (1988)	Copper	9.52	0.40 0.50	0.2 0.38	60 21	18 30	50 10	3.67
Schlager et al. (1989)	Copper	9.52	0.30	0.2 – 0.15	60	18 – 25	40	3.67
Shinohara and Tobe (1985)	Copper	9.52	0.30	0.12– 0.20	60 65	7 – 25	35, 50, 90	0.50
Tang et al. (2000)	Copper	9.52	0.36	0.2	60 72	0 18	15 40	2.83
Uchida et al. (1996)	Copper	7.0	0.30	0.163	60	18	40	1.09
Yasuda et al. (1990)	Copper	9.52 7.94	0.30	0.2 – 0.25	60 50	18 30	40	3.05

Table 3.3 Flow Conditions for Refrigerant Mixtures Flowing inside Micro-Fin Tubes

Reference	Runs	Fluid	P_{sat} (kPa)	T_{sat} (°C)	q (kW/m^2)	G (kg/m^2-s)	x (mean)
Bogart and Thors (1999)	11	R410a		40.6		200 – 850	0.80 – 0.10
Ebisu et al. (1994)	7	R32+ R134a		50		85 – 530	0.80 – 0.10
Ebisu et al. (1998)	4	R407c	1974.4	47	7.5	140 – 400	0.10 – 0.70
Eckels et al. (1999)	13 9	R410a R407c		40 40		100 – 630	0.95 – 0.05
Goto et al. (1995)	28	R407c		40		70 – 600	0.50
Jeong et al. (2000)	21	R410a		31		90 – 210	0.10 – 0.90
Tang et al. (2000)	37	R410a		40		250 – 850	0.50

Table 3.4 Tube Geometries for Refrigerant Mixtures Flowing inside Micro-Fin Tubes

Reference	Tube Material	d_o (mm)	th (mm)	e (mm)	n_g	γ (°)	β (°)	L (m)
Bogart and Thors (1999)	Copper	9.53	0.33	0.203	60	18	50	3.66
Ebisu et al. (1994)	Copper	7.0	0.30	0.18	50	18	40	3.0
Ebisu et al. (1998)	Copper	7.0	0.25	0.18	50	18	40	0.54
Eckels et al. (1999)	Copper	9.53 15.88 7.94	0.305 0.635 0.3	0.203 0.305 0.203	60 60 50	18 27 18	51 45 57	3.78 3.81 3.78
Goto et al. (1995)	Copper	9.52 6.35	0.36 0.34	0.17 0.14	60 55	25 16	50 50	1.0 1.0
Jeong et al. (2000)	Copper	9.52	0.30	0.20	60	18	53	0.63
Tang et al. (2000)	Copper	9.52	0.36	0.2	60 72	0 18	15 40	2.83

Most of the experimental data were presented at constant vapor quality with varying mass flux. The Jeong et al. (2000) experimental data were presented at constant mass flux with varying vapor quality. Almost all the experimental data were collected

from the graphs inserted in the published technical papers except the experimental data from Schlager (1988), which was collected from the tables presented in his thesis. The extraction of the data points from the graphs was accomplished with the aid of computer software, Digitize XY Data (DigXY). A graph containing experimental data was first scanned in bitmap format. Then, the experimental data points were analyzed and collected by the DigXY.

The thermodynamic and transport properties for pure refrigerants and refrigerant mixtures are obtained from REFPROP 6.01 computer software. REFPROP 6.01 is capable of generating thermodynamic and transport properties for pure refrigerants and mixture refrigerants at specified saturation conditions (saturation temperature or saturation pressure).

The mean absolute deviation (*MAD*) is set as the criterion to determine the effectiveness of a heat transfer model. *MAD* is defined as the average of the normalized difference between the predicted heat transfer coefficient and the experimental heat transfer coefficient.

$$MAD = \frac{1}{N} \cdot \sum \frac{\left| h_{\exp erimental} - h_{predicted} \right|}{h_{\exp erimental}} \tag{3.1}$$

The heat transfer model is considered acceptable if the achieved *MAD* value is less than 30%.

Cavallini et al. (1999) Heat Transfer Model for Pure Refrigerants

The Cavallini et al. (1999) model is a modified heat transfer model for condensation inside micro-fin tubes based on the Cavallini and Zecchin equation for smooth tubes. The condensation heat transfer coefficient for pure refrigerant is written as

$$h = \frac{Nu \cdot k_l}{d_i} = \frac{0.05 \cdot k_l \cdot \mathrm{Re}_{eq}^{0.8} \cdot \mathrm{Pr}_l^{\frac{1}{3}} \cdot Rx^s (Bo \cdot Fr)^t}{d_i} \tag{3.2}$$

The exponents *s* and *t* were derived by a best-fitting procedure from the available experimental data. The exponents for the Cavallini et al. (1999) model are listed in Table 3.5.

Table 3.5 Exponents in the Cavallini et al. (1999) Model

	Low-fins ($e/d_i \geq 0.04$)	Micro-fins ($e/d_i < 0.04$)	Cross-grooved
s	1.40	2.00	2.10
t	-0.08	-0.26	-0.26

The Cavallini et al. (1999) model is validated using 20 pure refrigerant data sets from 12 different researchers with a total of 414 data points. The tested refrigerants include R22, R134a, and R12. A majority of these experiments used R22 as the working fluid. Table 3.6 shows the range of the experimental conditions for all the data sets used to validate the Cavallini et al. (1999) model.

Table 3.6 Range of the Experimental Conditions

Experimental Condition	Range
Mass flux (kg/m^2-s)	40 – 850
Mean vapor quality	0.05 – 0.90
Outer tube diameter (mm)	8.00 – 1600
Maximum tube thickness (mm)	0.3 – 1.0
Fin height (mm)	0.12 – 0.30
Number of fins	21 – 75
Helix angle (°)	7 – 30
Apex angle (°)	0 – 90

The experimental data and the Cavallini et al. (1999) model are computed in MathCAD environment. A MathCAD property file is programmed with an interpolation function (cubic spline function) such that it will obtain the required refrigerant properties from the property table (text files) generated from REFPROP 6.01. A sample MathCAD data file, a model file, and a property file are in Appendix A. Another worksheet is created in MathCAD to extract the required information and generate the necessary results. A sample MathCAD calculation file for the Cavallini et al. (1999) model is presented in Appendix A.

The Cavallini et al. (1999) model is first validated with the available R22 data. There are total of 14 sets of experimental data that use R22 as working fluid. The prediction results for these R22 data sets are shown in Figure 3.1. The symbols indicate the experimental data points from different sources. The diagonal solid line shows a perfect match for the predicted heat transfer coefficient and the experimental heat transfer coefficient. The dashed lines represent the ±30% mean absolute deviation lines.

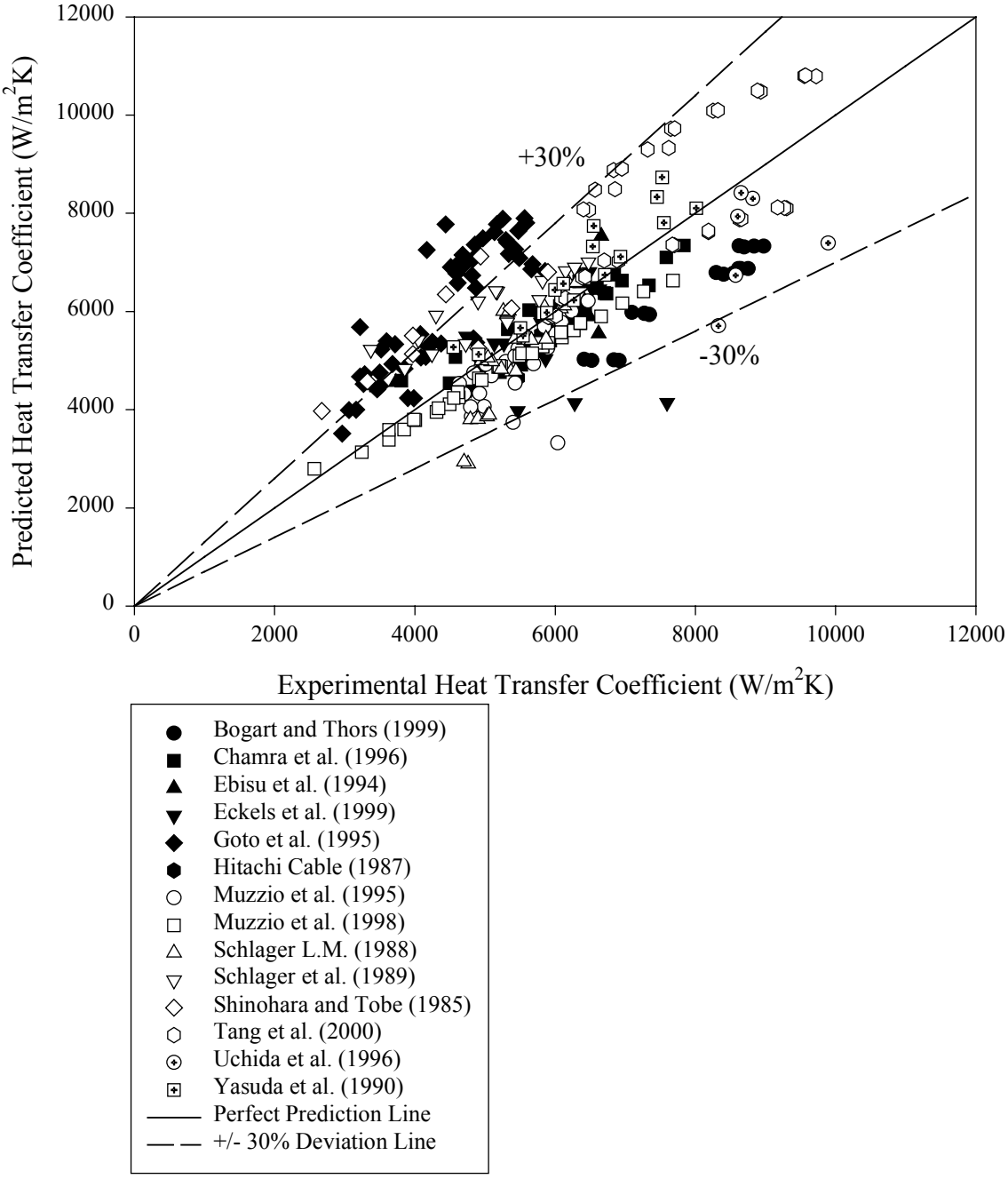

Figure 3.1 Cavallini et al. (1999) Model for all the Available R22 Data Sets

Figure 3.1 shows that the model successfully predicts most of the R22 data sets within 30% of the mean absolute deviation value. However, the Cavallini et al. (1999)

model fails to predict the R22 data sets from Shinohara and Tobe (1985) and Goto et al. (1995). Generally, the model over-predicts the R22 experimental data from Goto et al. (1995). Large deviations are observed as the mass flux increases. However, the model exhibits a consistent condensation heat transfer coefficient variation as the mass flux increases.

The Cavallini et al. (1999) model is further tested with the five R134a data sets. The prediction results for these R134a data sets are illustrated in Figure 3.2.

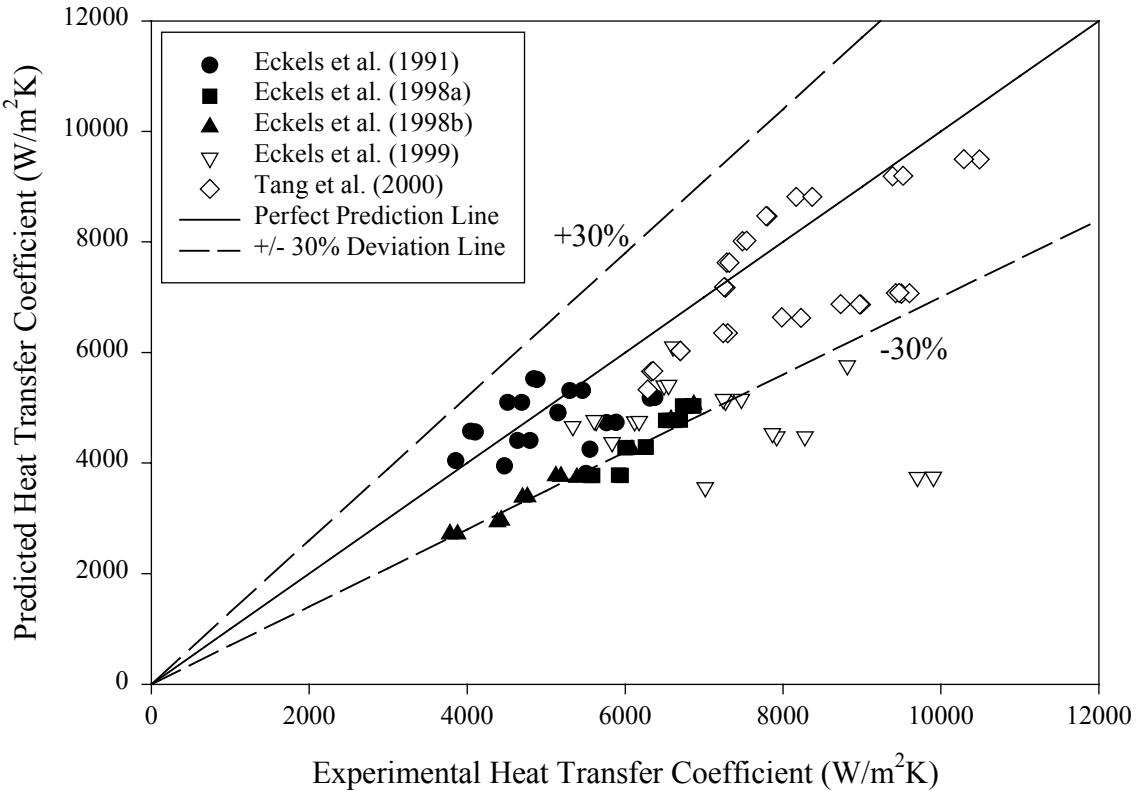

Figure 3.2 Cavallini et al. (1999) Model for all the Available R134a Data Sets

Figure 3.2 reflects that the Cavallini et al. (1999) model successfully predicts the R134a experimental data from Tang et al. (2000) and Eckels et al. (1991). The R134a

data sets of Eckels et al. (1998a), Eckels et al. (1998b), and Eckels et al. (1999) are predicted fairly well with mean absolute deviation about 30%. However, the model under predicts most of the Eckels et al. (1999) R134a data points.

Beside the R134a data sets, the R12 data set from Eckels et al. (1991) is also used for validation process. The model achieves the mean absolute deviation of 17% as shown in Figure 3.3.

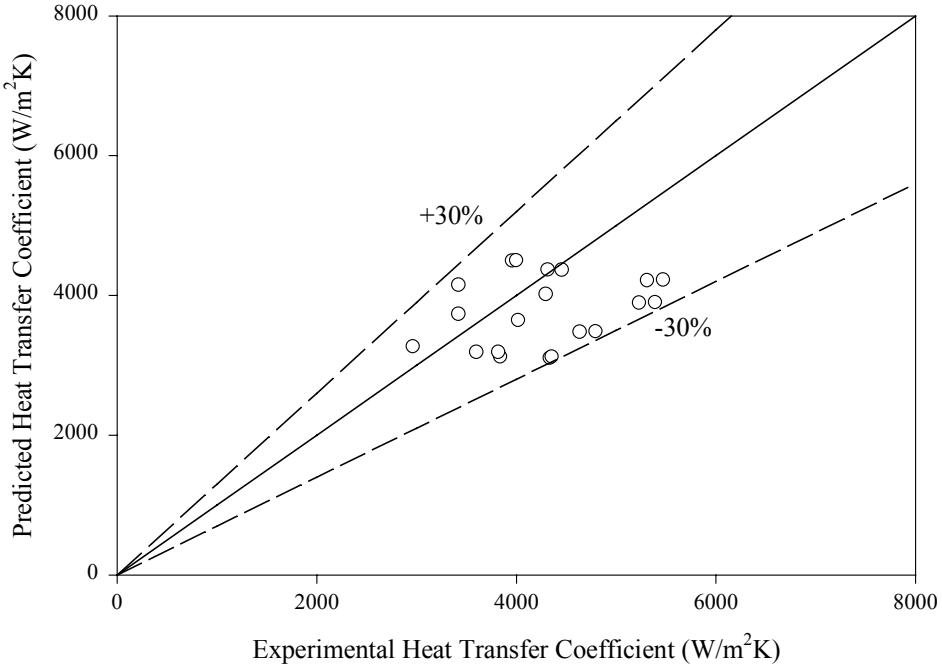

Figure 3.3 Cavallini et al. (1999) Model for the Eckels et al. (1991) R12 Data Set

Table 3.7 summarizes the mean absolute deviations achieved by Cavallini et al. (1999) model for the pure-refrigerant data sets. The prediction results for the Hitachi Cable (1987), Muzzio et al. (1998), Schlager (1988), Shinohara and Tobe (1985) and Yasuda et al. (1990) R22 data sets agree closely with the results claimed by Cavallini et al. (1999).

Table 3.7 Mean Absolute Deviation (*MAD*) Between the Experimental Data and the Prediction Results from the Cavallini et al. (1999) Pure-Refrigerant Model

No.	Reference	Refrigerant	MAD value (%)
1	Bogart and Thors (1999)	R22	19.9
2	Chamra et al. (1996)	R22	6.1
3	Ebisu et al. (1994)	R22	11.2
4	Eckels et al. (1991)	R134a R12	21.5 16.9
5	Eckels et al. (1998a)	R134a	29.1
6	Eckels et al. (1998b)	R134a	29.5
7	Eckels et al. (1999)	R22 R134a	11.4 30.7
8	Goto et al. (1995)	R22	37.3
9	Hitachi Cable (1987)	R22	8.0
10	Muzzio et al. (1995)	R22	10.3
11	Muzzio et al. (1998)	R22	7.7
12	Schlager L.M. (1988)	R22	10.7
13	Schlager et al. (1989)	R22	21.4
14	Shinohara and Tobe (1985)	R22	30.7
15	Tang et al. (2000)	R22 R134a	13.8 12.2
16	Uchida et al. (1996)	R22	15.8
17	Yasuda et al. (1990)	R22	6.4

Overall, the Cavallini et al. (1999) pure refrigerant model is considered successful of predicting most of the experimental data sets within 30% of mean absolute deviation. However, the model fails to predict the Goto et al. (1995) R22 data set. The achieved mean absolute deviation for this data set is 37%.

Yu and Koyama (1998) Heat Transfer Model for Pure Refrigerants

The Yu and Koyama (1998) model is a modified correlation for condensation inside micro-fin tubes based on the Haraguchi et al. (1994) model for smooth tubes. Yu and Koyama found that the condensation heat transfer coefficients in a horizontal tube are about two times higher than those of a smooth tube with the same inner diameter. They believed that the enhancement effect on heat transfer coefficients was mainly caused by the increased of heat transfer area. The Yu and Koyama (1998) model was developed for the condensation in micro-fin tube and is written as

$$Nu = \frac{h \cdot d_i}{k_l} = \left(Nu_F{}^2 + Nu_B{}^2\right)^{0.5} \tag{3.3}$$

where

$$Nu_F = 0.152 \cdot \left(\frac{\Phi_v}{X_{tt}}\right) \cdot \left(0.3 + 0.1 \cdot \mathrm{Pr}_l{}^{1.1}\right) \tag{3.4}$$

$$Nu_B = \frac{0.725}{\eta_A{}^{1/4}} \cdot H(\varepsilon) \cdot \left(\frac{Ga \cdot \mathrm{Pr}_l}{Ph_l}\right)^{0.25} \tag{3.5}$$

The Yu and Koyama (1998) model introduced a new dimensionless parameter, η_A, which is the enlargement ratio of heat transfer area. This new parameter is used to account for the enhancement in heat transfer surface due to the presence of micro-fins.

The Yu and Koyama (1998) model is evaluated using nine pure-refrigerant data sets, which include R22, R134a, and R12. These data sets were collected from five different researchers. The validation process is similar to that in the previous section. A sample model file is in Appendix B.

The Yu and Koyama (1998) model is first validated with the available R22 data sets. The prediction results for these R22 data sets are presented in Figure 3.4.

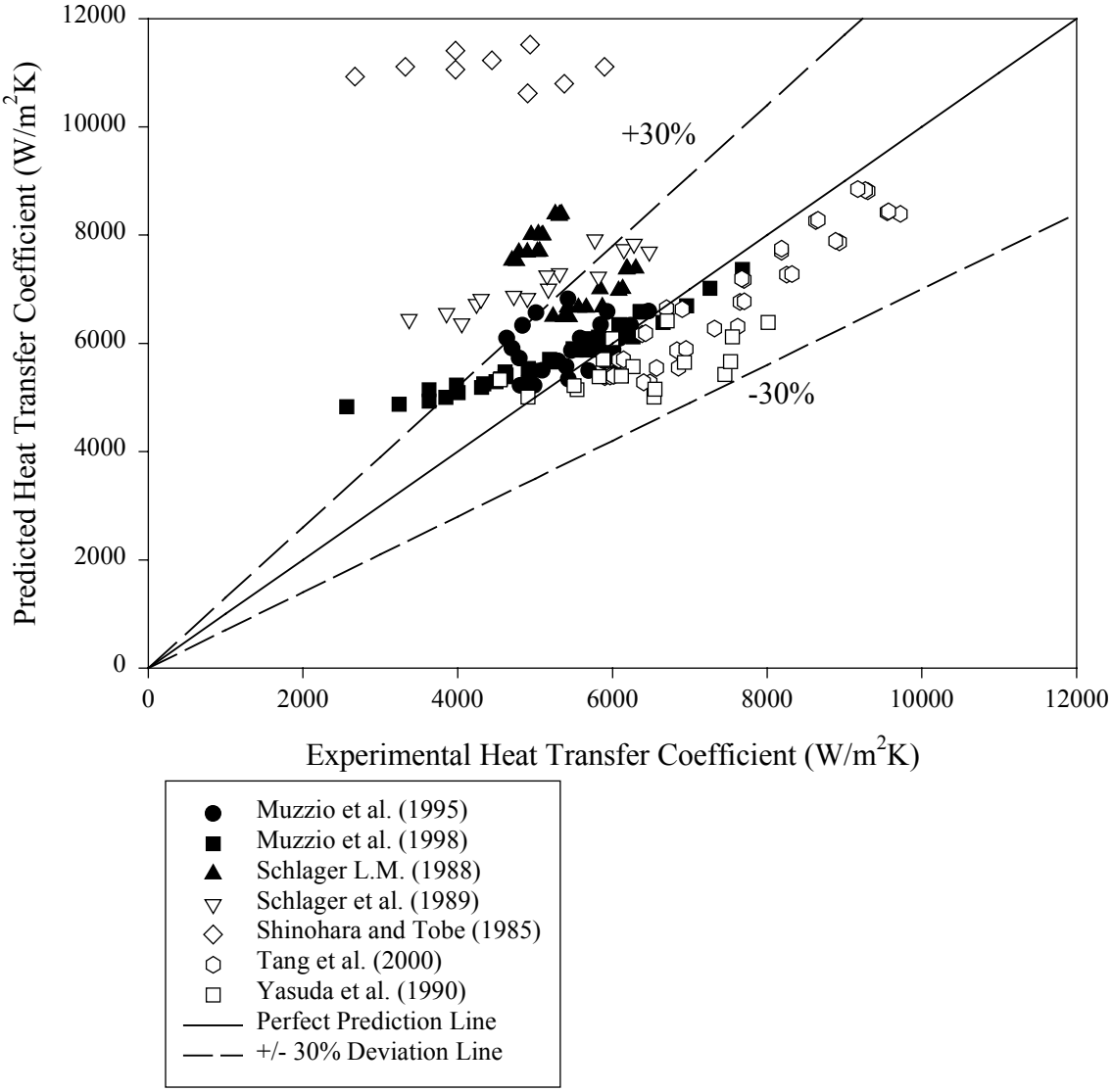

Figure 3.4 Yu and Koyama (1998) Model for all the Available R22 Data Sets

The Yu and Koyama (1998) model predicts most of the R22 data within 30% of mean absolute deviation values. However, the model over predicts the R22 data sets from Schlager L.M. (1988), Schlager et al. (1989), and Shinohara and Tobe (1985) with mean absolute deviations over 35%. The model predicts the correct trend of the heat transfer coefficient variation with mass flux increases.

The Yu and Koyama (1998) model is further evaluated with the R134a data. The prediction results for two R134a data sets are shown in Figure 3.5. The Yu and Koyama (1998) model successfully predicts the R134a data sets from Tang et al. (2000) and Eckels et al. (1991) with achieved mean absolute deviations within 30%. However, the model over predicts some of the experimental data points of Eckels et al. (1991) R134a data set.

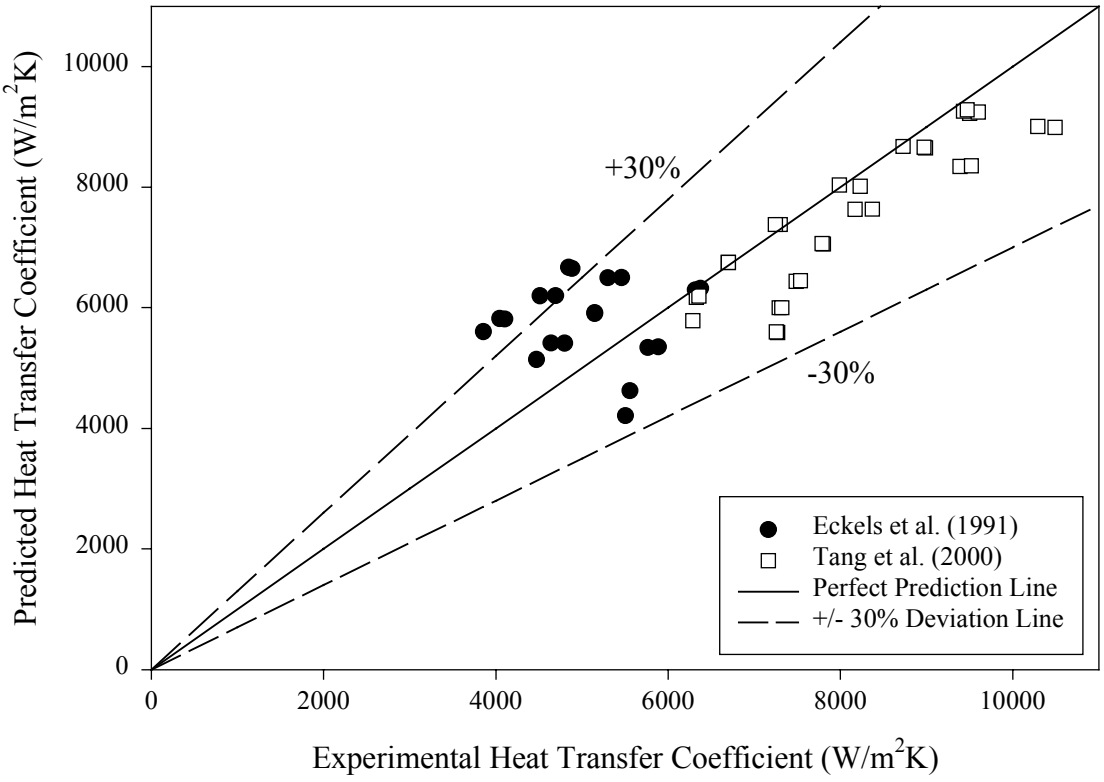

Figure 3.5 Yu and Koyama (1998) Model for all the Available R134a Data Sets

Figure 3.6 illustrates the prediction results of the Yu and Koyama (1998) model for the Eckels et al. (1991) R12 data set. The model achieves a mean absolute deviation of 25%, but the model over-predicts some of the experimental data points.

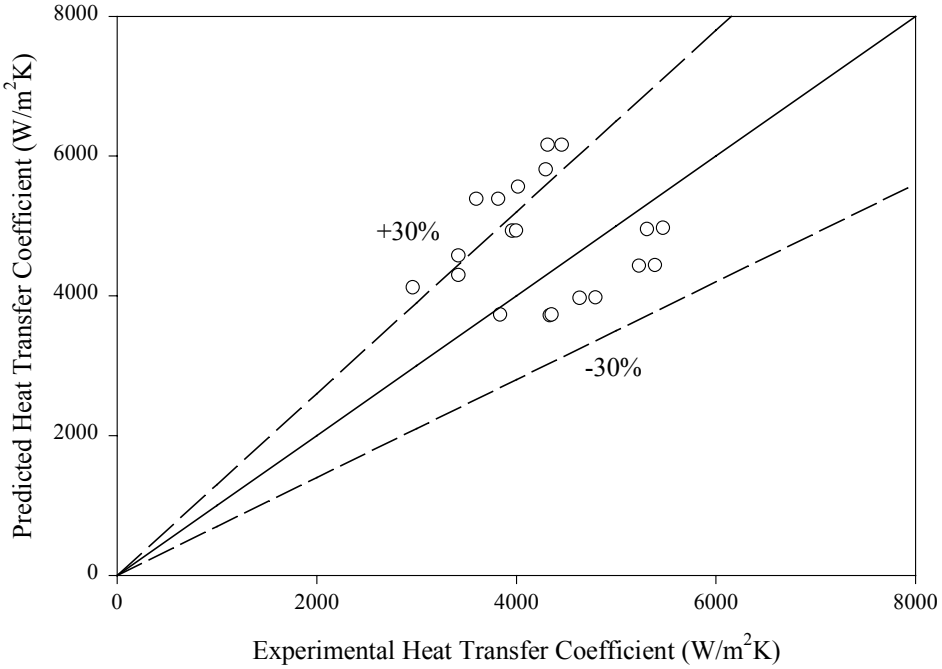

Figure 3.6 Yu and Koyama (1998) Model for the Eckels et al. (1991) R12 Data Set

Table 3.8 summarizes the mean absolute deviations of the Yu and Koyama (1998) model for the nine different data sets that were previously discussed. The Yu and Koyama (1998) model predicts most of the pure refrigerant data sets within 30%. However, the model over predicts the R22 data sets of Schlager with over 35% mean absolute deviations. The Shinohara and Tobe (1985) R22 data are also over predicted with very high mean absolute deviations. The Yu and Koyama (1998) model is limited because some of the available experimental data sets do not provide enough details to compute the parameter, η_A, which accounts for the heat transfer enhancement due to the presence of the micro-fins. Overall, the Yu and Koyama (1998) model predicts most of the pure-refrigerant data sets fairly well, within a 30% mean absolute deviation.

However, the proposed parameter, η_A, limits the usage of the model because lack of information in most of the experimental data sets to calculate this parameter.

Table 3.8 Mean Absolute Deviation (*MAD*) Between the Experimental Data and the Prediction Results from the Yu and Koyama (1998) Pure-Refrigerant Model

No.	Reference	Refrigerant	MAD value (%)
1	Eckels et al. (1991)	R134a R12	22.4 25.1
2	Muzzio et al. (1995)	R22	11.0
3	Muzzio et al. (1998)	R22	15.2
4	Schlager L.M. (1988)	R22	38.9
5	Schlager et al. (1989)	R22	44.3
6	Shinohara and Tobe (1985)	R22	166.8
6	Tang et al. (2000)	R22 R134a	9.7 7.8
7	Yasuda et al. (1990)	R22	13.2

Kedzierski and Goncalves (1999) Heat Transfer Model for Pure Refrigerants and Refrigerant Mixtures

The Kedzierski and Goncalves (1999) model correlates the measured convective-condensation Nusselt numbers for the refrigerants used in their experiment with a single expression consisting of the products of dimensionless parameters. They were refrigerants R134a, R410a, R125, and R32. The Kedzierski and Goncalves (1999) model is an empirical correlation that can be applied to both pure refrigerants and refrigerant mixtures. The Kedzierski and Goncalves (1999) correlation is written as

$$Nu = \frac{h \cdot d_h}{k_l} = 2.256 \cdot \mathrm{Re}^{\beta_1} \cdot Ja^{\beta_2} \cdot \mathrm{Pr}_l^{\beta_3} \cdot p_R^{\beta_4} \cdot \left(-\log_{10}\left(p_R\right)\right)^{\beta_5} \cdot S_v^{\beta_6} \qquad (3.6)$$

where $\beta_1 = 0.303$, $\beta_2 = 0.232 \cdot x$, $\beta_3 = 0.393$, $\beta_4 = -0.578 \cdot x^2$,

$\beta_5 = -0.474 \cdot x^2$, $\beta_6 = 2.531 \cdot x$

The Kedzierski and Goncalves (1999) model is first evaluated with twenty pure refrigerant experimental data sets, which include refrigerants R22, R134a, and R12. A sample model file is in Appendix C. The validity of the Kedzierski and Goncalves (1999) model is examined with fourteen R22 data sets. The prediction results for these available R22 data sets are presented in Figure 3.7.

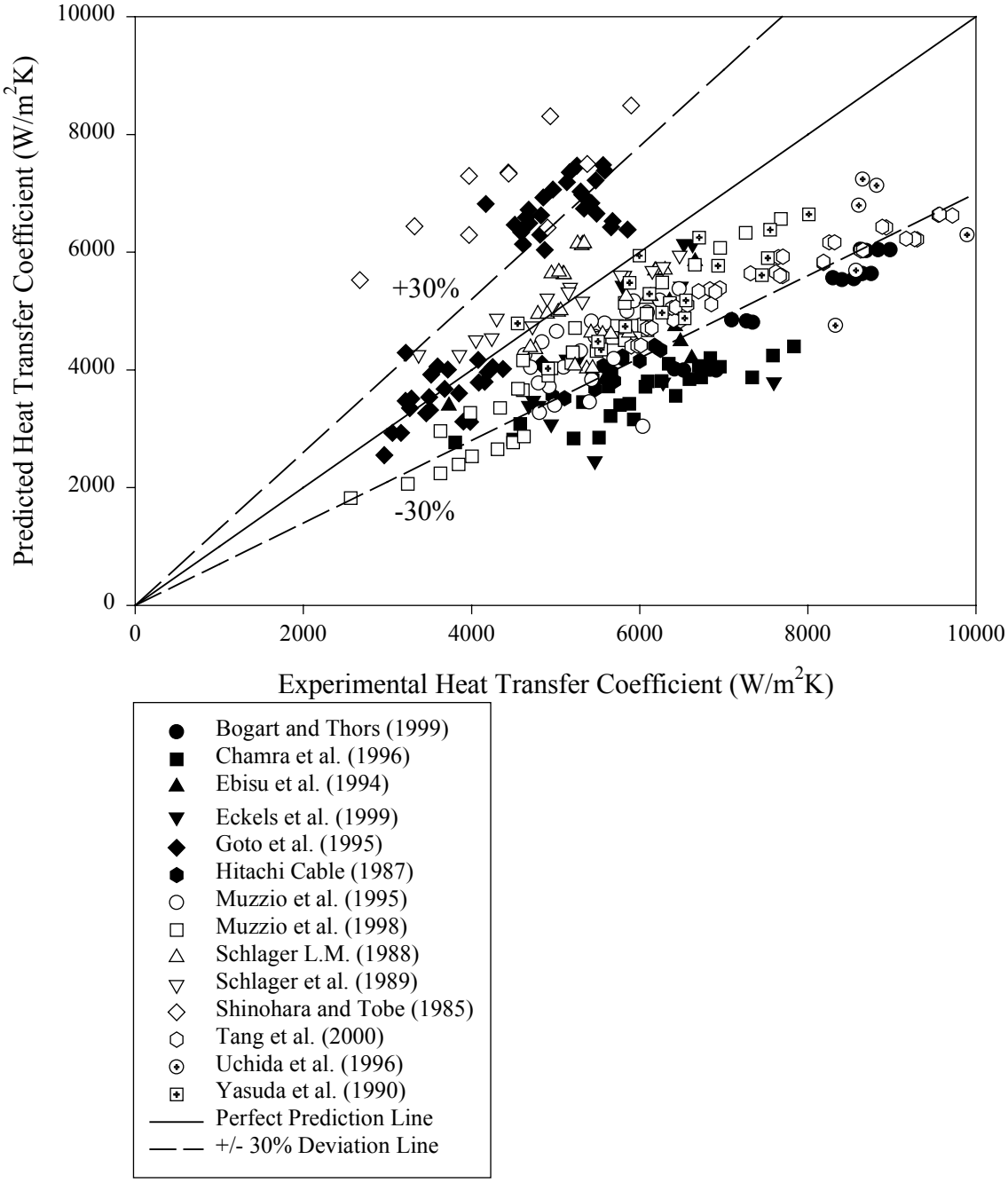

Figure 3.7 Kedzierski and Goncalves (1999) Model for all the Available R22 Data Sets

Figure 3.7 shows that the model successfully predicts most of the R22 data with mean absolute deviations within 30%. However, the model under predicts the R22 data sets from Bogart and Thors (1999), Uchida et al. (1996), and Chamra et al. (1996). The model fails to predict the Shinohara and Tobe (1985) R22 data set. Some of the Goto et al. (1995) R22 data points are over predicted as well.

Besides the R22 data sets, the Kedzierski and Goncalves (1999) model is also validated with five R134a data sets. The prediction results for these R134a data sets are illustrated in Figure 3.8.

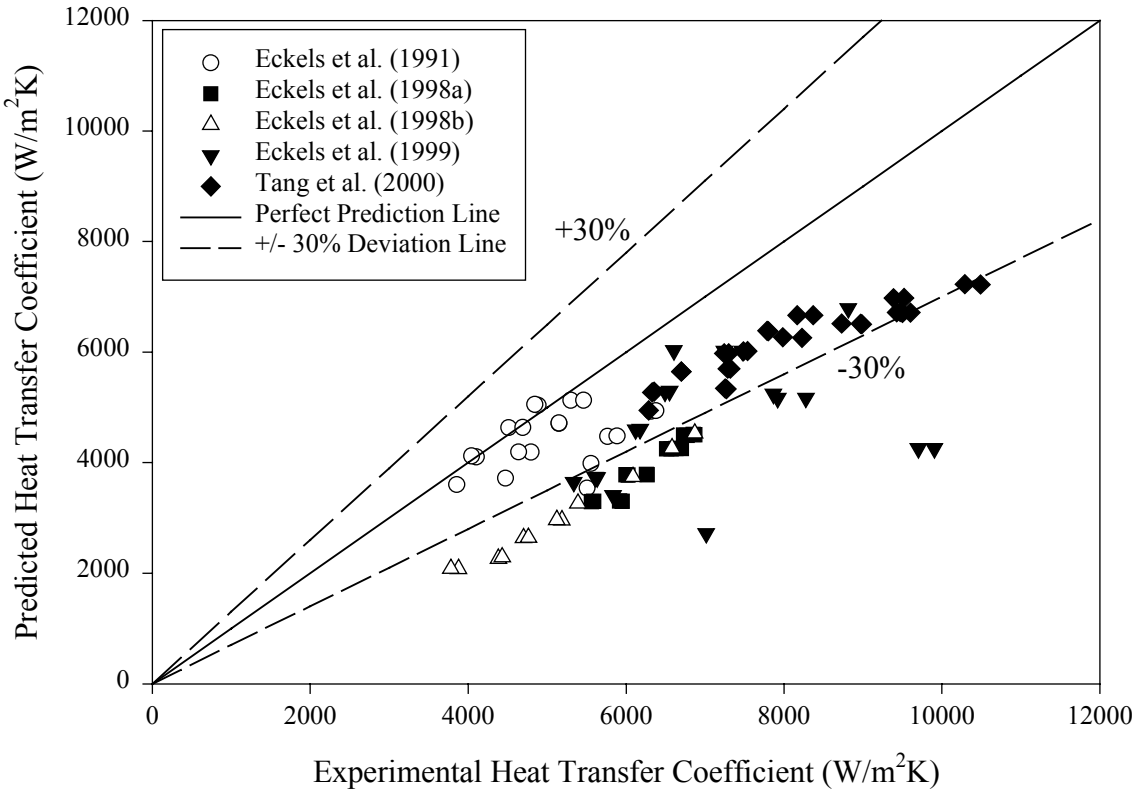

Figure 3.8 Kedzierski and Goncalves (1999) Model for all the Available R134a Data Sets

The Kedzierski and Goncalves (1999) model successfully predicts the Eckels et al. (1991) R134a data set and the Tang et al. (2000) R134a data set with mean absolute deviations less than 30%. However, as shown in Figure 3.8 the model under predicts most of the R134a data points from Eckels et al. (1998a, 1998b, 1999).

Figure 3.9 shows the prediction results of the Kedzierski and Goncalves (1999) model for the Eckels et al. (1991) R12 data set. As observed from the figure, the model successfully predicts the Eckels et al. (1991) data set with mean absolute deviations about 18%, but some of the data points are under predicted.

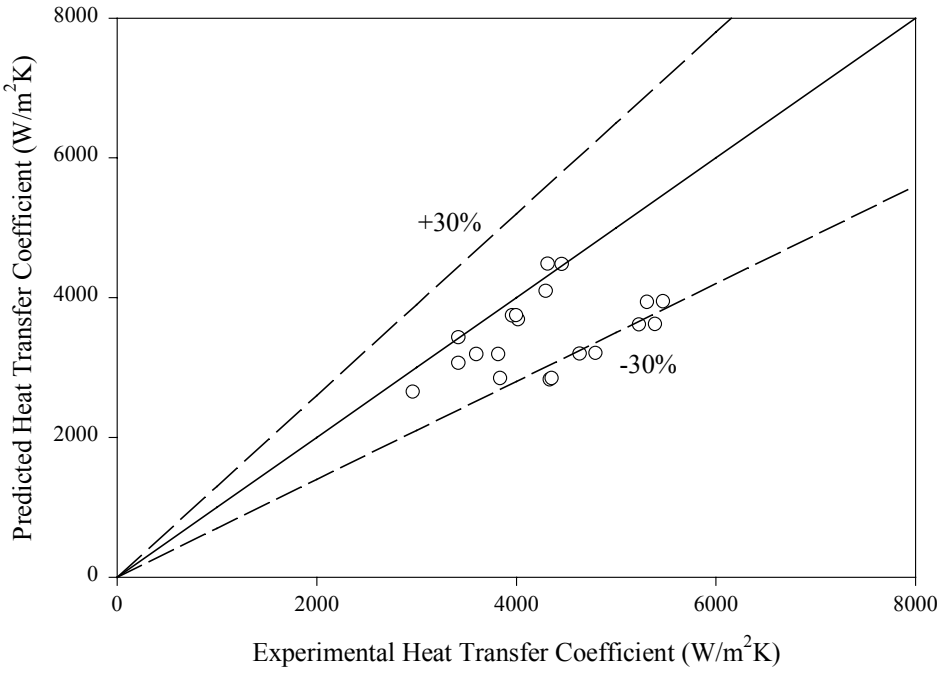

Figure 3.9 Kedzierski and Goncalves (1999) Model for the Eckels et al. (1991) R12 Data Set

Table 3.9 summarizes the mean absolute deviations of the Kedzierski and Goncalves (1999) model on the pure-refrigerants data sets. The model predicts most of

the experimental data sets with mean absolute deviations over 20%. The model fails to predict the Chamra et al. (1996) R22 data set, the Eckels et al. (1998a) R134a data set, Shinohara and Tobe (1985) R22 data set, and Uchida et al. (1996) R22 data set.

Table 3.9 Mean Absolute Deviation (*MAD*) Between the Pure-Refrigerant Experimental Data and the Prediction Results from the Kedzierski and Goncalves (1999) Model

No.	Reference	Refrigerant	MAD value (%)
1	Bogart and Thors (1999)	R22	34.8
2	Chamra et al. (1996)	R22	40.3
3	Ebisu et al. (1994)	R22	23.5
4	Eckels et al. (1991)	R134a R12	12.0 17.7
5	Eckels et al. (1998a)	R134a	42.4
6	Eckels et al. (1998b)	R134a	37.6
7	Eckels et al. (1999)	R22 R134a	25.3 31.3
8	Goto et al. (1995)	R22	22.7
9	Hitachi Cable (1987)	R22	29.7
10	Muzzio et al. (1995)	R22	20.6
11	Muzzio et al. (1998)	R22	21.7
12	Schlager L.M. (1988)	R22	12.6
13	Schlager et al. (1989)	R22	7.8
14	Shinohara and Tobe (1985)	R22	65.6
15	Tang et al. (2000)	R22 R134a	26.2 22.9
16	Uchida et al. (1996)	R22	49.7
17	Yasuda et al. (1990)	R22	16.1

The Kedzierski and Goncalves (1999) model is also validated with eight refrigerant mixture data sets. A total of 130 refrigerant mixtures data points were used for the validation process. The refrigerant mixtures used in the data sets consist of R410a, R407c and R32/R134a (30%/70%). The R410a data sets are first tested with the

Kedzierski and Goncalves (1999) model. The prediction results for these R410a data sets are shown in Figure 3.10.

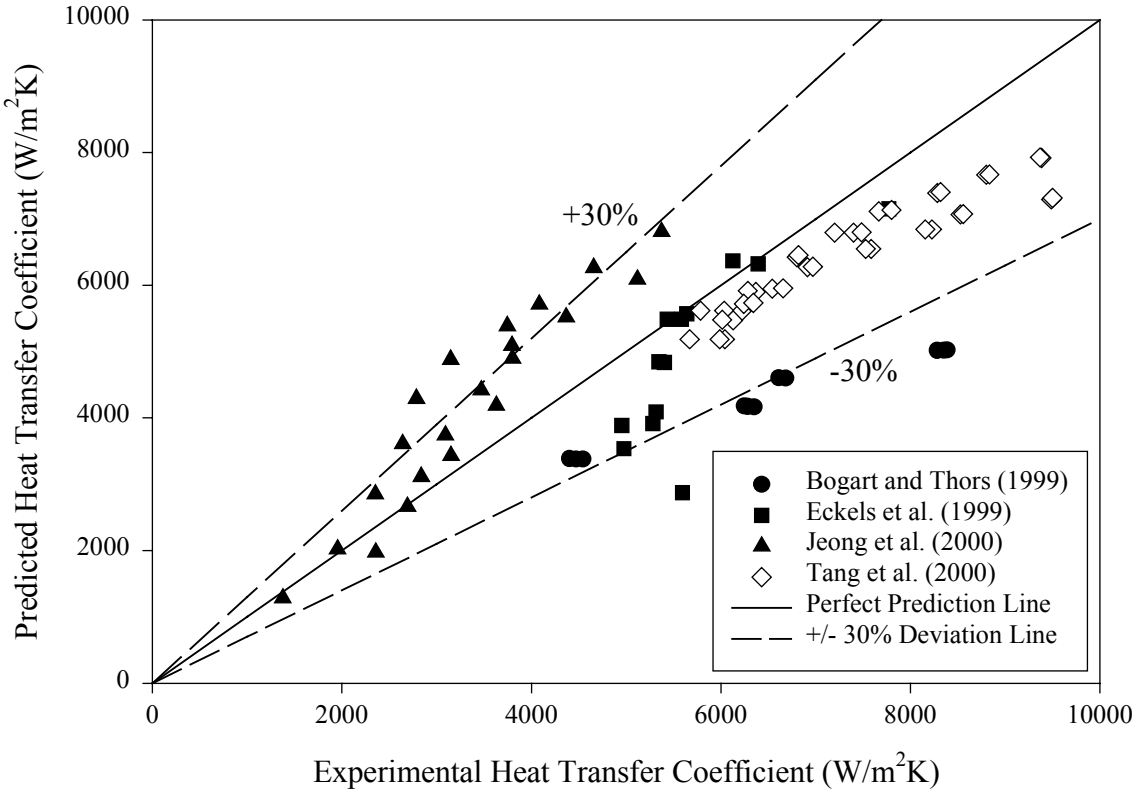

Figure 3.10 Kedzierski and Goncalves (1999) Model for all the Available R410a Data Sets

The Kedzierski and Goncalves (1999) model successfully predicts the R410a data sets from the Tang et al. (2000) and the Eckels et al. (1999) within 15%. This model also predicts the Jeong et al. (2000) R410a data set within 30%. However, the model under predicts the Bogart and Thors (1999) R410a data with mean absolute deviations over 30%.

Three R407c data sets were selected to evaluate the Kedzierski and Goncalves (1999) model. The prediction results for these R407c data sets are presented in Figure 3.11. The model adequately predicts the R407c data sets from Ebisu et al. (1998) and from Eckels et al. (1999). The model achieves a mean absolute deviation of less than 30% for these two data sets. However, the model over predicts the Goto et al. (1995) R407c data set with mean absolute deviations of about 50%.

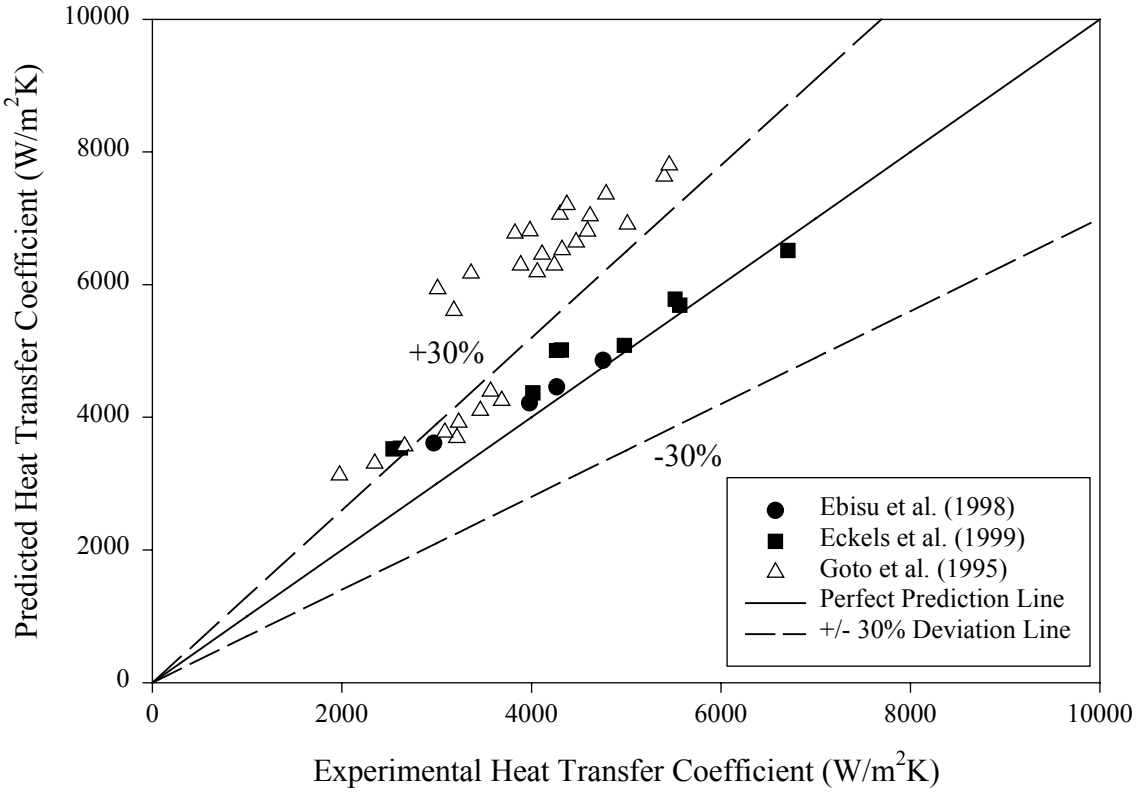

Figure 3.11 Kedzierski and Goncalves (1999) Model for all the Available R407c Data Sets

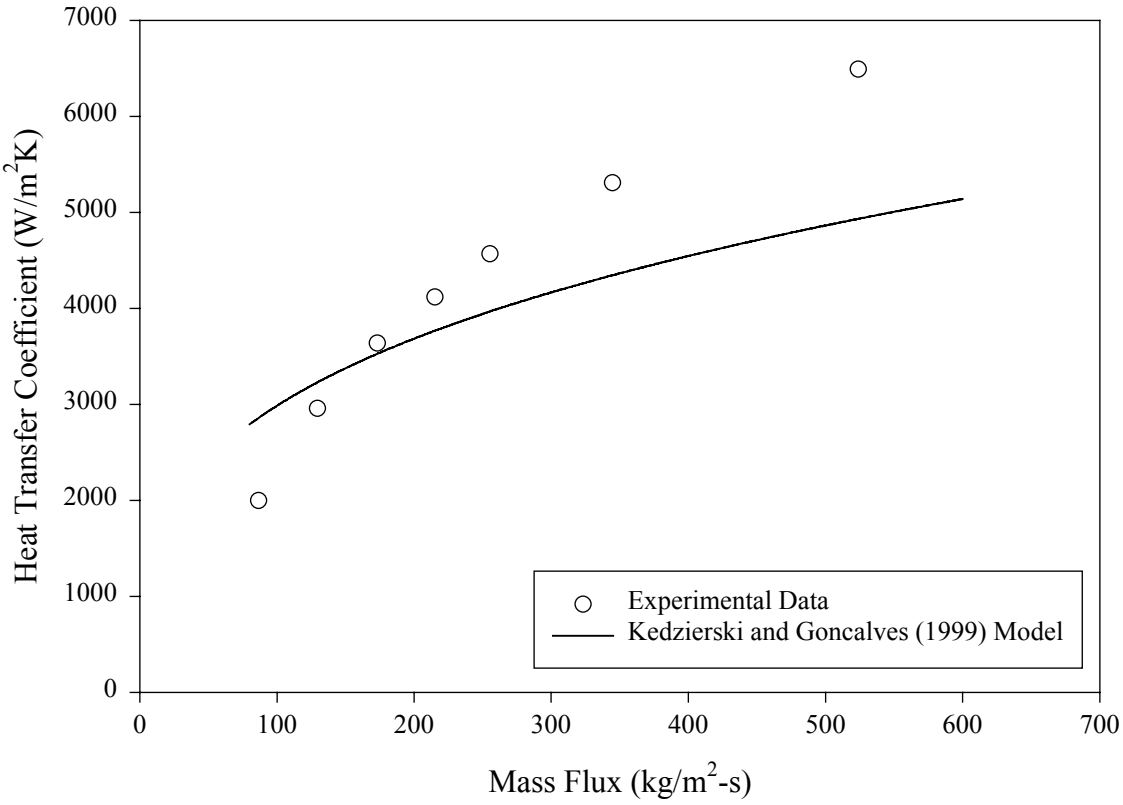

Figure 3.12 Kedzierski and Goncalves (1999) Model for the Ebisu et al. (1994) R32/R134a (30%/70%) Data Set

The Kedzierski and Goncalves (1999) model is also assessed with the Ebisu et al. (1994) R32/R134a (30%/70%) data set. The mean absolute deviation observed is around 17%. However, as shown in Figure 3.12 the model fails to predict the behavior of the heat transfer coefficient with increasing mass flux. It over predicts the experimental data at low mass flux (G<200 kg/m^2-s), but it under predicts the data in the high mass flux region.

Table 3.10 summarizes the predictions results of Kedzierski and Goncalves (1999) model for the refrigerant-mixture data sets. Except the Bogart and Thors (1999)

R410a and the Goto et al. (1995) R407c data sets, the model predicts most of the refrigerant mixture data sets successfully. The model predicts both of these data sets with mean absolute deviations over 30%.

Table 3.10 Mean Absolute Deviation (*MAD*) Between the Refrigerant-Mixture Experimental Data and the Prediction Results from the Kedzierski and Goncalves (1999) Model

No.	Reference	Refrigerant	MAD value (%)
1	Bogart and Thors (1999)	R410a	32.3
2	Ebisu et al. (1994)	R32/R134a (30%/70%)	17.0
3	Ebisu et al. (1998)	R407c	8.5
4	Eckels et al. (1999)	R410a R407c	14.3 14.3
5	Goto et al. (1995)	R407c	49.2
6	Jeong et al. (2000)	R410a	25.2
7	Tang et al. (2000)	R410a	11.2

Cavallini et al. (1999) Heat Transfer Model for Zeotropic Mixtures

The Cavallini et al. (1999) pure-refrigerant model is extended to predict heat transfer performance for refrigerant mixtures inside micro-fin tubes. The final form of the model is written as

$$h_m = \left[\frac{1}{h} + \frac{\frac{\delta Q_{SV}}{\delta Q_T}}{h_v} \right]^{-1} \tag{3.7}$$

where

$$\frac{\delta Q_{SV}}{\delta Q_T} \approx x \cdot c_{pv} \cdot \left(\frac{\Delta TG}{i_{fg\_m}} \right) \tag{3.8}$$

This model is validated for the R407c, R410a, and R32/R134a (30%/70%) refrigerant mixtures experimental data sets. A total of 130 experimental data points were available for the evaluation of the model. A sample model file is attached in Appendix D. The refrigerant-mixture model used the same property file and the same data file as generated for the pure-refrigerant model calculation process.

The Cavallini et al. (1999) refrigerant-mixture model was first validated with the R410a data sets. The prediction results for these R410a data sets are presented in Figure 3.13.

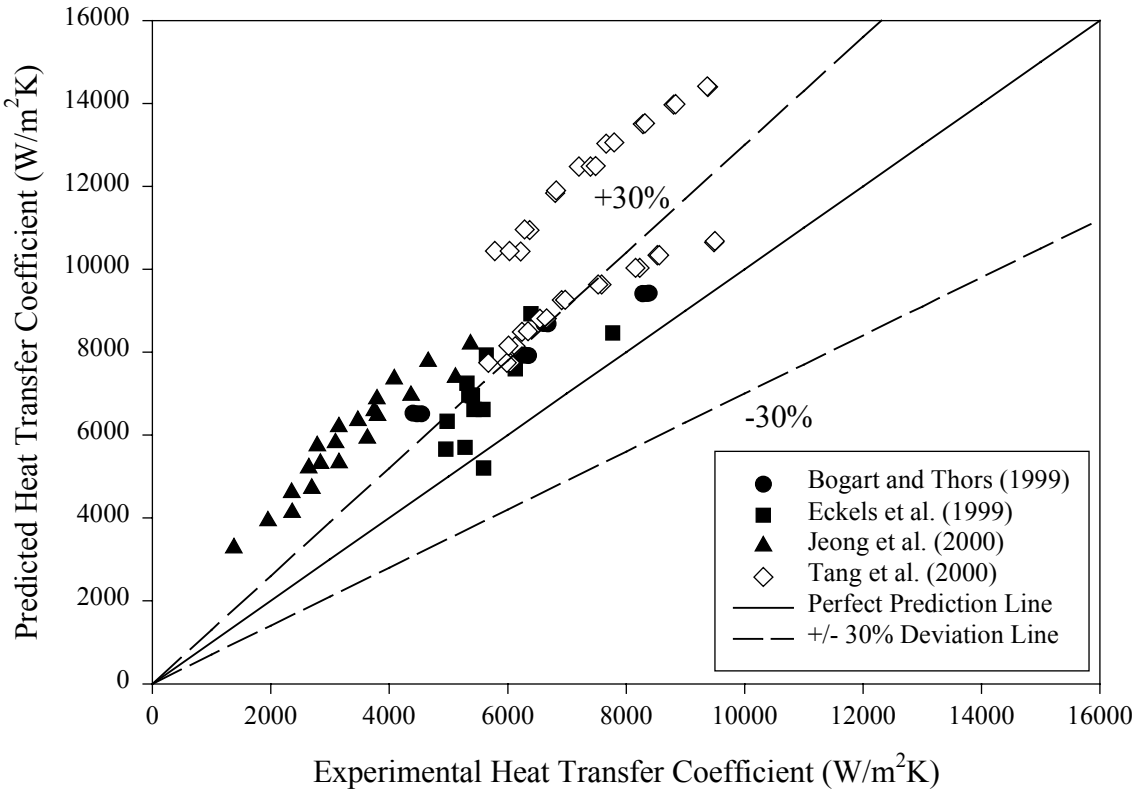

Figure 3.13 Cavallini et al. (1999) Model for all the Available R410a Data Sets

The Cavallini et al. (1999) refrigerant-mixture model failed to predict the R410a data sets accurately. It predicts most of the R410a experimental data sets with mean absolute deviations over 30%. As demonstrated in the Figure 3.13, the Jeong et al. (2000) R410a data set was not accurately predicted by the Cavallini et al. (1999) refrigerant-mixture model. The model predicted the R410a experimental data points from Tang et al. (2000) with a mean absolute deviation of about 47%.

The Cavallini et al. (1999) refrigerant-mixture model was also tested against the R407c data. The prediction results for these R407c data sets are shown in Figure 3.14.

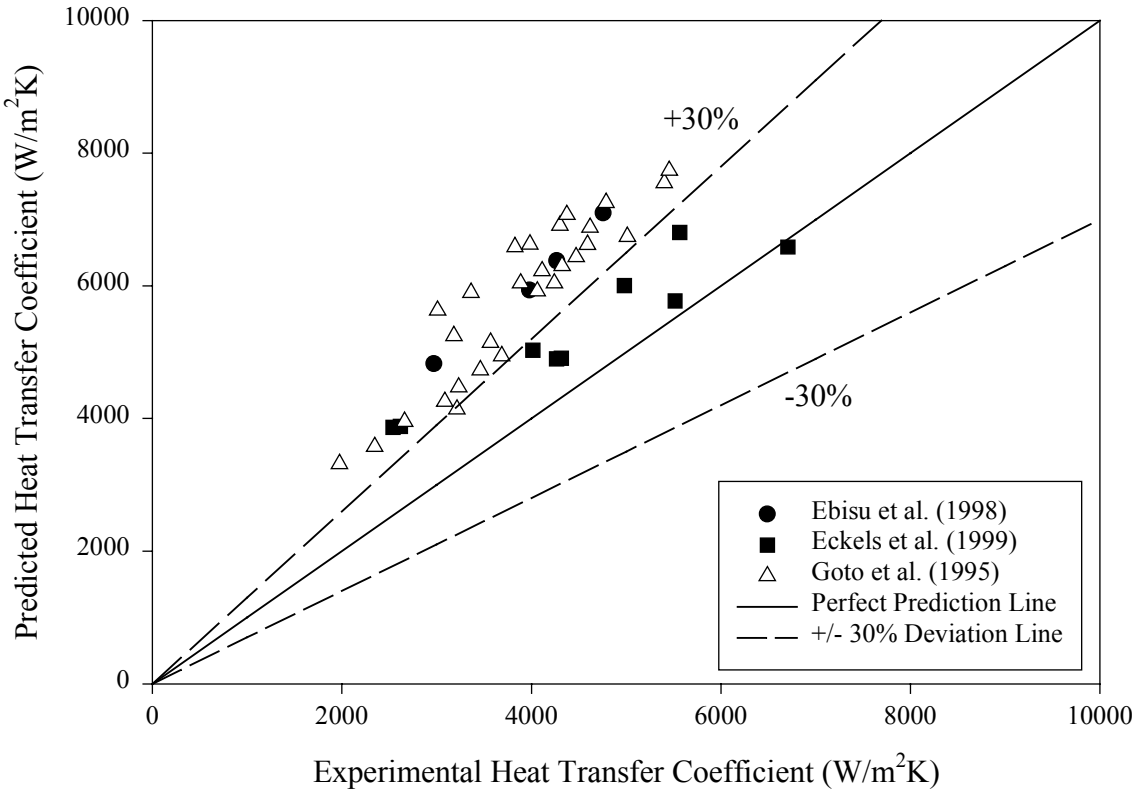

Figure 3.14 Cavallini et al. (1999) Model for all the Available R407c Data Sets

As shown in Figure 3.14, the model also failed to predict most of the R407c data sets. The model over predicts the Ebisu et al. (1998) and the Goto et al. (1995) R407c data sets with mean absolute deviations over 50%.

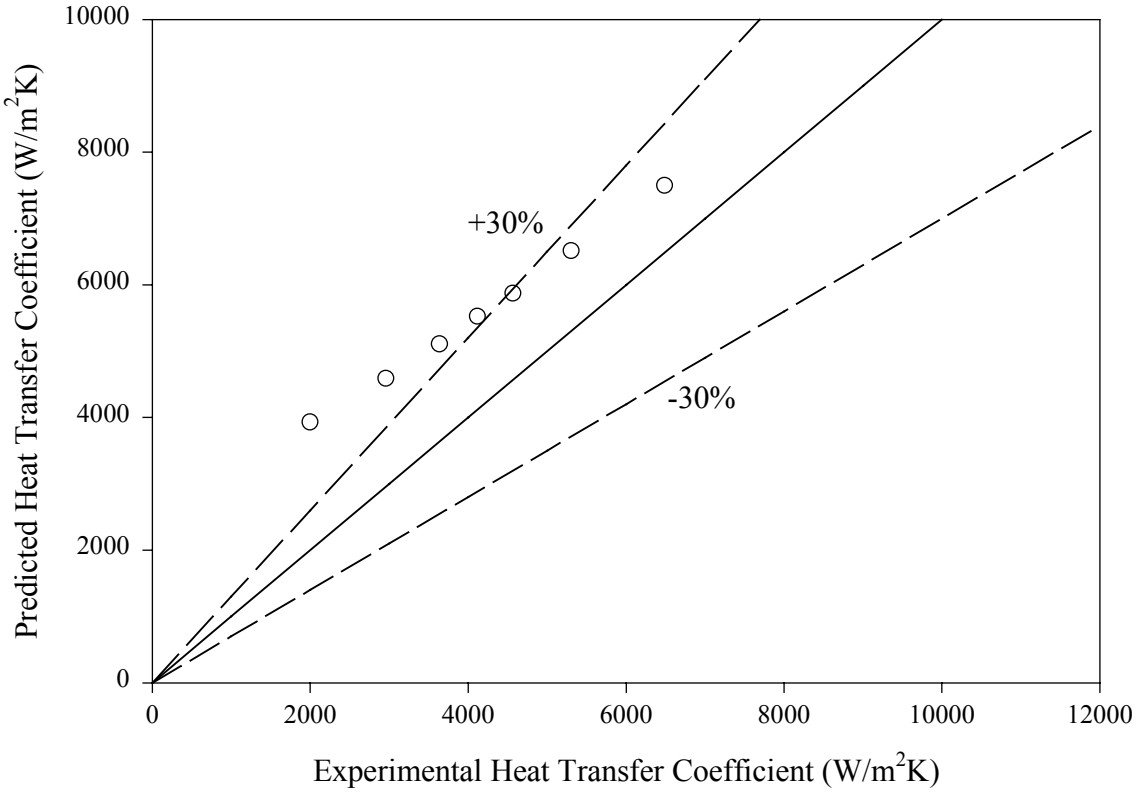

Figure 3.15 Cavallini et al. (1999) Model for the Ebisu et al. (1994) R32/R134a (30%/70%) Data Set

The model is also evaluated with the Ebisu et al. (1994) R32/R134a (30%/70%) data set. As presented in Figure 3.15, the model over predicts this data set with mean absolute deviations about 40%.

Table 3.11 summarizes the mean absolute deviations of the Cavallini et al. (1999) refrigerant-mixture model for the refrigerant-mixture data sets. The model over predicts

most of the refrigerant-mixture data sets with the achieved mean absolute deviation over 30%.

Table 3.11 Mean Absolute Deviation (*MAD*) Between the Experimental Data and the Prediction Results from the Cavallini et al. (1999) Refrigerant-Mixture Model

No.	Reference	Refrigerant	MAD value (%)
1	Bogart and Thors (1999)	R410a	28.5
2	Ebisu et al. (1994)	R32/R134a (30%/70%)	41.9
3	Ebisu et al. (1998)	R407c	52.5
4	Eckels et al. (1999)	R410a R407c	23.5 22.6
5	Jeong et al. (2000)	R410a	81.2
6	Goto et al. (1995)	R407c	50.8
7	Tang et al. (2000)	R410a	47.1

Except the Goto et al. (1995) R22 data set and Shinohara and Tobe (1985) R22 data set, the Cavallini et al. (1999) pure-refrigerant model predicts the available experimental data sets for pure refrigerants very well with mean absolute deviations within 30%. However, the Cavallini et al. (1999) refrigerant-mixture model results in high mean absolute deviations on most of the available refrigerant-mixture data sets.

Except the Schlager L.M. (1988), Schlager et al. (1989), and Shinohara and Tobe (1985) R22 data sets, the Yu and Koyama (1998) model, which is applicable for pure refrigerants only, predicts most of the available pure-refrigerant data sets fairly well with mean absolute deviation within 30%. However, the model does not capture the effects of tube geometry on the heat transfer coefficient in micro-fin tubes.

The Kedzierski and Goncalves (1999) model predicts the pure-refrigerant data sets fairly well with mean absolute deviations over 20% for most of the pure-refrigerant data sets. Except the Bogart and Thors (1999) R410a and the Goto et al. (1995) R407c refrigerant-mixture data sets, the model is able to predict most of these data within 30%. The Kedzierski and Goncalves (1999) model is an empirical correlation applicable to both pure refrigerants and refrigerant mixtures. The model does not account for mass transfer thermal resistance in the refrigerant mixtures.

Generally, the existing condensation heat transfer models are not very accurate for predicting the heat transfer coefficients of most of the available experimental data sets. The predictions of the existing condensation heat transfer models are not consistent. Furthermore, some of the existing condensation heat transfer models are too complicated to be used. Thus, a better and more general model is needed to compute the heat transfer coefficients of pure refrigerants and refrigerant mixtures flowing inside micro-fin tubes. A new semi-empirical model is introduced and evaluated in the next chapter.

CHAPTER IV

NEW CORRELATION AND VALIDATION

Dukler (1960) presented a method of predicting the hydrodynamics and heat transfer in vertical film-wise condensation. Dukler obtained the velocity distributions in the liquid film as a function of the interfacial shear and film thickness by working from the definition of eddy viscosity and using the Deissler equation for its variation near a solid boundary. The method presented by Dukler will be expanded for condensation in horizontal micro-fin tube.

New Correlation for Pure Refrigerants Flowing inside Micro-Fin Tubes

In order to determine the condensation heat transfer coefficient for a turbulent film, the transport of heat in the film, neglecting downstream convection compared to cross-stream diffusion, is given by

$$q = -\left(k + \rho c_p \varepsilon_H\right)\frac{dT}{dy} \tag{4.1}$$

where ε_H is the turbulent eddy conductivity. By substituting the thermal diffusivity, Equation (4.1) becomes

$$q = -\rho c_p \left(\alpha_T + \varepsilon_H\right)\frac{dT}{dy} \Rightarrow q = -\rho c_p \nu\left(\frac{1}{\mathrm{Pr}} + \frac{\varepsilon_H}{\nu}\right)\frac{dT}{dy} \tag{4.2}$$

where α_T is the thermal diffusivity and Pr is the Prandtl number. Equation (4.2) can be expressed in dimensionless form as

$$\frac{q}{q_w} = \left(\frac{1}{\Pr} + \frac{\varepsilon_H}{\nu} \right) \frac{dT^+}{dy^+} \tag{4.3}$$

where $$y^+ = y \frac{u^*}{\nu} \qquad with \qquad u^* = \sqrt{\frac{\tau_w}{\rho}} = \sqrt{g\delta} \tag{4.4}$$

$$T^+ = \frac{\rho c_p u^*}{q_w} (T_w - T) \tag{4.5}$$

If the turbulent Prandtl number, Pr_t, is equal to one, then

$$\Pr_t = \frac{\varepsilon_M}{\varepsilon_H} = 1 \Rightarrow \varepsilon_M = \varepsilon_H \tag{4.6}$$

where ε_M is the eddy diffusivity of momentum. Equation (4.3) becomes

$$\frac{q}{q_w} = \left(\frac{1}{\Pr} + \frac{\varepsilon_M}{\nu} \right) \frac{dT^+}{dy^+} \tag{4.7}$$

Equation (4.7) can be integrated from zero to δ^+, where δ^+ is the dimensionless liquid film thickness,

$$\delta^+ = \frac{\delta u^*}{\nu} \tag{4.8}$$

at $y = \delta^+$, $T = T_{sat}$ and at the surface, $y = 0$, $T = T_w$

Therefore,

$$\frac{T_{sat} - T_w}{\left(q_w / \rho c_p u^* \right)} = \int_0^{\delta^+} \frac{dy^+}{\frac{1}{\Pr} + \frac{\varepsilon_M}{\nu}} \tag{4.9}$$

Equation (4.9) can be integrated if the relationship between ε_M/ν and y^+ is known. This relationship is established by using the universal velocity distribution equations,

$$\tau = (\mu + \rho\varepsilon_M)\frac{du}{dy} \Rightarrow \frac{\tau}{\tau_w} = \left(1 + \frac{\varepsilon_M}{\nu}\right)\frac{du^+}{dy^+} \tag{4.10}$$

Therefore,

$$1 + \frac{\varepsilon_M}{\nu} = \frac{\tau/\tau_w}{du^+/dy^+} \Rightarrow \frac{\varepsilon_M}{\nu} = \frac{1}{\dfrac{du^+}{dy^+}} - 1 \tag{4.11}$$

The von Karman velocity distribution can be used to evaluate ε_M/ν.

$$y^+ \le 5 \Rightarrow u^+ = y^+ \Rightarrow \frac{\varepsilon_M}{\nu} = 0 \qquad \text{Viscous sublayer} \tag{4.12a}$$

$$5 \le y^+ \le 30 \Rightarrow u^+ = -3.05 + 5\ln(y^+) \Rightarrow \frac{\varepsilon_M}{\nu} = \frac{y^+}{5} - 1 \quad \text{Buffer sublayer} \tag{4.12b}$$

$$y^+ > 30 \Rightarrow u^+ = 5.5 + 2.5\ln(y^+) \Rightarrow \frac{\varepsilon_M}{\nu} = \frac{y^+}{2.5} - 1 \qquad \text{Turbulent region} \tag{4.12c}$$

$$u^+ = \frac{\overline{u}}{u^*} \tag{4.12d}$$

Equation (4.9) can now be integrated to evaluate the condensation heat transfer coefficient,

$$h = \frac{q}{T_{sat} - T_w} \Rightarrow \frac{\rho c_p u^*}{h} = T^+ = \underbrace{\int_0^5 \frac{dy^+}{1/\mathrm{Pr}}}_{Viscous,sublayer} + \underbrace{\int_5^{26} \frac{dy^+}{\dfrac{1}{\mathrm{Pr}} + \left(\dfrac{y^+}{5} - 1\right)}}_{Buffer,sublayer} + \underbrace{\int_{26}^{\delta^+} \frac{dy^+}{\dfrac{1}{\mathrm{Pr}} + \left(\dfrac{y^+}{2.5} - 1\right)}}_{Turbulent,region} \tag{4.13}$$

The dimensionless temperature, T^+, is defined using the equations below.

$$T^+ = \delta^+ \cdot \mathrm{Pr}_l \qquad \delta^+ \le 5 \tag{4.14}$$

$$T^+ = 5 \cdot \left[\mathrm{Pr}_l + \ln\left[1 + \mathrm{Pr}_l\left(\frac{\delta^+}{5} - 1\right)\right]\right] \qquad 5 < \delta^+ \le 30 \tag{4.15}$$

$$T^+ = 5 \cdot \left[\mathrm{Pr}_l + \ln\left(1 + 5 \cdot \mathrm{Pr}_l\right) + 0.5 \cdot \ln\left(\frac{\delta^+ - 2.5}{27.5} \right) \right] \qquad \delta^+ > 30 \tag{4.16}$$

The dimensionless condensate film thickness, δ^+, is defined as follow:

For laminar flow,

$$\delta^+ = 0.866\,\mathrm{Re}_l^{\,0.5} \qquad \text{for } \mathrm{Re}_l \le 1600 \tag{4.17}$$

For turbulent flow, the dimensionless film thickness can be found by using the Ganchev et al. (1976) empirical correlation,

$$\delta^+ = 0.051\,\mathrm{Re}_l^{\,0.87} \qquad \text{for } \mathrm{Re}_l > 1600 \tag{4.18}$$

Where the Reynolds number, Re_l, is

$$\mathrm{Re}_l = \frac{4 \cdot m_l}{\pi \cdot d_i \cdot \mu_l} = \frac{G \cdot (1 - x) \cdot d_i}{\mu_l} \tag{4.19}$$

The original model is used to predict the heat transfer coefficient during condensation inside smooth tubes.

$$h = \frac{\rho_l \cdot c_{pl} \cdot \left(\frac{\tau_w}{\rho_l} \right)^{0.5}}{T^+} \tag{4.20}$$

where τ_w is the wall shear stress and $T^+$is the dimensionless temperature. The frictional component of the two-phase flow pressure gradient $(dp/dz)_f$ is related to the wall shear stress, τ_w, as

$$\pi d \tau_w = \left(\frac{dp}{dz} \right)_f \cdot \frac{\pi d_i^{\,2}}{4} \Rightarrow \tau_w = \left(\frac{dp}{dz} \right)_f \cdot \frac{d_i}{4} \tag{4.21}$$

$(dp/dz)_f$ is defined as the frictional pressure gradient. The value of the frictional pressure gradient is calculated by using the following equations:

$$\left(\frac{dp}{dz}\right)_f = \Phi_{LO}{}^2 \cdot \left(\frac{dp_f}{dz}\right)_{LO} = \frac{\Phi_{LO}{}^2 \cdot 2 \cdot f_{LO} \cdot G^2}{d_i \cdot \rho_l} \tag{4.22}$$

where Φ_{LO} is the two-phase multiplier and f_{LO} is the single-phase friction multiplier. The two-phase multiplier is evaluated by using Friedel (1979) correlations.

$$\Phi_{LO}{}^2 = E + \frac{3.24 \cdot F \cdot H}{Fr^{0.045} We^{0.035}} \tag{4.23}$$

$$E = (1-x)^2 + x^2 \cdot \frac{\rho_l \cdot f_{GO}}{\rho_v \cdot f_{LO}} \tag{4.24}$$

$$F = x^{0.78}(1-x)^{0.224} \tag{4.25}$$

$$H = \left(\frac{\rho_l}{\rho_v}\right)^{0.91} \cdot \left(\frac{\mu_v}{\mu_l}\right)^{0.19} \cdot \left(1 - \frac{\mu_v}{\mu_l}\right)^{0.7} \tag{4.26}$$

$$We = \frac{G^2 \cdot d_i}{\rho_m \cdot \sigma} \tag{4.27}$$

$$Fr = \frac{G^2}{g \cdot d_i \cdot \rho_m^2} \tag{4.28}$$

$$\rho_m = \left(\frac{x}{\rho_v} + \frac{(1-x)}{\rho_l}\right)^{-1} \tag{4.29}$$

The single-phase friction factors, f_{GO} and f_{LO}, are used in the calculation of the frictional pressure gradient. For micro-fin tubes, Cavallini et al. (1999) suggested that the single-phase friction factor to be taken as the higher value of that obtained from the Blausius equation for smooth tubes and that estimated from the Moody diagram under fully-developed turbulent flow and at a relative roughness (empirically fitted). The method is applied to compute the friction factors

$$f_{LO} = \max(f_{LO1}, f_{LO2}) \qquad f_{GO} = \max(f_{GO1}, f_{GO2})$$

Using the Blasius equation for the turbulent flow

$$f_{LO1} = 0.079 \cdot \left(\frac{G \cdot d_i}{\mu_l} \right)^{-0.25} \qquad f_{GO1} = 0.079 \cdot \left(\frac{G \cdot d_i}{\mu_v} \right)^{-0.25} \qquad \text{when } \frac{G \cdot d_i}{\mu_v} > 2000 \tag{4.30}$$

and for laminar flow

$$f_{LO1} = \frac{16}{\left(\frac{G \cdot d_i}{\mu_l} \right)} \qquad f_{GO1} = \frac{16}{\left(\frac{G \cdot d_i}{\mu_v} \right)} \qquad \text{when } \frac{G \cdot d_i}{\mu_v} \le 2000 \tag{4.31}$$

or for both laminar and turbulent flow,

$$f_{LO2} = \frac{\left[1.74 - 2 \cdot \log\left(2 \cdot Rx_f\right)\right]^{-2}}{4} \tag{4.32}$$

$$f_{GO2} = \frac{\left[1.74 - 2 \cdot \log\left(2 \cdot Rx_f\right)\right]^{-2}}{4} \tag{4.33}$$

where Rx_f is an empirically-fitted relative roughness that is used to model the micro-fin tubes.

$$Rx_f = \frac{0.18 \cdot \left(\frac{e}{d_i} \right)}{(0.1 + \cos\beta)} \tag{4.34}$$

In order to expand the original smooth-tube model to the micro-fin tubes, a new geometry-enhancement factor, which was introduced by Hori and Shinohara (1991), is used in the new model. The equation for the geometry-enhancement factor which accounts for the effects of the heat transfer area increase and the spiral angle is

$$Rx = \left[\frac{2 \cdot e \cdot n_g \cdot \left(1 - \sin\left(\frac{\beta}{2}\right)\right)}{\pi \cdot d_i \cdot \cos\left(\frac{\beta}{2}\right)} + 1 \right] \cdot \frac{1}{\cos(\gamma)} \tag{4.35}$$

where *Rx* is the geometry-enhancement factor. Equation (4.20) will be multiplied by the enhancement factor for the micro-fin tubes. In addition, three empirical constants (P_1, P_2, and P_3) will be generated from the available experimental database.

$$h = \frac{P_1 \cdot \rho_l \cdot c_{pl} \cdot \left(\frac{\tau_w}{\rho_l}\right)^{P_2}}{T^+} \cdot Rx^{P_3} \tag{4.36}$$

MathCad minimize function is used to generate the three new empirical constants. The new empirical constants for the new pure-refrigerant model are generated using the 174 data points collected from the seven different sources presented in Table 4.1. A detailed MathCAD worksheet for the entire process and a sample model file are presented in Appendix E and Appendix F.

Table 4.1 Pure-Refrigerant Data Sets Used for Generating the New Empirical Constants

Reference	Refrigerant	Number of data points
Hitachi Cable (1987)	R22	12
Muzzio et al. (1995)	R22	24
Schlager et al. (1989)	R22	15
Shinohara and Tobe (1985)	R22	9
Tang et al. (2000)	R22	35
Yasuda et al. (1990)	R22	17
Eckels et al. (1998a)	R134a	12
Tang et al. (2000)	R134a	30
Eckels et al. (1991)	R12	20

The new pure-refrigerant model to compute the heat transfer coefficient during the condensation inside the micro-fin tubes using pure refrigerants is

$$h = \frac{0.208 \cdot \rho_l \cdot c_{pl} \cdot \left(\frac{\tau_w}{\rho_l}\right)^{0.224}}{T^+} \cdot Rx^{1.321} \tag{4.37}$$

The constant P_1 must have the dimension $m^{0.552}/s^{0.552}$ in order for the equation to yield the correct dimensions, W/m^2-K, for the heat transfer coefficient. The new pure-refrigerant model is used to predict existing experimental data and the mean absolute deviation (*MAD*) value is calculated. The mean absolute deviation (*MAD*) is set as the criterion to determine the effectiveness of the heat transfer model. The heat transfer model is considered acceptable if the *MAD* is less than 30%. For the pure refrigerants, the available experimental data have been used to validate the prediction results of the new pure-refrigerant model. The accuracy of the new model in predicting the pure-refrigerant data is presented in Table 4.2.

Table 4.2 Mean Absolute Deviation (*MAD*) Achieved by the New Pure-Refrigerant Model for the Data Sets Used in Generating the New Empirical Constants

Reference	Refrigerant	*MAD* Value (%)
Hitachi Cable (1987)	R22	9.9
Muzzio et al. (1995)	R22	10.7
Schlager et al. (1989)	R22	17.9
Shinohara and Tobe (1985)	R22	18.4
Tang et al. (2000)	R22	5.6
Yasuda et al. (1990)	R22	4.8
Eckels et al. (1998a)	R134a	14.8
Tang et al. (2000)	R134a	5.4
Eckels et al. (1991)	R12	12.7

Table 4.2 shows that the prediction results are excellent with the new pure-refrigerant model. The mean absolute deviations for all these pure-refrigerant data sets are less than 19%. In addition, the new model produces more reliable and consistent prediction results. The prediction results for the nine data sets are illustrated in Figure 4.1 – 4.3. The symbols indicate the experimental data points.

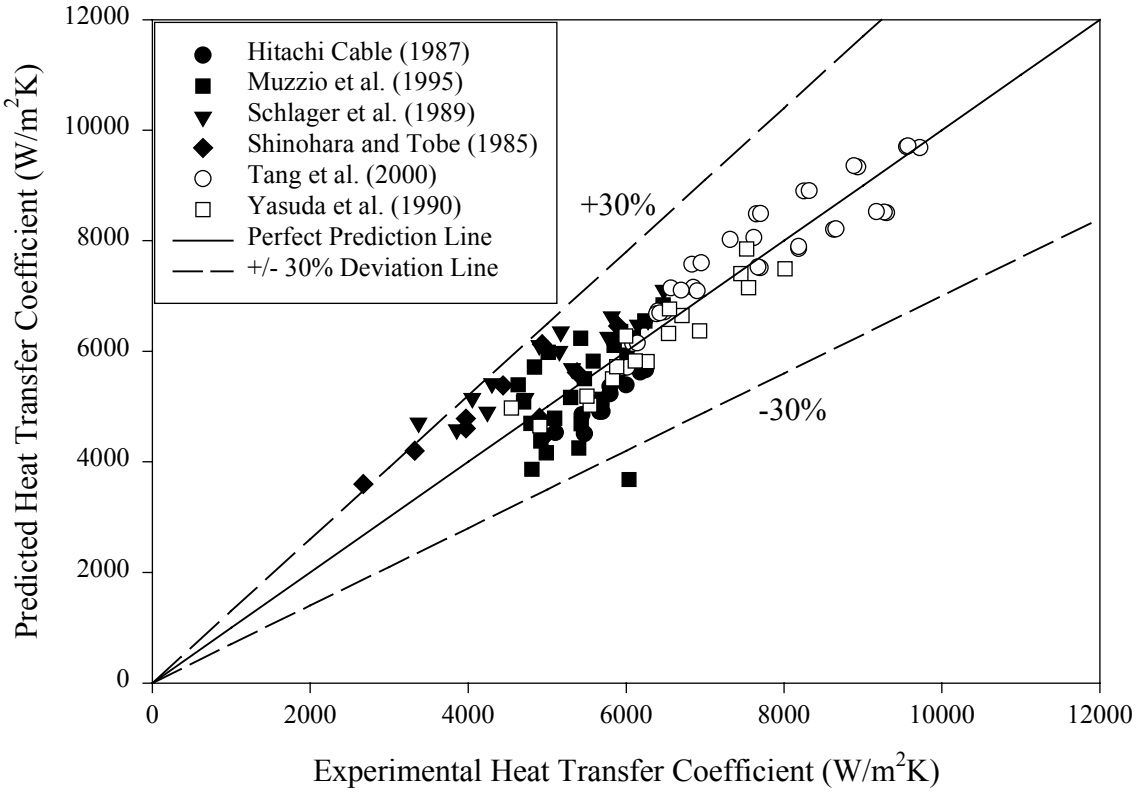

Figure 4.1 New Pure-Refrigerant Model for the R22 Data Sets Used in Generating the New Empirical Constants

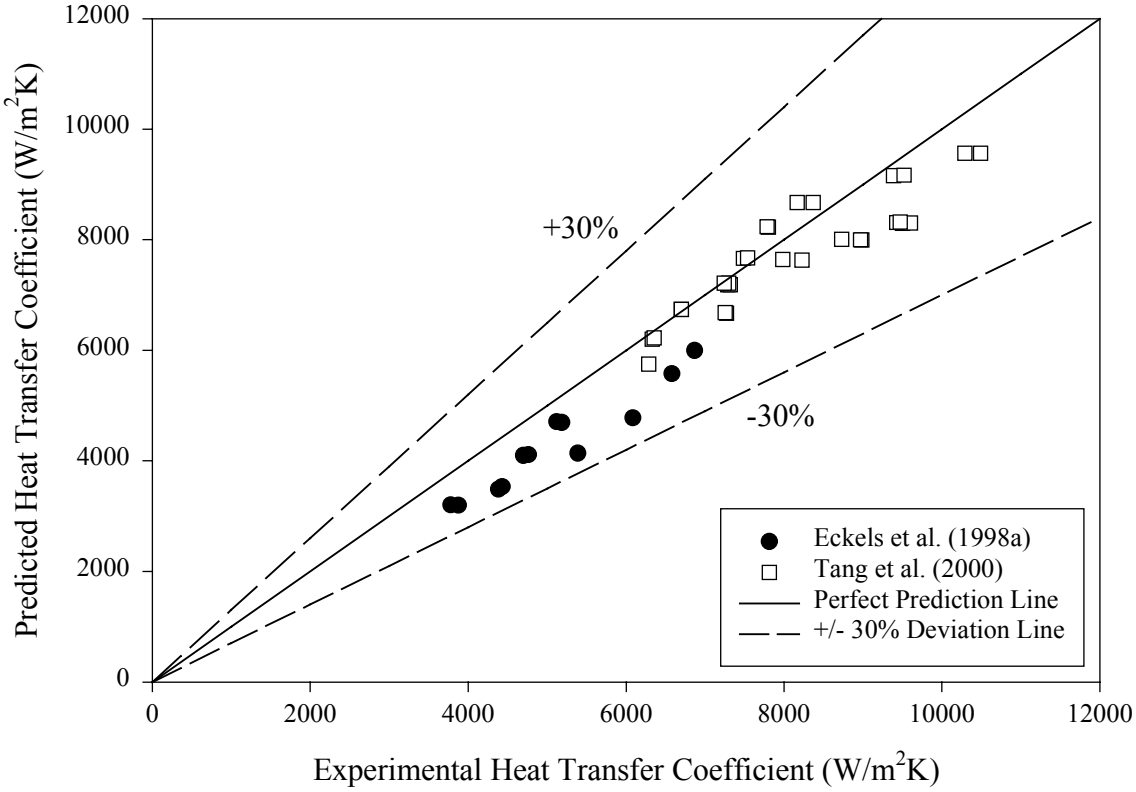

Figure 4.2 New Pure-Refrigerant Model for the R134a Data Sets Used in Generating the New Empirical Constants

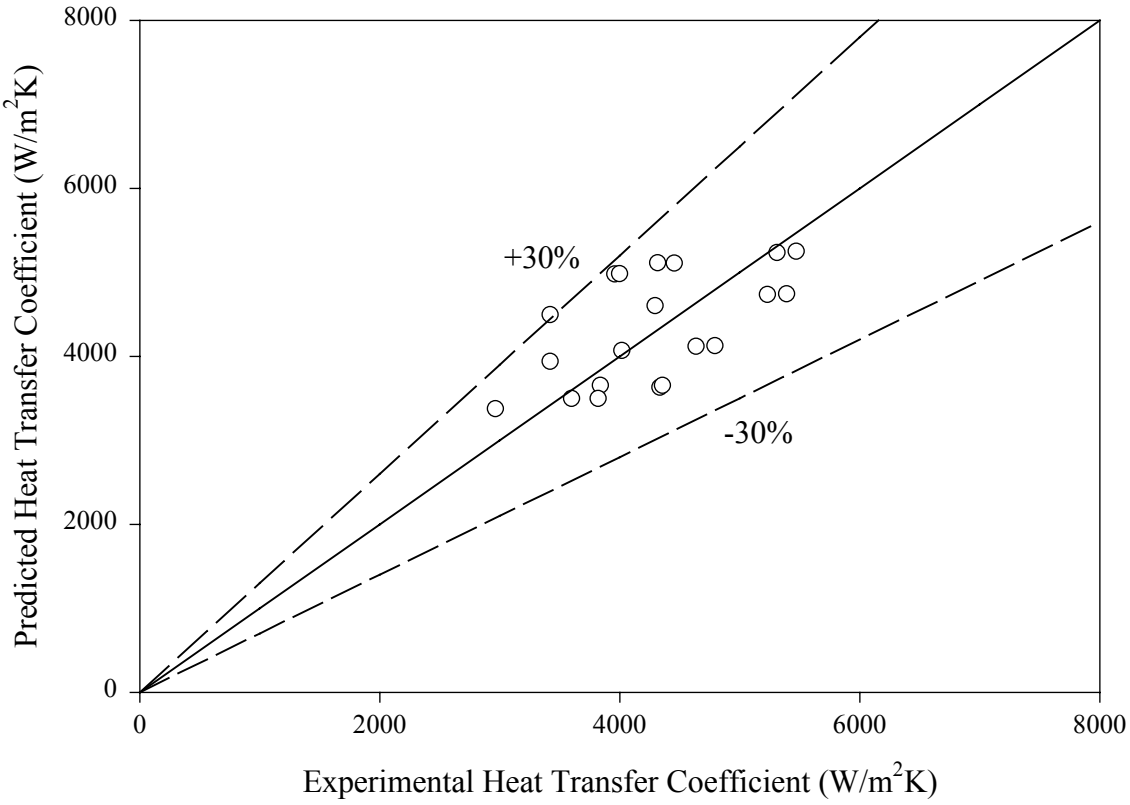

Figure 4.3 New Pure-Refrigerant Model for the Eckels et al. (1991) R12 Data Set

The new pure-refrigerant model is further tested with data sets not included in developing the model. The validation process is important to prove the capability of the new model in accurately predicting condensation heat transfer coefficients in micro-fin tubes.

Comparison Between the Prediction Results of the New Pure-Refrigerant Model and the Experimental Data from Wolverine

Wolverine Tube Company provided two experimental condensation data sets for micro-fin tubes using R22 as the working fluid. The data were for the Turbo-A and the Turbo-A crosscut geometries. The flow conditions of the experimental data are listed in Table 4.3. Table 4.4 presents the geometries of the micro-fin tubes used by Wolverine.

Table 4.3 Flow Conditions for R22 Flowing inside Micro-Fin Tubes from Wolverine

Experimental Condition	Range
Saturation temperature (°C)	37.8
Saturation pressure (kPa)	1450
Mass flux (kg/m^2-s)	60 – 1100
Mean vapor quality	0.5

Table 4.4 Tube Geometries of the Micro-Fin Tubes Used by Wolverine

Tube Type	Tube Material	d_o (mm)	th (mm)	e (mm)	n_g	γ (°)	β (°)	L (m)
Turbo-A	Copper	9.53	0.33	0.203	60	18	50	3.66
Turbo-A Crosscut	Copper	9.53	0.33	0.203	60	18	50	3.66

The experimental data sets were plotted for comparison with the prediction results of the new pure-refrigerant model. Figures 4.4 and 4.5 present the results of the two R22 data sets.

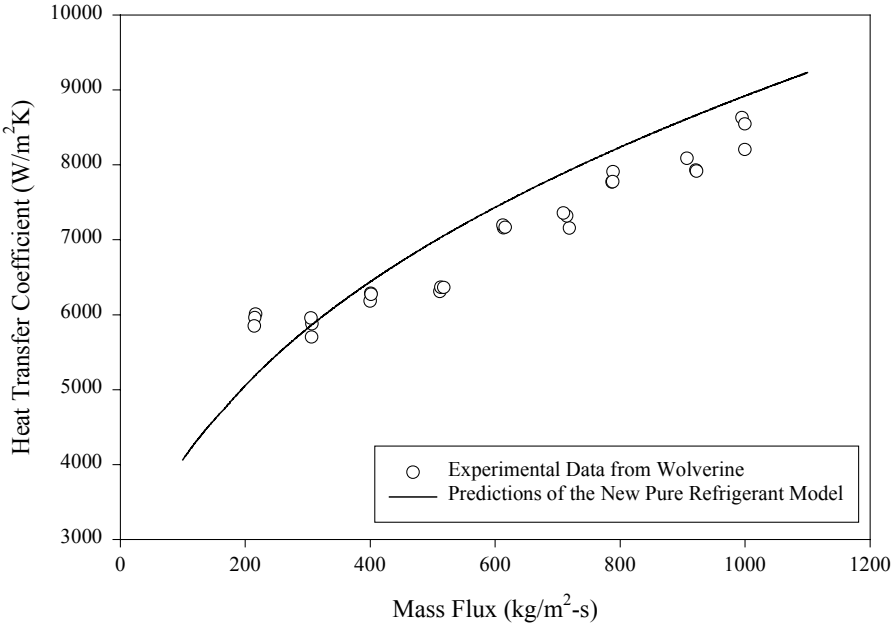

(a)

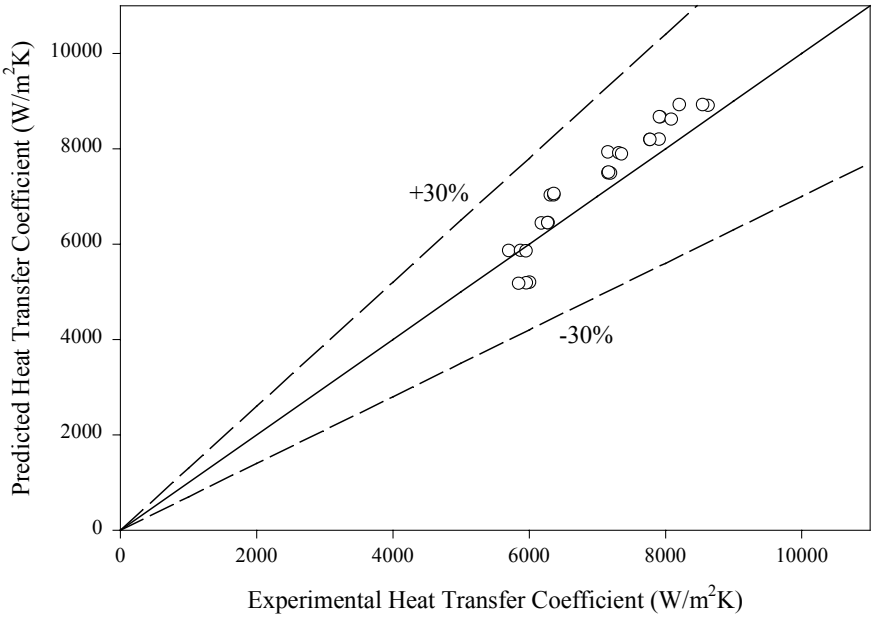

(b)

Figure 4.4 New Pure-Refrigerant Model for the R22 Turbo-A Data Set from Wolverine

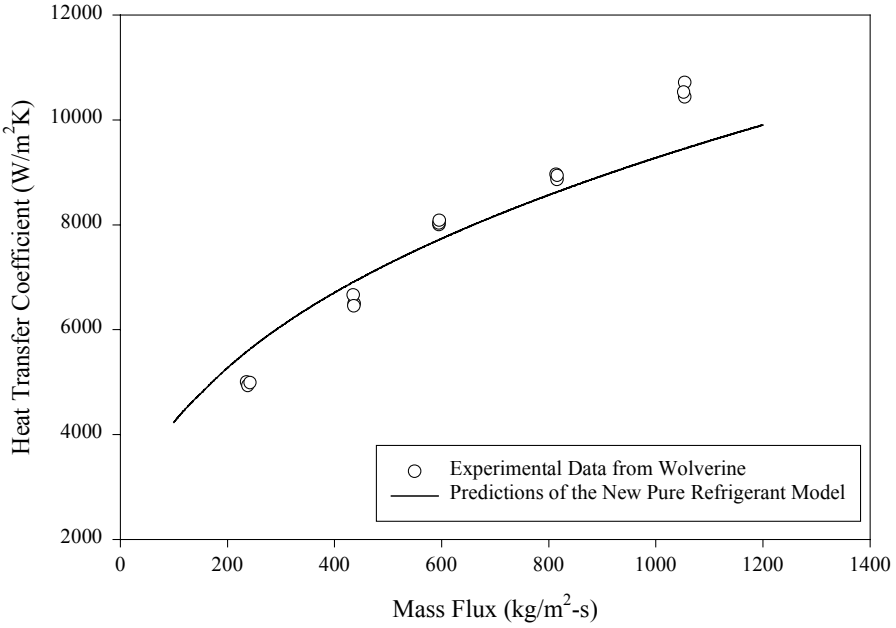

(a)

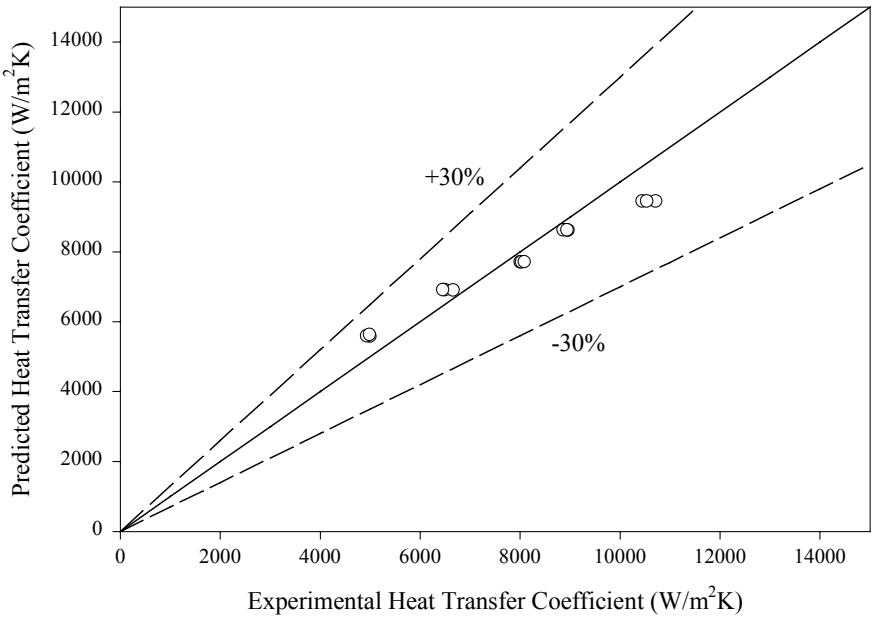

(b)

Figure 4.5 New Pure-Refrigerant Model for the R22 Turbo-A Crosscut Data Set from Wolverine

The mean absolute deviation for R22 in the Turbo-A tube is found to be 7.522%. The new pure-refrigerant model predicts this data set with good accuracy. Figure 4.5 shows the comparison between the experimental data for R22 in the Turbo-A Crosscut tube and the predicted results. The mean absolute deviation for R22 in the Turbo-A Crosscut tube is 7.164%. The prediction results prove that the new pure-refrigerant model has the capability to predict the R22 data sets from Wolverine within 8%. Table 4.5 presents a summary of the *MAD* achieved by the new pure-refrigerant model on the two data sets.

Table 4.5 Mean Absolute Deviation (*MAD*) Achieved by the New Pure-Refrigerant Model for the R22 Data Sets from Wolverine

Refrigerant	Tube Type	*MAD* (%)
R22	Turbo-A	7.522
R22	Turbo-A with Crosscut	7.164

Comparison Between the New Experimental Data Sets and the Prediction Results of the New Pure-Refrigerant Model

Additional pure-refrigerant experimental data sets were collected and compared with the prediction results of the new pure-refrigerant model. These new data sets were not included in developing the new pure-refrigerant model. The capability of the new model to predict the experimental data from other researchers is evaluated. The flow conditions of the new experimental data points and the tube geometries used for the new data sets are listed in Table 3.1 and Table 3.2. The predictions of the new pure-refrigerant model for the new experimental data points are shown in Table 4.6.

Table 4.6 Mean Absolute Deviation (*MAD*) Achieved by the New Pure-Refrigerant Model on the Pure-Refrigerant Data Sets

No.	Reference	Refrigerant	*MAD* value (%)
1	Bogart and Thors (1999)	R22	13.7
2	Chamra et al. (1996)	R22	7.7
3	Ebisu et al. (1994)	R22	12.6
4	Eckels et al. (1991)	R134a	12.6
5	Eckels et al. (1998b)	R134a	18.1
6	Eckels et al. (1999)	R22 R134a	16.5 19.1
7	Goto et al. (1995)	R22	29.2
8	Muzzio et al. (1998)	R22	6.8
9	Schlager L.M. (1988)	R22	11.9
10	Uchida et al. (1996)	R22	22.9

A total number of 250 new experimental data points were collected from 10 different sources. These new experimental data were compared with the prediction results from the new pure-refrigerant model. The achieved *MAD* values are within 20% for most of the experimental data points. This shows that the new pure-refrigerant model is capable of predicting the experimental data points accurately. The prediction results of the new pure-refrigerant model on the additional experimental data sets are shown in the Figures 4.6 and 4.7. The prediction results for the Goto et al. (1995) R22 data set of the new pure-refrigerant model are relatively high because the experiment is run using a short length of micro-fin tube with low mass flux. The flow configuration inside the Goto et al. (1995) experiment may be in the other flow regime instead of the annular flow. Thus, the new pure-refrigerant model, which is applicable for annular flow regime only, achieves high mean absolute deviation for this particular data set.

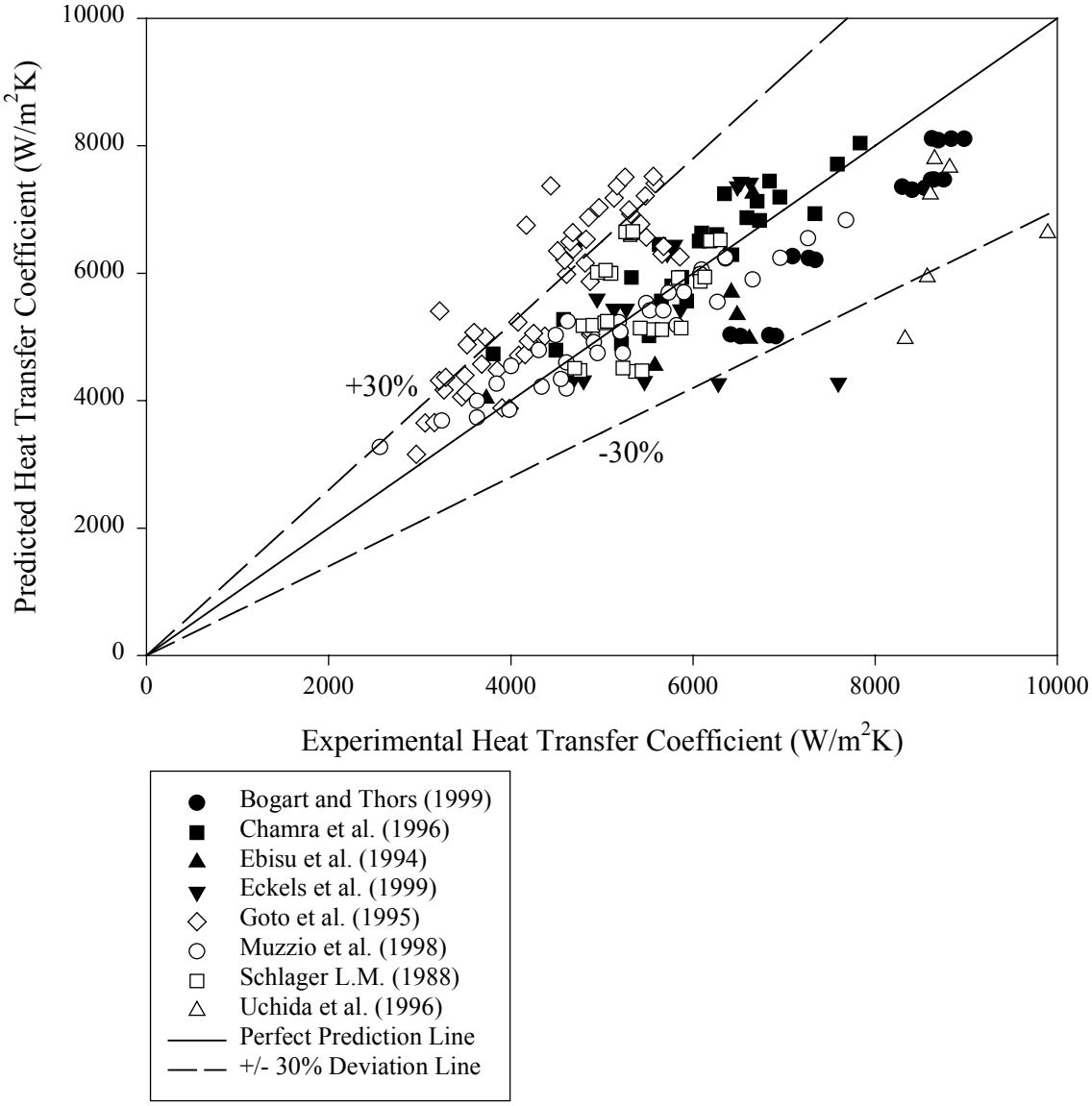

Figure 4.6 New Pure-Refrigerant Model for the New R22 Data Sets

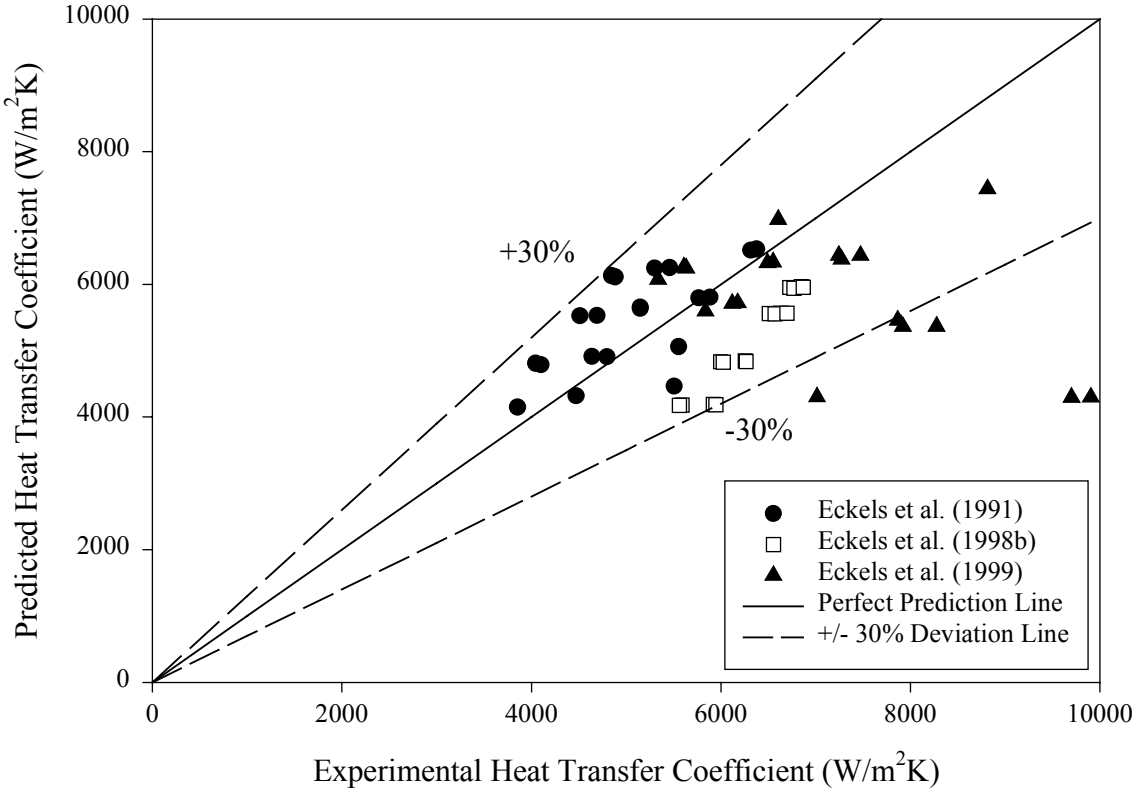

Figure 4.7 New Pure-Refrigerant Model on the New R134a Data Sets

New Correlation for Refrigerant Mixtures Flowing inside Micro-Fin Tubes

The new pure-refrigerant model is extended to predict the heat transfer performance for refrigerant mixtures. The Silver (1947) and Bell and Ghaly (1973) correction to account for mass transfer thermal resistance, which was suggested by Cavallini et al. (1999), is applied to the new refrigerant-mixture model. The final form of the model is written as

$$h_m = \left[\frac{1}{\frac{M_1 \cdot \rho_l \cdot c_{pl} \cdot \left(\frac{\tau_w}{\rho_l} \right)^{M_2}}{T^+} \cdot Rx^{M_3}} + \frac{\frac{\delta Q_{SV}}{\delta Q_T}}{h_v} \right]^{-1} \tag{4.38}$$

where h_v is the heat transfer coefficient of the vapor phase flowing alone in the duct (the value computed by the Dittus-Boelter equation) and $\frac{\delta Q_{SV}}{\delta Q_T}$ is the ratio between the sensible heat duty removed by cooling the vapor and the total heat flow rate exchanged.

$$h_v = 0.023 \cdot \frac{k_v}{d_i} \cdot \left(\frac{G \cdot d_i}{\mu_v} \right)^{0.8} \cdot \left(\frac{c_{pv} \cdot \mu_v}{k_v} \right)^{0.3} \tag{4.39}$$

$$\frac{\delta Q_{SV}}{\delta Q_T} = x \cdot c_{pv} \cdot \left(\frac{\Delta TG}{i_{fg\_m}} \right) \tag{4.40}$$

where ΔTG is the temperature glide and i_{fg_m} is the enthalpy of isobaric condensation of the mixture.

Similar concepts in generating the empirical constants for the new pure-refrigerant model are applied to the new refrigerant-mixture model. The refrigerant-mixture data are obtained from the 110 data points presented in Table 4.7.

Table 4.7 Refrigerant-Mixture Data Sets Used for Generating the New Empirical Constants

Reference	Refrigerant	Number of data points
Bogart and Thors (1999)	R410a	11
Jeong et al. (2000)	R410a	21
Tang et al. (2000)	R410a	37
Ebisu et al. (1998)	R407c	4
Eckels et al. (1999)	R407c	9
Goto et al. (1995)	R407c	28

The variables M_1, M_2, and M_3 are the new empirical constants to be determined from the refrigerant mixture data. A detailed MathCAD worksheet for the calculation process and a sample model file are presented in Appendix G and Appendix H.

The new refrigerant-mixture model to compute the heat transfer during the condensation inside micro-fin tubes is written as

$$h_m = \left[\frac{1}{\dfrac{0.31\rho_l \cdot c_{pl} \cdot \left(\dfrac{\tau_w}{\rho_l}\right)^{0.314}}{T^+} \cdot Rx^{0.993}} + \frac{\dfrac{\delta Q_{SV}}{\delta Q_T}}{h_v} \right]^{-1} \tag{4.41}$$

The constant M_1 must have the dimension $m^{0.338}/s^{0.338}$ in order for the equation to yield the correct dimensions, W/m^2-K, for the heat transfer coefficient. The new refrigerant-mixture model is used to predict the existing experimental data. The prediction results using the new refrigerant-mixture model for the available refrigerant-mixture data sets are presented in Table 4.8.

Table 4.8 Mean Absolute Deviation (*MAD*) Achieved by the New Refrigerant-Mixture Model for the Data Sets Used in Generating the New Empirical Constants

Reference	Refrigerant	*MAD* Value (%)
Bogart and Thors (1999)	R410a	3.7
Jeong et al. (2000)	R410a	21.4
Tang et al. (2000)	R410a	5.8
Ebisu et al. (1998)	R407c	7.9
Eckels et al. (1999)	R407c	4.8
Goto et al. (1995)	R407c	10.9

Table 4.8 shows that the prediction results are excellent with the new refrigerant-mixture model. The mean absolute deviations for all these mixture-refrigerant data sets are less than 22%. Most of the mixture-refrigerant data sets are predicted within 10%. The prediction results for the six data sets using the new refrigerant-mixture model are illustrated in Figures 4.8 and 4.9.

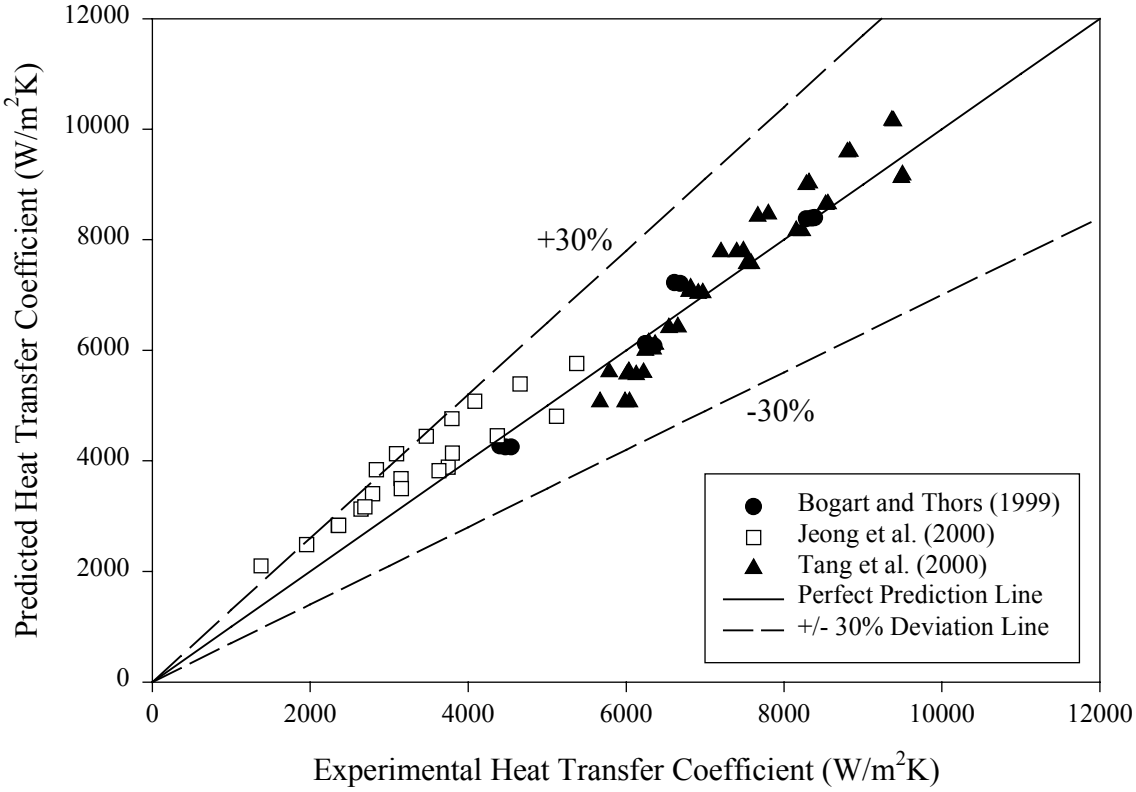

Figure 4.8 New Refrigerant-Mixture Model for the R410a Data Sets Used in Generating the New Empirical Constants

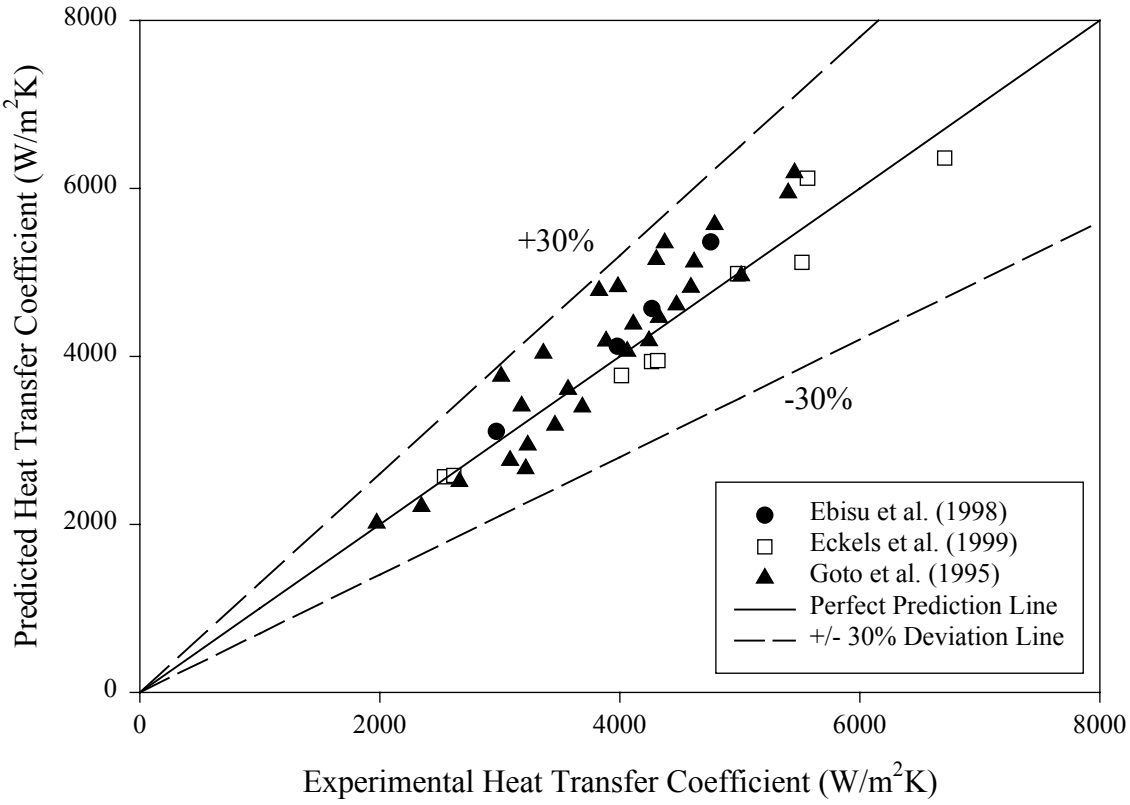

Figure 4.9 New Refrigerant-Mixture Model for the R407c Data Sets Used in Generating the New Empirical Constants.

The new refrigerant-mixture model has the capability to produce better prediction results for the available data sets. Furthermore, the new refrigerant-mixture model is more reliable. The new refrigerant-mixture model is further tested with additional data sets not used in developing the model.

Comparison Between the Prediction Results of the New Refrigerant-Mixture Model and the Experimental Data from Wolverine

Beside the R22 data sets, Wolverine Tube Company also provided two experimental condensation data sets for the Turbo-A and the Turbo-A crosscut geometries using R410a as the working fluid. The flow conditions of the R410a experimental data are listed in Table 4.9, and the geometries of the micro-fin tubes used are presented in Table 4.4.

Table 4.9 Flow Conditions for R410a Flowing inside Micro-Fin Tubes from Wolverine

Experimental Condition	Range
Saturation temperature (°C)	37.8
Saturation pressure (kPa)	2290
Mass flux (kg/m^2-s)	180 – 1100
Mean vapor quality	0.5

The experimental data are plotted for comparison with the predicted results of the new refrigerant-mixture model. Figures 4.10 and 4.11 present the comparison for the R410a data sets.

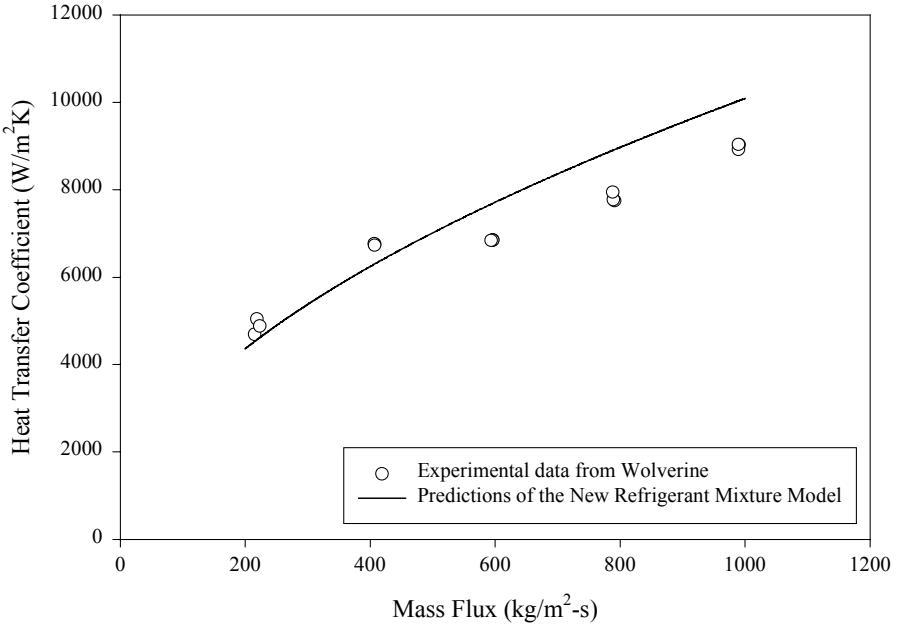

(a)

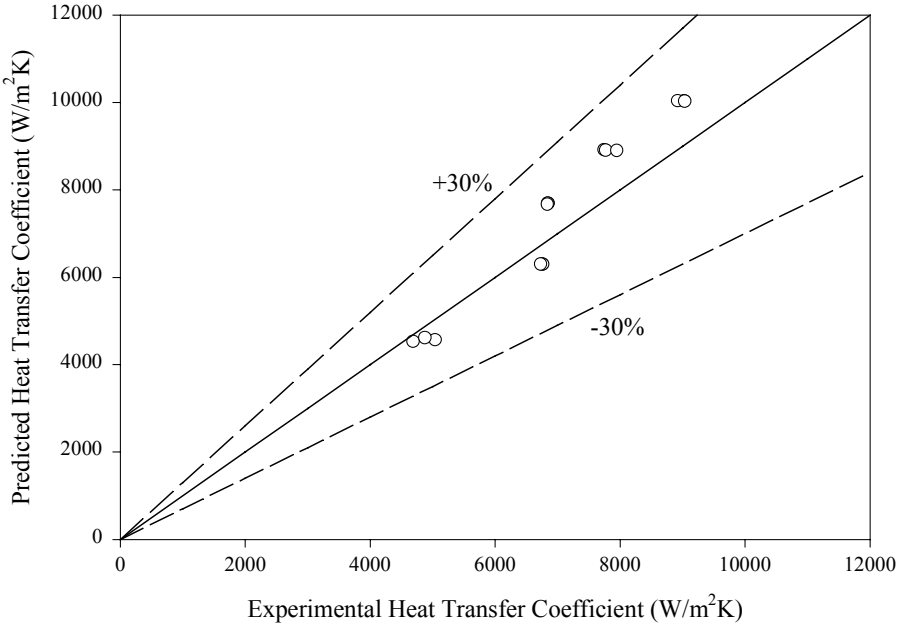

(b)

Figure 4.10 New Refrigerant-Mixture Model for the R410a Turbo-A Data Set from Wolverine

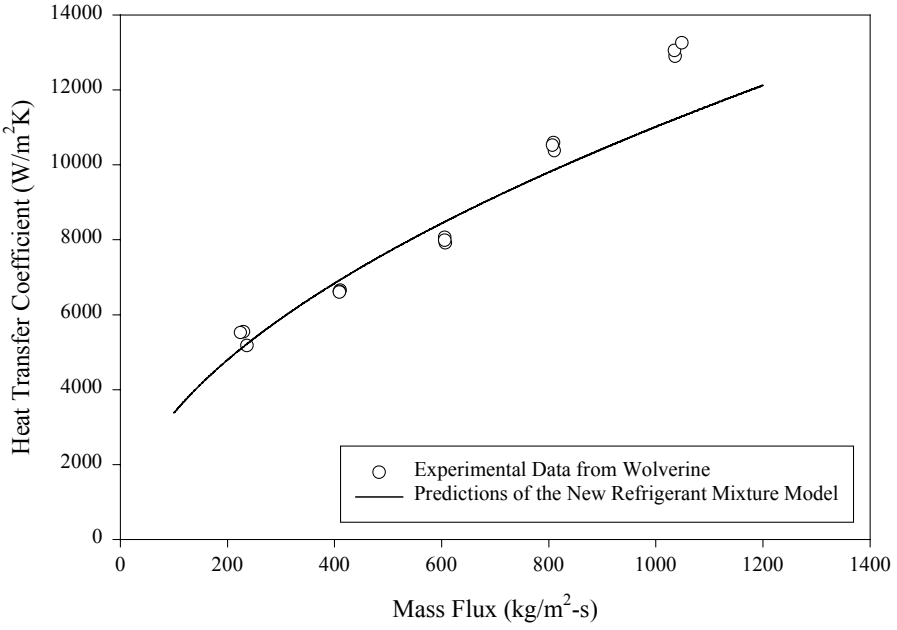

(a)

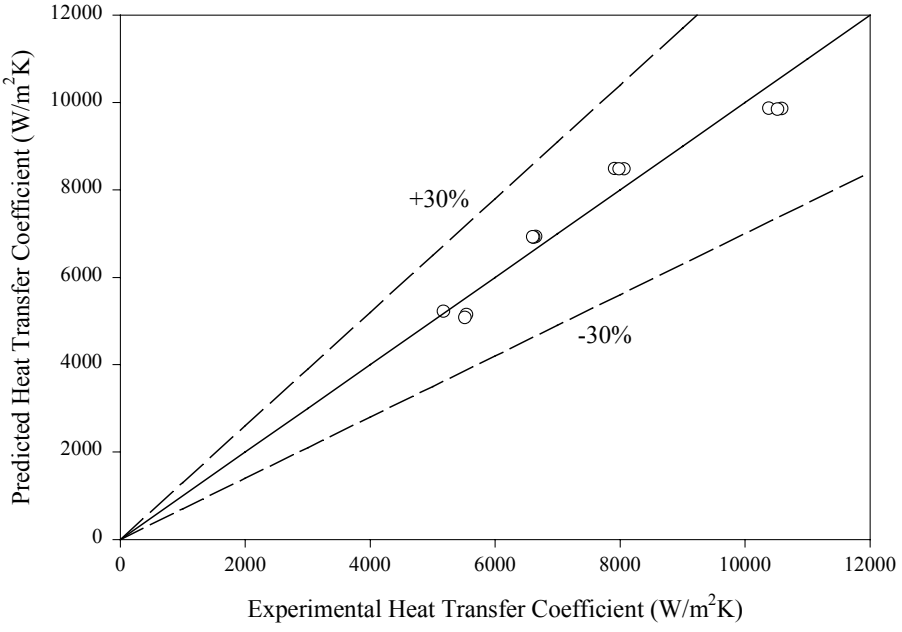

(b)

Figure 4.11 New Refrigerant-Mixture Model for the R410a Turbo-A Crosscut Data Set from Wolverine

The mean absolute deviation for R410a Turbo-A data set is 10.51%. The mean absolute deviation for R410a Turbo-A with crosscut data set is 7.243%. The new refrigerant-mixture model accurately predicts both the R410a data sets from Wolverine.

Table 4.10 shows the summary of the MAD achieved by all the R410a data sets. The new refrigerant-mixture model is capable to predict the data set well with low *MAD* value.

Table 4.10 Mean Absolute Deviation (*MAD*) Achieved by the New Refrigerant-Mixture Model for the R410a Data Sets from Wolverine

Refrigerant	Tube Type	*MAD* (%)
R410a	Turbo-A	10.51%
R410a	Turbo-A with Crosscut	7.243%

Comparison Between the New Experimental Data Sets and the Prediction Results of the New Refrigerant-Mixture Model

Besides the pure refrigerant data sets, the new refrigerant-mixture model was also tested with new experimental data from other sources. These new data sets were not included in developing the new refrigerant-mixture model. The flow conditions of the new experimental data points and the tube geometries used for the new data sets are listed in Table 3.3 and Table 3.4, respectively. The predictions of the new refrigerant-mixture model for the new experimental data points are presented in Table 4.11.

Table 4.11 Mean Absolute Deviation (*MAD*) Achieved by the New Refrigerant-Mixture Model on the Refrigerant-Mixture Data Sets

No.	Reference	Refrigerant	*MAD* Value (%)
1	Ebisu et al. (1994)	R32/R134a (30%/70%)	9.2
2	Eckels et al. (1999)	R410a	16.2

Two new experimental data sets for refrigerant mixtures were collected. These two new experimental data sets were compared with the prediction results of the new refrigerant-mixture model. The achieved *MAD* value is within 17%. This shows that the new refrigerant-mixture model is capable of predicting the experimental data sets accurately. The prediction results of the new refrigerant-mixture model for these two new data sets are illustrated in the Figures 4.12 and 4.13.

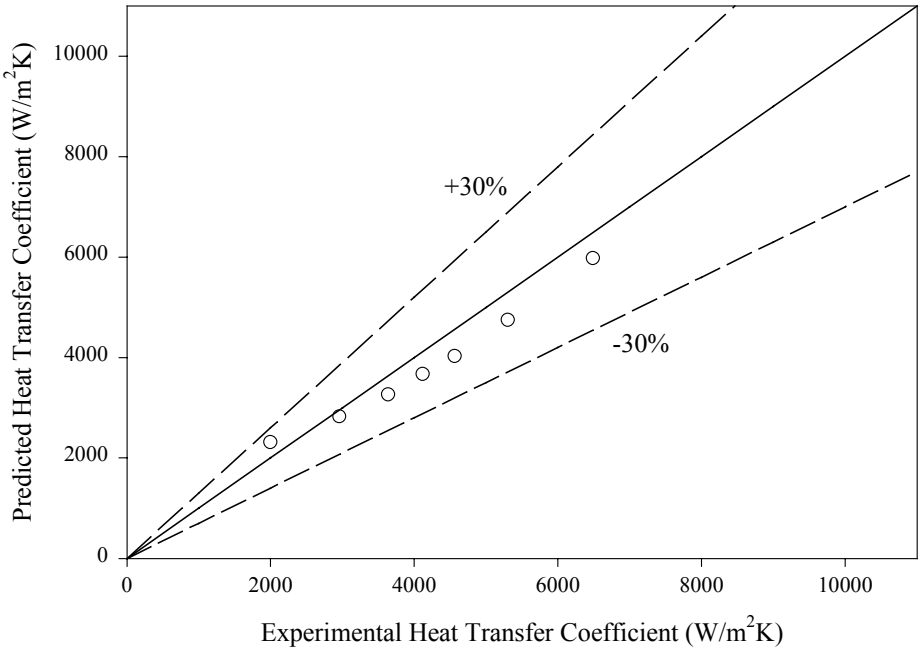

Figure 4.12 New Refrigerant-Mixture Model for the Ebisu et al. (1994) R32/R134a (30%/70%) Data Set

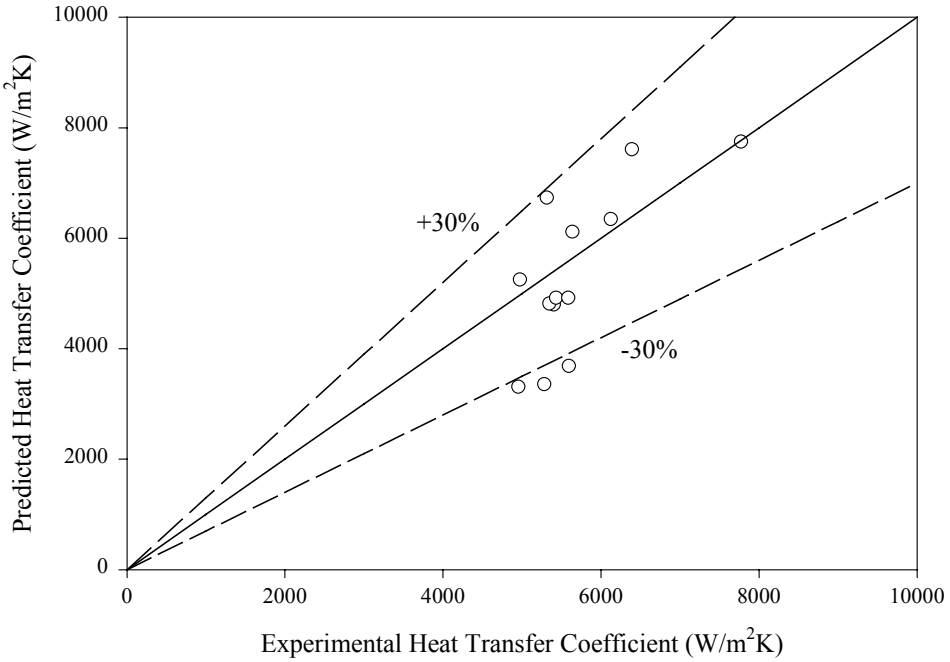

Figure 4.13 New Refrigerant-Mixture Model for the Eckels et al. (1999) R410a Data Set

CHAPTER V

CONCLUSIONS

Three existing condensation heat transfer models have been validated with the available experimental data sets to predict the condensation heat transfer coefficients. These models are the Cavallini et al. (1999) model, the Yu and Koyama (1998) model, and the Kedzierski and Goncalves (1999) model. The Cavallini et al. (1999) model adequately predicts most of the pure-refrigerant data sets. However, the model fails to provide accurate predictions for most of the refrigerant-mixture data sets.

The Yu and Koyama (1998) model is only applicable for pure-refrigerant data sets. However, the model fails, mean absolute deviation over 30%, to predict most of the R22 data sets.

The Kedzierski and Goncalves (1999) model is applicable for both pure-refrigerant and refrigerant-mixture data sets because the model is generated by correlating the convective-condensation Nusselts number of all the tested refrigerants to a single expression that consists of products of dimensionless parameters. The model does not account for the mass transfer thermal resistance in refrigerant mixtures. The model results in relatively high mean absolute deviation for most of the pure-refrigerant data sets. Even so, the model provides relatively good predictions for most of the refrigerant-mixture data sets.

Table 5.1 presents a comparison of the mean absolute deviations of the new pure-refrigerant model, the Cavallini et al. (1999) model, the Kedzierski and Goncalves (1999) model, and the Yu and Koyama (1998) model with the pure-refrigerant data sets. Table 5.2 delineates a comparison of the mean absolute deviations of the new refrigerant-mixture model, the Cavallini et al. (1999) model, and the Kedzierski and Goncalves (1999) model with the refrigerant-mixture data sets. The operating ranges for both the new models are listed in Table 5.3.

Table 5.1 Comparison of the Mean Absolute Deviation (*MAD*) of Different Models for the Pure-Refrigerant Data Sets

	Reference	Refrigerant	*MAD* Value (%)			
			New Pure Model	Cavallini et al. (1999) Model	Kedzierski and Goncalves (1999) Model	Yu and Koyama (1998) Model
1	Eckels et al. (1991)	R134a R12	12.6 12.7	21.5 16.9	12.0 17.7	22.4 25.1
2	Muzzio et al. (1995)	R22	10.7	10.3	20.6	11.0
3	Muzzio et al. (1998)	R22	6.8	7.7	21.7	15.2
4	Schlager L.M. (1988)	R22	11.9	10.7	12.6	38.9
5	Schlager et al. (1989)	R22	16.6	21.4	7.8	44.3
6	Shinohara and Tobe (1985)	R22	18.4	30.7	65.6	166.8
7	Tang et al. (2000)	R22 R134a	5.6 5.4	13.8 12.2	26.2 22.9	9.7 7.8
8	Yasuda et al. (1990)	R22	4.8	6.4	16.1	13.2

Table 5.2 Comparison of the Mean Absolute Deviation (*MAD*) of Different Models for the Refrigerant-Mixture Data Sets

	Reference	Refrigerant	*MAD* Value (%)		
			New Mixture Model	Cavallini et al. (1999) Model	Kedzierski and Goncalves (1999) Model
1	Bogart and Thors (1999)	R410a	3.7	28.5	32.3
2	Ebisu et al. (1994)	R32/R134a (30%/70%)	9.2	41.9	17.0
3	Ebisu et al. (1998)	R407c	7.9	52.5	8.5
4	Eckels et al. (1999)	R410a R407c	16.2 4.8	23.5 22.6	14.3 14.3
5	Goto et al. (1995)	R407c	10.9	50.8	49.2
6	Jeong et al. (2000)	R410a	21.4	81.2	25.2
7	Tang et al. (2000)	R410a	5.8	47.1	11.2

Table 5.3 Operating Ranges for Both the New Pure-refrigerant Model and the New Refrigerant-Mixture Model

Mass Flux	$40\ kg/m^2\text{-}s < G < 850\ kg/m^2\text{-}s$
Saturation Temperature	$30°C < T_{sat} < 50°C$
Helix Angle	$0° < \gamma < 30°$
Fin Height	$0.12\ mm < e < 0.38\ mm$

Overall, both the new pure-refrigerant model and the new refrigerant-mixture model successfully achieved the preliminary objective of generating more reliable prediction results with lower mean absolute deviations. The mean absolute deviations are relatively low when compared to the other models. Besides, these two semi-empirical models are developed with only three empirical constants, which are less than the empirical constants generated in other models.

REFERENCES

Bell, K. J.; Ghaly, M. A. An Approximate Generalized Design Method for Multi-component/partial Condenser. *AIChE Symp. Ser.*, **1973**, 69, 72-79.

Bogart, J.; Thors, P. In-tube Evaporation and Condensation of R-22 and R-410A with Plain and Internally Enhanced Tubes. *Enhanced Heat Transfer*, **1999**, 6, 37-50.

Cavallini, A.; Zecchin, R. High Velocity Condensation of Organic Refrigerants Inside Tubes. *Proceedings of the 8th International Congress of Refrigeration*, **1971**, 2, 193-200.

Cavallini, A.; Zecchin, R. A Dimensionless Correlation for Heat Transfer in Forced Convection Condensation. *Proceedings of the 6th International Heat Transfer Conference*, **1974**, 3, 309-313.

Cavallini, A.; Del Col, D.; Doretti, L.; Longo,G.A.; Rossetto, L. A New Computational Procedure for Heat Transfer and Pressure Drop During Refrigerant Condensation Inside Enhanced Tubes. *Enhanced Heat Transfer*, **1999**, 6, 441-456.

Cavallini, A.; Del Col, D.; Doretti, L.; Longo,G.A.; Rossetto, L. Review Paper Heat Transfer and Pressure Drop During Condensation of Refrigerants inside Horizontal Enhanced Tubes. *International Journal of Refrigeration*, **2000**, 23, 4-25.

Cavallini, A.; Doretti, L.; Klammesteiner, N.; Longo, G. A.; Rossetto, L. Condensation of New Refrigerants Inside Smooth and Enhanced Tubes. *Proceedings of the 19th International Congress of Refrigeration, The Hague*, **1995**, 4, 105-114.

Chamra, L. M.; Webb, R. L.; Randlett, M. R. Advanced Micro-fin Tubes for Condensation. *International Journal of Heat and Mass Transfer*, **1996**, 39(9), 1839-1846.

Collier, J. G.; Thome, J. R. *Convective Boiling and Condensation*. 3rd ed.; Oxford University Press Inc.: New York, 1994.

Cooper, M. G. Saturation Nucleate Pool Boiling – A Simple Correlation. *Department of Engineering Science, Oxford University, England*, **1984**, 86, 785-793.

Dukler, A. E. Fluid Mechanics and Heat Transfer in Vertical Falling Film Systems. *Chem. Engng. Prog. Symp. Series No.30*, **1960**, 56, 1.

Ebisu, T.; Torikoshi, K. In-tube Heat Transfer Characteristics of Refrigerant Mixtures of HFC-32/134a And HFC-32/125/134a. *International Refrigeration Conference (1994: Purdue University)*, **1994**, 293-298.

Ebisu, T.; Torikoshi K. Experimental Study on Evaporation and Condensation Heat Transfer Enhancement for R-407c Using Herringbone Heat Transfer Tube. *ASHRAE Transactions*, **1998,** 104(2), 1044-1052.

Eckels, S. J.; Pate, M. B. Evaporation and Condensation of HFC-134a and CFC-12 in a Smooth Tube and a Micro-fin Tube. *ASHRAE Transactions*, **1991,** 97(2), 71-81.

Eckels, S. J.; Pate, M. B. An Experimental Comparison of Evaporation and Condensation Heat Transfer Coefficients for HFC-134a and CFC-12. *Revue Internationale du froid*, **1991**, 14, 70-77.

Eckels, S. J.; Doerr, T. M.; Pate, M. B. In-tube Heat Transfer and Pressure Drop of R-134a and Ester Lubricant Mixtures in a Smooth Tube and a Micro-fin Tube: Part I - Evaporation. *ASHRAE Transactions*, **1994**, 100(2), 265-282.

Eckels, S. J.; Doerr, T. M.; Pate, M. B. Heat Transfer Coefficients and Pressure Drops for R-134a and an Ester Lubricant Mixture in a Smooth Tube and a Micro-fin Tube. *ASHRAE Transactions*, **1998a**, 104(1a), 366-375.

Eckels, S. J.; Doerr, T. M.; Pate, M. B. A Comparison of the Heat Transfer and Pressure Drop Performance of R134a-lubricant Mixtures in Different Diameter Smooth Tubes and Micro-fin Tubes. *ASHRAE Transactions*, **1998b,** 104(1a), 376-386.

Eckels, S. J.; Tesene, B. A. A comparison of R22, R134a, R410a, and R407c Condensation Performance in Smooth and Enhanced Tubes: Part 1, Heat Transfer. *ASHRAE Transaction*, **1999**, 4313, 428-441.

Friedel, L. Improved Friction Pressure Drop Correlations for Horizontal and Vertical Two Phase Pipe Flow, paper E2. European Two Phase Flow Group Meeting, Ispra, Italy, 1979.

Ganchev, B. G.; Musvik, A. B. Experimental Study of Hydrodynamic and Heat-Transfer Processes in the Downward Motion of a Two-phase Flow under Annular and Dispersed-annular Conditions. *Journal of Engineering Physics*, **1976**, 31, 1, 760-766.

Goto, M.; Inoue, N.; Koyama, K. Condensation Heat Transfer of HFC-22 and Its Alternative Refrigerants Inside an Internally Grooved Horizontal Tube. *Proceedings of 19th International Congress on Refrigeration, The Hagul*, **1995**, 4A, 254-260.

Haraguchi, H.; Koyama, S.; Fujii, T. Condensation of Refrigerants HFC22, HFC134a and HCFC123 in a Horizontal Smooth Tube (2nd Report, Proposals of Empirical Expressions for Local Heat Transfer Coefficient). *Transactions JSME*, **1994**, 60, 574, 245-252 (in Japanese).

Hayashi, T. Enhanced Condensation Heat Transfer of Refrigerant HFC134a in Horizontal Tubes. Master Theses, Kyushu University, Japan, 1998 (in Japanese).

Hitachi Cable, Ltd.; Technical Data 14-958. Effect on Performance of Expanding the Thermofin-EX and Thermofin-HEX, Tube; Hitachi Cable, Ltd.: **1987**; p14-958.

Hori, M.; Shinohara, H. Internal Heat Transfer Characteristics of Small-diameter Thermofin Tubes. *Hitachi Cable Review*, **1991**, 10, 85-90.

Jeong, K. T.; Park, S. K.; Kim, M. H. Enhanced Effect of a Horizontal Micro-fin Tube for Condensation Heat Transfer with R22 and R410A. *Enhanced Heat Transfer*, **2000**, 7, 97-107.

Kedzierski, M. A.; Goncalves, J. M. Horizontal Convective Condensation of Alternative Refrigerants Within a Microfin Tubes. *Enhanced Heat Transfer*, **1999**, 6, 161-178.

Koyama, S.; Miyara, H.; Takamatsu, H.; Yonemoto, K.; Fujii, T. Condensation and Evaporation of Non-azeotropic Refrigerant Mixtures of R22 and R114 inside a Spirally Grooved Horizontal Tube. *The Reports of Institute of Advanced Material Study, Kyushu University*, **1988**, 1, 1, 57-75 (in Japanese).

MathCAD 2000 Professional; Mathsoft Inc.: Cambrigde, MA, 1995.

Miyara, A.; Nonaka, K.; Yoshida, K.; Nakashima, T.; Uehara, H.; Taniguchi, M. Condensation Heat Transfer and Flow Pattern of a W-shaped Microfin Tube. *Proceedings 1998 JAR Annual Conference, Tokyo*, **1998** (in Japanese).

Muzzio, A.; Niro, A.; Arosio, S. Heat Transfer and Pressure Drop During Evaporation and Condensation of R22 Inside 9.52-mm O.D. Microfin Tubes of Different Geometries. *Enhanced Heat Transfer,* **1998,** 5(1), 39-52.

Muzzio, A.; Niro, A.; Garavaglia, M. Flow Patterns and Heat Transfer Coefficients in Flow-Boiling and Convective Condensation of R22 Inside a Microfin Tube of New Design. *Proceedings of 11th International Heat Transfer Conference*, **1998**, 2(11), 291-296.

Newell, T. A.; Shah, R. K. An Assessment of Refrigerant Heat Transfer, Pressure Drop, and Void Fraction Effects In Microfin Tubes. *International Journal of Heating, Ventilating, Air-Conditioning and Refrigerating Research*, **2001**, 7, 125-153.

REFPROP, 6.01; National Institute of Standards and Technology: Boulder, CO, 1998.

Schlager, L. M. The Effect of Oil on Heat Transfer and Pressure Drop During Evaporation and Condensation of Refrigerant Inside Augmented Tubes. Ph. D. Dissertation, Iowa State University, Ames, Iowa, 1988.

Schlager, L. M.; Pate, M. B.; Bergles, A. E. Heat Transfer and Pressure Drop During Evaporation and Condensation of R22 in Horizontal Micro-fin Tubes. *International Journal of Refrigeration*, **1989**, 12, 6-14.

Shikazono, N.; Itoh, M.; Uchida, M.; Fukushima, T.; Hatada, T. An Analytical Model to Predict the Condensation Heat Transfer Coefficient in Horizontal Microfin Tubes. *ASHRAE Transaction*, **1998**, 104(2), 143-152.

Shinohara, Y.; Tobe, M. Development of an Improved "Thermofin Tube". *Hitachi Cable Review*, **1985,** 4, 47-50.

Silver, L. Gas cooling with aqueous condensation. *Trans. Inst. Chem. Eng.*, **1947**, 25, 30-42.

Smith, S.L. Void Fraction in Two-phase Flow: A Correlation Based on Equal Velocity Head Model. *Heat and Fluid Flow*, **1970**, 1, 1, 22-39.

Tang, L. Y.; Ohadi, M. M.; Johnson, A. T. Flow Condensation in Smooth and Micro-fin Tubes with HFC-22, HFC-134a and HFC-410A Refrigerants Part I: Experimental Results. *Enhanced Heat Transfer*, **2000**, 7, 289-310.

Tang, L. Y.; Ohadi, M. M.; Johnson, A. T. Flow Condensation in Smooth and Micro-fin Tubes with HFC-22, HFC-134a and HFC-410A Refrigerants Part II: Design Equations. *Enhanced Heat Transfer*, **2000**, 7, 311-325.

Uchida, M.; Itoh, M.; Shikazono, N.; Kudoh, M. Expeimental Study on the Heat Transfer Performance of a Zeotropic Refrigerant Mixture in Horizontal Tubes. *Proceedings of the 1996 International Refrigeration Conference at Purdue*, **1996**, 133-138.

Webb, R. L. Enhancement of film condensation. *International Com. Heat Mass Transfer*, **1988**, 15, 475-507.

Yasuda, K; Ohizumi, K.; Makoto, H.; Kawamata, O. Development of Condensing "Thermofin-Hex-C Tube". *Hitachi Cable Review,* **1990,** 9, 27-30.

Yu, J.; Koyama, S. Condensation Heat Transfer of Pure Refrigerants in Microfin Tubes. *Proceedings of the 1998 International Refrigeration Conference at Purdue*, **1998**, 325-330.

APPENDIX A

MathCAD Files for the Cavallini et al. (1999)

Pure-Refrigerant Model

Sample Data File

Experimental Data for
for R22 in Micro-Fin Tubes
from Hitachi Cable TD 14-958, 1987

R22

Define flow condition (Source: ASHRAE fundamental 1997):

$T_{sat} := 40$ C $P_{sat} := 1540000$ Pa

$q := 10000$ $W \cdot m^{-2}$

$G := 100 .. 250$ $kg \cdot m^{-2} \cdot s^{-1}$

$g := 9.807$ $m \cdot s^{-2}$

Import property table generated by REFPROP.

:= C:\..\R22.txt := C:\..\R22 Info.txt

Calculate thermodynamics and transport properties by Mathcad cubic spline interpola

Reference:C:\MFT Project\Condensation\Properties_Condensation.mcd

TUBE = Thermofin EX

Define tube configuration:
Tube Materials ==> Cooper

Tube properties,

$d_o := 9.52 \cdot 10^{-3}$ m $th := 0.48 \cdot 10^{-3}$ m

$d_i := d_o - 2 \cdot th$ $d_i = 8.56 \times 10^{-3}$ m

Micro-fin properties, (assumption: equal triangular micro-fin)

$\gamma := 18deg$ $\beta := 53 \cdot deg$ $n_f := 60$ $e := 0.2 \cdot 10^{-3}$ m

$L := 3.05$ m $b := \frac{\pi \cdot d_i}{n_f} - 2 \cdot e \cdot \tan\left(\frac{\beta}{2}\right)$ m $p := \frac{\pi \cdot d_i}{n_f}$

Experimental Data

$x := 0.5$

$Data_{expG\_TFINEX} :=$

	0	1
0	144.38	5.47
1	185.79	5.67
2	202.47	5.57
3	223.19	5.8

$h_{cond\_expG\_TFINEX} := Data_{expG\_TFINEX}^{\langle 1 \rangle} \cdot 1000$

$G_{exp\_TFINEX} := Data_{expG\_TFINEX}^{\langle 0 \rangle}$

Sample Model File

Define empirical constants,

$$A := 0.05 \qquad B := 0.8 \qquad C := \frac{1}{3}$$

$$s := \begin{cases} 2.00 & \text{if } \frac{e}{d_i} < 0.04 \\ 1.40 & \text{if } \frac{e}{d_i} \geq 0.04 \end{cases} \qquad t := \begin{cases} -0.26 & \text{if } \frac{e}{d_i} < 0.04 \\ -0.08 & \text{if } \frac{e}{d_i} \geq 0.04 \end{cases}$$

Define Reynolds Number,

$$Re_{eq}(G, x) := \frac{4 \cdot G \cdot A_c \cdot \left[(1 - x) + x \cdot \left(\frac{\rho_l}{\rho_v} \right)^{\frac{1}{2}} \right]}{\pi \cdot d_i \cdot \mu_l}$$

Define geometry enhancement factor,

$$Rx := \left[\frac{2 \cdot e \cdot n_f \cdot \left(1 - \sin\left(\frac{\beta}{2} \right) \right)}{\pi \cdot d_i \cdot \cos\left(\frac{\beta}{2} \right)} + 1 \right] \cdot \frac{1}{\cos(\gamma)}$$

Define Froude Number,

$$Fr(G) := \left(\frac{G}{\rho_v} \right)^2 \cdot \frac{1}{g \cdot d_i}$$

Bond Number

$$Bo := \frac{g \cdot \rho_l \cdot e \cdot \pi \cdot d_i}{8 \cdot \sigma \cdot n_f}$$

Define Nusselt number,

$$Nu(G,x) := A \cdot Re_{eq}(G,x)^{B} \cdot Pr_l^{C} \cdot Rx^{s} \cdot (Bo \cdot Fr(G))^{t}$$

Define two-phase heat transfer coefficient (Cavallini, 19

$$h(G,x) := \frac{A \cdot Re_{eq}(G,x)^{B} \cdot Pr_l^{C} \cdot Rx^{s} \cdot (Bo \cdot Fr(G))^{t} \cdot k_l}{d_i}$$

Sample Property File

Cubic Spline interpolation for all required properties.

$P := \text{TABLE}\ \langle 0 \rangle$ $T_{l\_} := \text{TABLE}\ \langle 1 \rangle$ $T_{v\_} := \text{TABLE}\ \langle 13 \rangle$

$\rho_{l\_} := \text{TABLE}\ \langle 2 \rangle$ $\rho_{v\_} := \text{TABLE}\ \langle 3 \rangle$ $i_{l\_} := \text{TABLE}\ \langle 4 \rangle$ $i_{v\_} := \text{TABLE}\ \langle 5 \rangle$

$c_{p\_l\_} := \text{TABLE}\ \langle 6 \rangle$ $c_{p\_v\_} := \text{TABLE}\ \langle 7 \rangle$ $\mu_{l\_} := \text{TABLE}\ \langle 8 \rangle$ $\mu_{v\_} := \text{TABLE}\ \langle 9 \rangle$

$k_{l\_} := \text{TABLE}\ \langle 10 \rangle$ $k_{v\_} := \text{TABLE}\ \langle 11 \rangle$ $\sigma\_ := \text{TABLE}\ \langle 12 \rangle$

$\rho_{l\_s} := \text{cspline}(P, \rho_{l\_})$ $\rho_{v\_s} := \text{cspline}(P, \rho_{v\_})$ $i_{l\_s} := \text{cspline}(P, i_{l\_})$

$c_{p\_l\_s} := \text{cspline}(P, c_{p\_l\_})$ $c_{p\_v\_s} := \text{cspline}(P, c_{p\_v\_})$ $\mu_{l\_s} := \text{cspline}(P, \mu_{l\_})$

$k_{l\_s} := \text{cspline}(P, k_{l\_})$ $k_{v\_s} := \text{cspline}(P, k_{v\_})$ $\sigma_s := \text{cspline}(P, \sigma\_)$

$T_{l\_s} := \text{cspline}(P, T_{l\_})$ $T_{v\_s} := \text{cspline}(P, T_{v\_})$ $i_{v\_s} := \text{cspline}(P, i_{v\_})$

$\mu_{v\_s} := \text{cspline}(P, \mu_{v\_})$

$\rho_l(PP) := \text{interp}(\rho_{l\_s}, P, \rho_{l\_}, PP)$ $\rho_v(PP) := \text{interp}(\rho_{v\_s}, P, \rho_{v\_}, PP)$

$i_l(PP) := \text{interp}(i_{l\_s}, P, i_{l\_}, PP)$ $i_v(PP) := \text{interp}(i_{v\_s}, P, i_{v\_}, PP)$

$c_{p\_l}(PP) := \text{interp}(c_{p\_l\_s}, P, c_{p\_l\_}, PP)$ $c_{p\_v}(PP) := \text{interp}(c_{p\_v\_s}, P, c_{p\_v\_}, PP)$

$\mu_l(PP) := \text{interp}(\mu_{l\_s}, P, \mu_{l\_}, PP)$ $\mu_v(PP) := \text{interp}(\mu_{v\_s}, P, \mu_{v\_}, PP)$

$k_l(PP) := \text{interp}(k_{l\_s}, P, k_{l\_}, PP)$ $k_v(PP) := \text{interp}(k_{v\_s}, P, k_{v\_}, PP)$

$\sigma(PP) := \text{interp}(\sigma_s, P, \sigma\_, PP)$

$T_l(PP) := \text{interp}(T_{l\_s}, P, T_{l\_}, PP)$ $T_v(PP) := \text{interp}(T_{v\_s}, P, T_{v\_}, PP)$

Define fluid properties: (Source: REFPROP 6.01)

$\rho_l := \rho_l\left(P_{sat}\cdot 10^{-6}\right)$ $\quad \rho_l = 1127.778 \quad kg\cdot m^{-3}$

$\rho_v := \rho_v\left(P_{sat}\cdot 10^{-6}\right)$ $\quad \rho_v = 66.492 \quad kg\cdot m^{-3}$

$c_{p\_l} := c_{p\_l}\left(P_{sat}\cdot 10^{-6}\right)\cdot 10^{3}$ $\quad c_{p\_l} = 1.34\times 10^{3} \quad J\cdot kg^{-1}\cdot K^{-1}$

$c_{p\_v} := c_{p\_v}\left(P_{sat}\cdot 10^{-6}\right)\cdot 10^{3}$ $\quad c_{p\_v} = 996.544 \quad J\cdot kg^{-1}\cdot K^{-1}$

$\mu_l := \mu_l\left(P_{sat}\cdot 10^{-6}\right)\cdot 10^{-6}$ $\quad \mu_l = 1.391\times 10^{-4}\left(10^{-6}\right) \quad Pa\cdot s$

$\mu_v := \mu_v\left(P_{sat}\cdot 10^{-6}\right)\cdot 10^{-6}$ $\quad \mu_v = 1.353\times 10^{-5}\left(10^{-6}\right) \quad Pa\cdot s$

$k_l := k_l\left(P_{sat}\cdot 10^{-6}\right)$ $\quad k_l = 0.077 \quad W\cdot m^{-1}\cdot K^{-1}$

$k_v := k_v\left(P_{sat}\cdot 10^{-6}\right)$ $\quad k_v = 0.013 \quad W\cdot m^{-1}\cdot K^{-1}$

$i_{fg} := \left(i_v\left(P_{sat}\cdot 10^{-6}\right) - i_l\left(P_{sat}\cdot 10^{-6}\right)\right)\cdot 10^{3}$ $\quad i_{fg} = 1.664\times 10^{5}\left(10^{3}\right) \quad J\cdot kg^{-1}$

$\sigma := \sigma\left(P_{sat}\cdot 10^{-6}\right)$ $\quad \sigma = 6.013\times 10^{-3} \quad N\cdot m^{-1}$

$\Delta T := \left|T_{sat} - T_l\left(P_{sat}\cdot 10^{-6}\right)\right|$ $\quad \Delta T = 0.171 \quad K$

$Pr_l := \dfrac{\mu_l\cdot c_{p\_l}}{k_l}$ $\quad Pr_l = 2.427$

$Pr_v := \dfrac{\mu_v\cdot c_{p\_v}}{k_v}$ $\quad Pr_v = 1.034$

$P_c := \left|\text{INFO}^{\langle 1\rangle}\right|\cdot 10^{6}$ $\quad P_c = 4.99\times 10^{6}$

Sample Calculation File

Correlation for Pure Refrigerant flowing inside Micro-fin Tubes

R22

Source of Correlations:
1. Cavallini et al. (1999)

Source of Experimental Data:
1. Hitachi Cable TD 14-958, 1987

Import experimental data from Hitachi (1987):

Define flow condition (Source: REFPROP 6.01) and tube configuration:

Tube ==> TFIN HEX

Reference:C:\MFT Project\Condensation\Data_Hitachi_R22_MFT_TFINHEX _1987.

Import Cavallini model (1999):

Reference:C:\MFT Project\Condensation\Cavallini_Condensation_Model.mcd

Tube ==> TFIN HEX

Define range of mass flux, $G := 100 .. 300 \quad kg \cdot m^{-2} \cdot s^{-1}$

$x = 0.5$

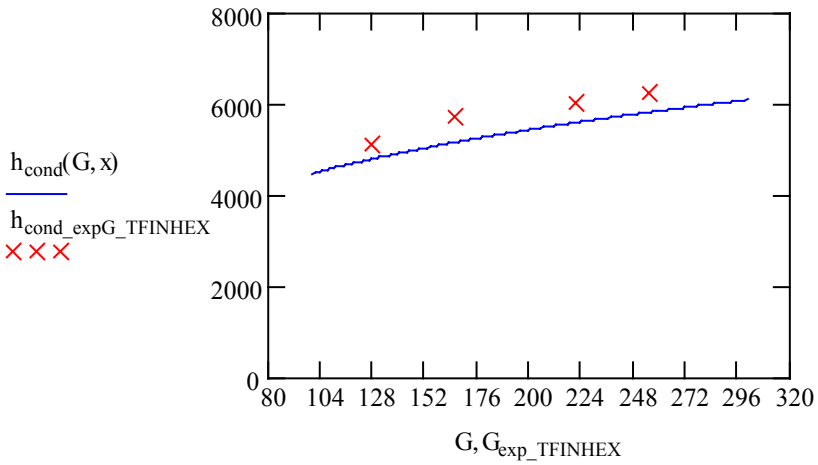

WRITEPRN("temp1.dat") := $\overrightarrow{h_{cond}(G_{exp\_TFINHEX}, x)}$

WRITEPRN("temp2.dat") := $h_{cond\_expG\_TFINHEX}$

$$\text{APPENDPRN("temp1.dat")} := \overrightarrow{h_{cond}\left(G_{exp\_TFINEX}, x\right)}$$

$$\text{APPENDPRN("temp2.dat")} := h_{cond\_expG\_TFINEX}$$

$$\text{APPENDPRN("temp1.dat")} := \overrightarrow{h_{cond}\left(G_{exp\_TFINEX'}, x\right)}$$

$$\text{APPENDPRN("temp2.dat")} := h_{cond\_expG\_TFINEX'}$$

Plot for $h_{predicted}$ versus $h_{experiment}$

$h_{predicted} := \text{READPRN("temp1.dat")}$ $h_{experiment} := \text{READPRN("temp2.dat")}$

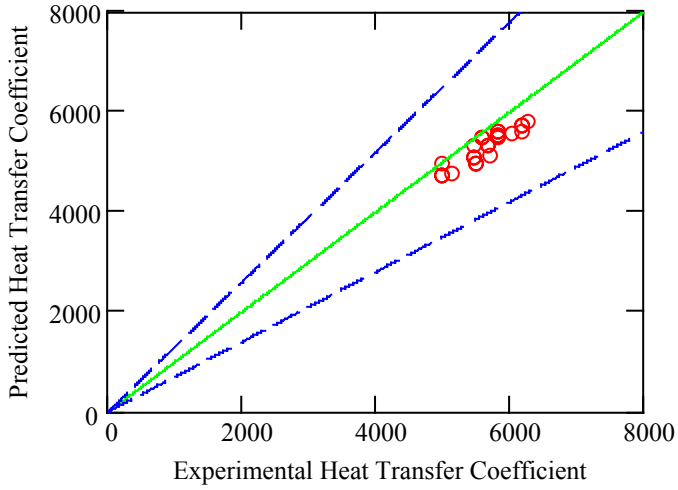

$$MAD := \frac{1}{N} \cdot \sum \overrightarrow{\frac{\left|h_{experiment} - h_{predicted}\right|}{h_{experiment}}} \qquad MAD = 8.051\,\%$$

APPENDIX B

MathCAD Files for the Yu and Koyama (1998) Model

Sample Model File

Source of Correlations: Yu and Koyama (1998)

Define Reynolds number,

$$Re_L(x,G) := \frac{G\cdot(1-x)\cdot d_i}{\mu_l}$$

Define Martinelli parameter,

$$X_{tt}(x) := \left(\frac{1-x}{x}\right)^{0.9}\cdot\left(\frac{\rho_v}{\rho_l}\right)^{0.5}\cdot\left(\frac{\mu_l}{\mu_v}\right)^{0.1}$$

Define Two-phase multiplier,

$$\Phi_v(x,G) := 1.1 + 1.3\cdot\left[\frac{G\cdot X_{tt}(x)}{\sqrt{g\cdot d_i\cdot\rho_v\cdot(\rho_l-\rho_v)}}\right]^{0.35}$$

Define Forced convective condensation component,

$$Nu_F(x,G) := 0.152\cdot\left(0.3 + 0.1\cdot Pr_l^{1.1}\right)\left(\frac{\Phi_v(x,G)}{X_{tt}(x)}\right)\cdot Re_L(x,G)^{0.68}$$

Define Void fraction,

$$\xi(x) := \left[1 + \frac{\rho_v}{\rho_l}\cdot\left(\frac{1-x}{x}\right)\cdot\left[0.4 + 0.6\cdot\sqrt{\frac{\frac{\rho_l}{\rho_v} + 0.4\cdot\left(\frac{1-x}{x}\right)}{1 + 0.4\cdot\left(\frac{1-x}{x}\right)}}\right]\right]^{-1}$$

$$A(x) := 10\cdot(1-\xi(x))^{0.1} - 8.0$$

$$H(x) := \xi(x) + A(x)\cdot\sqrt{\xi(x)}\cdot\left(1-\sqrt{\xi(x)}\right)$$

Define Galileo number,

$$Ga := \frac{g\cdot\rho_l^{\,2}\cdot d_i^{\,3}}{\mu_l^{\,2}}$$

Define Phase change number,

$$Ph_l := \frac{c_{p\_l} \cdot (\Delta T)}{i_{fg}}$$

Free Convection condensation,

$$Nu_B(x, G) := 0.725 \cdot \eta_A^{-0.25} \cdot H(x) \cdot \left(\frac{Ga \cdot Pr_l}{Ph_l} \right)^{0.25}$$

Define Nusselt number,

$$Nu(x, G) := \left(Nu_F(x, G)^2 + Nu_B(x, G)^2 \right)^{0.5}$$

Define Heat transfer coefficient,

$$h(G, x) := \frac{k_l \cdot Nu(x, G)}{d_i}$$

APPENDIX C

MathCAD Files for the Kedzierski and Goncalves (1999) Model

Sample Model File

Source of Correlations: Kedzierski and Goncalves(1999)

Define Reynolds Number,

$$Re(G) := \frac{G \cdot d_h}{\mu_l}$$

Define Reduced Pressure,

$$P_r := \frac{P_{sat}}{P_c}$$

Refrigerant Jakob number,

$$Ja := \frac{i_{fg}}{c_{p\_l} \cdot \Delta T}$$

Define Dimensionless Specific Volume,

$$Sv(x) := \frac{\left(\frac{\rho_l}{\rho_v}\right) - 1}{\left(x \cdot \frac{\rho_l}{\rho_v} + 1 - x\right)}$$

$$B(x) := -0.578 \cdot x^2 \qquad C(x) := -0.474x^2 \qquad D(x) := 2.531x$$

Define Nusselt Number,

$$Nu(x, G) := 2.256 \cdot Re(G)^{0.303} \cdot Ja^{0.232x} \cdot Pr_l^{0.393} \cdot P_r^{B(x)} \cdot \left(-\log\left(P_r\right)\right)^{C(x)} \cdot Sv(x)^{D(x)}$$

Define Heat Transfer Coefficient,

$$h(x, G) := \frac{k_l \cdot Nu(x, G)}{d_h}$$

APPENDIX D

MathCAD Files for the Cavallini et al. (1999)

Refrigerant-Mixture Model

Sample Model File

Source of Correlations:
1. Cavallini et al. (1999)

Define empirical constants,

$$A := 0.05 \qquad B := 0.8 \qquad C := \frac{1}{3}$$

$$s := \begin{cases} 2.00 & \text{if } \frac{e}{d_i} < 0.04 \\ 1.40 & \text{if } \frac{e}{d_i} \geq 0.04 \end{cases} \qquad t := \begin{cases} -0.26 & \text{if } \frac{e}{d_i} < 0.04 \\ -0.08 & \text{if } \frac{e}{d_i} \geq 0.04 \end{cases}$$

Define Reynolds Number,

$$Re_{eq}(G, x) := \frac{4 \cdot G \cdot A_c \cdot \left[(1 - x) + x \cdot \left(\frac{\rho_l}{\rho_v} \right)^{\frac{1}{2}} \right]}{\pi \cdot d_i \cdot \mu_l}$$

Define geometry enhancement factor,

$$Rx := \left[\frac{2 \cdot e \cdot n_f \cdot \left(1 - \sin\left(\frac{\beta}{2} \right) \right)}{\pi \cdot d_i \cdot \cos\left(\frac{\beta}{2} \right)} + 1 \right] \cdot \frac{1}{\cos(\gamma)}$$

Define Froude Number,

$$Fr(G) := \left(\frac{G}{\rho_v} \right)^2 \cdot \frac{1}{g \cdot d_i}$$

Define Bond Number,

$$Bo := \frac{g \cdot \rho_l \cdot e \cdot \pi \cdot d_i}{8 \cdot \sigma \cdot n_f}$$

Define Nusselt number,

$$Nu(G, x) := A \cdot Re_{eq}(G, x)^B \cdot Pr_l^C \cdot Rx^s \cdot (Bo \cdot Fr(G))^t$$

Define heat transfer coefficient (Cavallini, 1999),

$$h(G, x) := \frac{A \cdot Re_{eq}(G, x)^B \cdot Pr_l^C \cdot Rx^s \cdot (Bo \cdot Fr(G))^t \cdot k_l}{d_i}$$

Define the ratio between the sensible heat duty removed by cooling the vapour and the to heat flow rate exchanged,

$$\delta Q_{SV\_T}(x) := x \cdot c_{p\_v} \cdot \left(\frac{\Delta TG}{i_{fg}} \right)$$

Define the heat transfer coefficient of the vapour phase flowing alone in the duct, (Dittus-Boelter, 1930)

$$h_G(G, x) := 0.023 \cdot \frac{k_v}{d_i} \cdot \left(\frac{G \cdot d_i}{\mu_v} \right)^{0.8} \cdot \left(\frac{c_{p\_v} \cdot \mu_v}{k_v} \right)^{0.3}$$

Define the corrected heat transfer coefficient for zeotropic mixture,

$$h_m(G, x) := \left(\frac{1}{h(G, x)} + \frac{\delta Q_{SV\_T}(x)}{h_G(G, x)} \right)^{-1}$$

APPENDIX E

MathCAD Worksheet for Generating the New Empirical Constants for The New Pure-Refrigerant Model

Define independent parameter:

hcond := READPRN("hcond.dat")

τ := READPRN("Tao.dat")

T := READPRN("Temp.dat")

Rx := READPRN("Rx.dat")

F1 := READPRN("F1.dat")

N := length(hcond) N = 174
N := length(τ) N = 174
N := length(T) N = 174
N := length(Rx) N = 174
N := length(F1) N = 174

All N values must be equal

$$SER(P) := \sqrt{\frac{\sum_{i=1}^{N}\left[hcond_i - \left[\frac{P_1 \cdot F1_i \cdot (\tau_i)^{P_2}}{(T_i)} \cdot (Rx_i)^{P_3}\right]\right]^2}{N-3}}$$

$$P := \begin{pmatrix} 0.208 \\ 0.224 \\ 1.321 \end{pmatrix} \quad Min := Minimize(SER, P) \qquad Min = \begin{pmatrix} 0.213 \\ 0.219 \\ 1.249 \end{pmatrix} \qquad SER(Min) = 645.211$$

APPENDIX F

MathCAD Worksheet for the New Pure-Refrigerant Model

Define the Reynolds Number,

$$Re_L(x,G) := \frac{G\cdot(1-x)\cdot d_i}{\mu_l}$$

Define the dimensionless Condensate Film Thickness,

$$\delta(x,G) := \begin{cases} 0.866\,Re_L(x,G)^{0.5} & \text{if } Re_L(x,G) \le 1600 \\ 0.051\cdot Re_L(x,G)^{0.87} & \text{if } Re_L(x,G) > 1600 \end{cases}$$

Define the dimensionless temperature,

$$T(x,G) := \begin{cases} \delta(x,G)\cdot Pr_l & \text{if } \delta(x,G) \le 5 \\ 5\cdot\left[Pr_l + \ln\left[1 + Pr_l\cdot\left(\frac{\delta(x,G)}{5} - 1 \right) \right] \right] & \text{if } 5 < \delta(x,G) \le 30 \\ 5\cdot\left(Pr_l + \ln\left(1 + 5\cdot Pr_l\right) + 0.495\cdot\ln\left(\frac{\delta(x,G) - 2.5}{27.5} \right) \right) & \text{if } \delta(x,G) > 30 \end{cases}$$

Define the empirically fitted relative roughness,

$$Rx_f := \frac{0.18\cdot\left(\frac{e}{d_i}\right)}{0.1 + \cos(\beta)}$$

Define the Single-Phase friction factors,

$$f_{LO1}(G) := \begin{cases} 0.079\left(\frac{G\cdot d_i}{\mu_l}\right)^{-0.25} & \text{if } \frac{G\cdot d_i}{\mu_v} > 2000 \\ \frac{16}{\left(\frac{G\cdot d_i}{\mu_l}\right)} & \text{if } \frac{G\cdot d_i}{\mu_v} \le 2000 \end{cases}$$

$$f_{GO1}(G) := \begin{cases} 0.079 \cdot \left(\frac{G \cdot d_i}{\mu_v} \right)^{-0.25} & \text{if } \frac{G \cdot d_i}{\mu_v} > 2000 \\ \frac{16}{\left(\frac{G \cdot d_i}{\mu_v} \right)} & \text{if } \frac{G \cdot d_i}{\mu_v} \leq 2000 \end{cases}$$

$$f_{LO2}(G) := \frac{\left(1.74 - 2 \cdot \log\left(2 \cdot Rx_f\right)\right)^{-2}}{4}$$

$$f_{GO2}(G) := \frac{\left(1.74 - 2 \cdot \log\left(2 \cdot Rx_f\right)\right)^{-2}}{4}$$

$$f_{LO}(G) := \begin{cases} f_{LO1}(G) & \text{if } f_{LO1}(G) > f_{LO2}(G) \\ f_{LO2}(G) & \text{otherwise} \end{cases}$$

$$f_{GO}(G) := \begin{cases} f_{GO1}(G) & \text{if } f_{GO1}(G) > f_{GO2}(G) \\ f_{GO2}(G) & \text{otherwise} \end{cases}$$

$$E(x, G) := (1 - x)^2 + x^2 \cdot \frac{\rho_l \cdot f_{GO}(G)}{\rho_v \cdot f_{LO}(G)}$$

$$F(x) := x^{0.78} \cdot (1 - x)^{0.224}$$

$$H := \left(\frac{\rho_l}{\rho_v} \right)^{0.91} \cdot \left(\frac{\mu_v}{\mu_l} \right)^{0.19} \cdot \left(1 - \frac{\mu_v}{\mu_l} \right)^{0.7} \qquad \rho_m := \left(\frac{x}{\rho_v} + \frac{1 - x}{\rho_l} \right)^{-1}$$

Define the Weber Number,

$$We(G) := \frac{G^2 \cdot d_i}{\rho_m \cdot \sigma}$$

Define the Froude Number,

$$Fr(G) := \frac{G^2}{g \cdot d_i \cdot \rho_m{}^2}$$

Define the two-phase multiplier,

$$\Phi_{LO}(x,G) := \left[E(x,G) + \frac{(3.24 \cdot F(x) \cdot H)}{Fr(G)^{0.045} \cdot We(G)^{0.035}} \right]^{0.5}$$

Define the Interfacial Shear Stress,

$$dp_{dz}(x,G) := \frac{\Phi_{LO}(x,G)^2 \cdot 2 \cdot f_{LO}(G) \cdot G^2}{d_i \cdot \rho_l}$$

$$\tau(x,G) := dp_{dz}(x,G) \cdot \frac{d_i}{4}$$

Define geometry enhancement factor,

$$Rx := \left[\frac{\left[\left[2 \cdot e \cdot n_f \cdot \left(1 - \sin\left(\frac{\beta}{2} \right) \right) \right] \right]}{\pi \cdot d_i \cdot \cos\left(\frac{\beta}{2} \right)} + 1 \right] \cdot \frac{1}{\cos(\gamma)}$$

Define the heat transfer coefficient,

$$h(x,G) := \frac{0.208 \rho_l \cdot c_{p\_l} \cdot \left(\frac{\tau(x,G)}{\rho_l} \right)^{0.224}}{T(x,G)} \cdot Rx^{1.321}$$

APPENDIX G

MathCAD Worksheet for Generating the New Empirical Constants for The New Refrigerant-Mixture Model

Define independent parameter:

$hcond := READPRN("hcond.dat")$

$\tau := READPRN("Tao.dat")$

$T := READPRN("Temp.dat")$

$Rx := READPRN("Rx.dat")$

$F1 := READPRN("F1.dat")$

$F2 := READPRN("F2.dat")$

$h_G := READPRN("hG.dat")$

$N := length(hcond) \quad N = 110$
$N := length(\tau) \quad N = 110$
$N := length(T) \quad N = 110$
$N := length(Rx) \quad N = 110$
$N := length(F1) \quad N = 110$
$N := length(F2) \quad N = 110$
$N := length(h_G) \quad N = 110$

All N values must be equal

$$SER(M) := \sqrt{\frac{\sum_{i=1}^{N}\left[hcond_i - \left[\frac{1}{\frac{M_1 \cdot F1_i \cdot (\tau_i)^{M_2}}{(T_i)} \cdot (Rx_i)^{M_3}} + \frac{F2_i}{h_{G_i}}\right]^{-1}\right]^2}{N-3}}$$

$$M := \begin{pmatrix} 0.31 \\ 0.314 \\ 0.993 \end{pmatrix} \quad Min := Minimize(SER, M) \quad Min = \begin{pmatrix} 0.31 \\ 0.314 \\ 0.935 \end{pmatrix} \quad SER(Min) = 464.43$$

APPENDIX H

MathCAD Worksheet for the New Refrigerant-Mixture Model

Define the Reynolds Number,

$$Re_L(x,G) := \frac{G\cdot(1-x)\cdot d_i}{\mu_l}$$

Define the Condensate Film Thickness,

$$\delta(x,G) := \begin{cases} 0.866\,Re_L(x,G)^{0.5} & \text{if } Re_L(x,G) \le 1600 \\ 0.051\cdot Re_L(x,G)^{0.87} & \text{if } Re_L(x,G) > 1600 \end{cases}$$

Define the Temperature,

$$T(x,G) := \begin{cases} \delta(x,G)\cdot Pr_l & \text{if } \delta(x,G) \le 5 \\ 5\cdot\left[Pr_l + \ln\left[1 + Pr_l\cdot\left(\frac{\delta(x,G)}{5} - 1 \right)\right]\right] & \text{if } 5 < \delta(x,G) \le 30 \\ 5\cdot\left(Pr_l + \ln\left(1 + 5\cdot Pr_l\right) + 0.495\cdot\ln\left(\frac{\delta(x,G) - 2.5}{27.5} \right)\right) & \text{if } \delta(x,G) > 30 \end{cases}$$

Define the empirically relative roughness,

$$Rx_f := \frac{0.18\cdot\left(\frac{e}{d_i}\right)}{0.1 + \cos(\beta)}$$

Define the Single-Phase Friction Factor,

$$f_{LOl}(G) := \begin{cases} 0.079\left(\frac{G\cdot d_i}{\mu_l} \right)^{-0.25} & \text{if } \frac{G\cdot d_i}{\mu_v} > 2000 \\ \frac{16}{\left(\frac{G\cdot d_i}{\mu_l} \right)} & \text{if } \frac{G\cdot d_i}{\mu_v} \le 2000 \end{cases}$$

$$f_{GO1}(G) := \begin{cases} 0.079 \cdot \left(\frac{G \cdot d_i}{\mu_v}\right)^{-0.25} & \text{if } \frac{G \cdot d_i}{\mu_v} > 2000 \\ \frac{16}{\left(\frac{G \cdot d_i}{\mu_v}\right)} & \text{if } \frac{G \cdot d_i}{\mu_v} \le 2000 \end{cases}$$

$$f_{LO2}(G) := \frac{\left(1.74 - 2 \cdot \log\left(2 \cdot Rx_f\right)\right)^{-2}}{4}$$

$$f_{GO2}(G) := \frac{\left(1.74 - 2 \cdot \log\left(2 \cdot Rx_f\right)\right)^{-2}}{4}$$

$$f_{LO}(G) := \begin{cases} f_{LO1}(G) & \text{if } f_{LO1}(G) > f_{LO2}(G) \\ f_{LO2}(G) & \text{otherwise} \end{cases}$$

$$f_{GO}(G) := \begin{cases} f_{GO1}(G) & \text{if } f_{GO1}(G) > f_{GO2}(G) \\ f_{GO2}(G) & \text{otherwise} \end{cases}$$

$$E(x, G) := (1 - x)^2 + x^2 \cdot \frac{\rho_l \cdot f_{GO}(G)}{\rho_v \cdot f_{LO}(G)}$$

$$F(x) := x^{0.78} \cdot (1 - x)^{0.224}$$

$$H := \left(\frac{\rho_l}{\rho_v}\right)^{0.91} \cdot \left(\frac{\mu_v}{\mu_l}\right)^{0.19} \cdot \left(1 - \frac{\mu_v}{\mu_l}\right)^{0.7} \qquad \rho_m(x) := \left(\frac{x}{\rho_v} + \frac{1 - x}{\rho_l}\right)^{-1}$$

Define the Weber Number,

$$We(G, x) := \frac{G^2 \cdot d_i}{\rho_m(x) \cdot \sigma}$$

Define the Froude Number,

$$Fr(G, x) := \frac{G^2}{g \cdot d_i \cdot \rho_m(x)^2}$$

Define the two-phase multiplier,

$$\Phi_{LO}(x,G) := \left[E(x,G) + \frac{(3.24 \cdot F(x) \cdot H)}{Fr(G,x)^{0.045} \cdot We(G,x)^{0.035}} \right]^{0.5}$$

Define the Interfacial Shear Stress,

$$dp_{dz}(x,G) := \frac{\Phi_{LO}(x,G)^2 \cdot 2 \cdot f_{LO}(G) \cdot G^2}{d_i \cdot \rho_l}$$

$$\tau(x,G) := dp_{dz}(x,G) \cdot \frac{d_i}{4}$$

Define geometry enhancement factor,

$$Rx := \left[\frac{\left[2 \cdot e \cdot n_f \cdot \left(1 - \sin\left(\frac{\beta}{2} \right) \right) \right]}{\pi \cdot d_i \cdot \cos\left(\frac{\beta}{2} \right)} + 1 \right] \cdot \frac{1}{\cos(\gamma)}$$

Define the ratio between the sensible heat duty removed by cooling the vapour and the total heat flow rate exchanged,

$$\delta Q_{SV\_T}(x) := x \cdot c_{p\_v} \cdot \left(\frac{\Delta TG}{i_{fg}} \right)$$

Define the heat transfer coefficient of the vapour phase flowing alone in the duct, (Dittus-Boelter, 1930)

$$h_G(G,x) := 0.023 \cdot \frac{k_v}{d_i} \cdot \left(\frac{G \cdot d_i}{\mu_v} \right)^{0.8} \cdot \left(\frac{c_{p\_v} \cdot \mu_v}{k_v} \right)^{0.3}$$

Define the corrected heat transfer coefficient for zeotropic mixture,

$$h_m(x,G) := \left[\frac{1}{\frac{0.31 \rho_l \cdot c_{p\_l} \cdot \left(\frac{\tau(x,G)}{\rho_l} \right)^{0.314}}{T(x,G)} \cdot Rx^{0.993}} + \frac{\delta Q_{SV\_T}(x)}{h_G(G,x)} \right]^{-1}$$